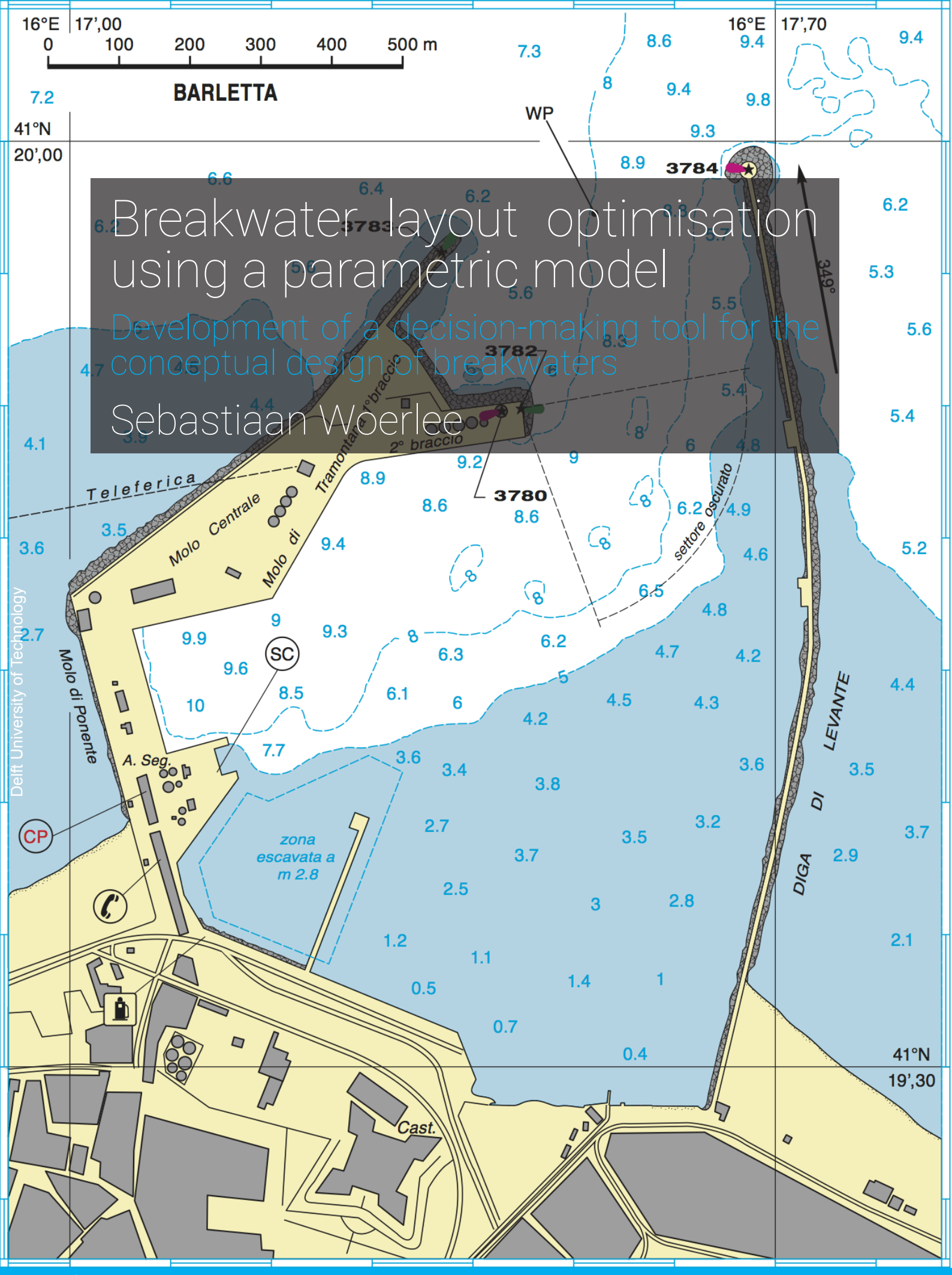

Breakwater layout optimisation using a parametric model

Development of a decision-making tool for the conceptual design of breakwaters

Sebastiaan Woerlee

TU Delft
ARCADIS

Breakwater layout optimisation using a parametric model

Development of a decision-making tool for the conceptual design of breakwaters

by

Sebastiaan Woerlee

in partial fulfilment of the requirements to obtain the degree of

Master of Science

in Hydraulic Engineering

at the faculty of

Civil Engineering and Geosciences

at

Delft University of Technology

to be defended publicly on Thursday September 12, 2019 at 2:00 PM.

Student number:	4234030	
Project duration:	October 15, 2018 – September 1, 2019	
Thesis committee:	Prof. dr. ir. S.G.J. Aarninkhof,	TU Delft, chair
	Ir. C. Parkinson,	Arcadis
	Ir. J. van Overeem,	TU Delft - Arcadis
	Ir. A.J. Lansen	TU Delft

Cover image: Porto di Barletta, edited from Istituto Idrografico della Marina, https://www.pagineazzurre.com/.

TU Delft Delft University of Technology

ARCADIS Design & Consultancy for natural and built assets

Preface

I am writing this preface with the knowledge that this will be the very last thing I will put on paper as a student. This thesis concludes my Master of Science program at the Delft University of Technology and therewith also my time as a student comes to an end. I can genuinely say that I have enjoyed this last year and that I have learned a lot along the way. It has been challenging, as I had to discover both the world of Python and that of genetic algorithms mostly on my own, which I could never have done without developing this much interest for programming and optimisation technologies. In addition, I really enjoyed my time at the office of Arcadis in Rotterdam, where I performed my research.

The past year would never have been such a success without the help I received. First of all, I would like to thank Jan van Overeem, for bringing me in touch with Arcadis and for the sympathetic ear concerning all the problems I faced. Your enthusiasm was contagious and I truly hope I managed to stimulate it during the process. In addition, I would like to thank Chris Parkinson, for his support at every stage of my work. I was able to ask you anything and you were always there to take another look at my report or sit around the table to talk about some points of discussion. Thank you for putting trust in the work I performed, as the knowledge that my work would be followed up kept me motivated until the very end. I would like to thank Stefan Aarninkhof for his enthusiasm and critical thoughts during my presentations at the TU Delft and Joost Lansen for the in-depth sessions we had concerning port layout related topics.

I would like to thank Arcadis for the opportunity to talk to all the people that were in the position to help me during the course of my research. A special thanks to Kasper, Matthijs and Wojciech for their input concerning breakwater, hydrodynamical and port layout related topics. To my friends and family, thank you for being there whenever I needed someone to talk to.

For now, I would like to say, enjoy reading. I would like to wish Jelle the best of luck in continuing what I started. I am really curious what kind of improvements another year of research will offer!

Sebastiaan Woerlee
Delft, September 2019

Summary

Nowadays, conceptual breakwater layout design mostly relies on experience and expert judgement, making it complicated to demonstrate that an economic optimum has been reached. Assurance of results, in combination with flexibility in design and approach, is becoming increasingly important due to rapid port modernisation, growing port competition and higher demands. This stresses the need to develop a tool that is able to establish the economically most attractive breakwater layout in the conceptual design phase for a certain set of requirements and site-specific data. This study provides a proof of concept for a generative breakwater layout design tool, applicable to projects all around the world. A suitable optimisation method, a universally applicable methodology for the determination of the economic optimum and the subsequent set-up of a *robust* and *flexible* parametric model result in a design that meets client expectations. In this way, breakwater projects can be forced into a spiral of increasing trust between the involved parties in an early design stage.

A fully quantitative optimisation approach has been established by defining the optimal breakwater layout as the layout inducing lowest total costs, therewith providing the opportunity to apply cost validation. Optimisation takes place based on two objectives, costs and performance, leading to a realistic representation of the problem and the ability to consider a wide range of alternatives. Costs, presented as capital and operational expenditures, have been divided into breakwater-related costs (production, transport and construction), dredging costs and land costs. Performance has been associated directly with the downtime costs that are induced by the respective layout alternative. Several output points for both operational and navigational downtime have been established, at which the hours of downtime per year are determined based on the prevailing environmental conditions.

Genetic algorithms are proven to be the most suitable optimisation method to examine the balance between costs and performance of a breakwater layout configuration. They are ideally suited to robustly find an optimum in the conceptual design phase. The specific genetic algorithm that has been chosen for this study, the non-dominated sorting genetic algorithm (*NSGA-II*), accomplishes this by laying its focus on three robustness indicators. First of all, the model *consistently* achieves the same results over several runs, therewith generating a robust concept. Besides, it ensures that the model *converges* towards the global optimum (rather than a local optimum), by efficiently evaluating and selecting the alternatives within a population. Ultimately, it strives to maintain *diversity* in the generated solutions, so that the model encompasses the entire solution space, and the possibility of encountering the neighbourhood containing the global optimum is maximised. This is realised by randomly generating fully parameterised breakwater layout alternatives that comply with the applied boundary conditions and model constraints. Layout alternatives are evaluated and improved over the course of generations by making use of evolutionary processes (selection, crossover and mutation) until sufficient convergence has been observed.

Model validation has taken place by comparing model results to actual design implementations for the port of Tanger Med 2 in Morocco. Total cost consistency has been valued at 1.4% over three separate model runs, therewith fulfilling the expectations applying to *NSGA-II*. Layout changes with respect to the actual layout could all be related to the applied model simplifications. The parametric model is *robust*, as total cost accuracy is consistently located well within the 30% range that is applicable to conceptual breakwater layout design (Ligteringen & Velsink, 2012), when performing at least two runs that generate comparable results. The total optimisation process now has an average duration amounting to somewhat over two hours, which guarantees an increase in the speed of the decision-making process, especially since the parametric model can be run in the background. The model is considered to be *flexible*, as it is able to efficiently deal with changes in design requirements and future port developments. Besides, it adequately reacts to changes in input and boundary conditions.

This research emphasises the opportunities that are present within conceptual breakwater layout design. The provided proof of concept for a generative breakwater layout design tool gives a significant amount of support to the design process and has a large potential of improving client relationships in an early design stage. Different parameters and phases of the port development can easily be modelled in a short period of time and presented in a visually attractive way. Therefore, fast mutual agreement in the decision-making process is enhanced. Building out the proposed model can result in its applicability for port realisation projects all around the world.

Contents

List of Figures

List of Tables

Nomenclature

Acronyms

ANN	Artificial Neural Network
CAPEX	Capital Expenditures
GA	Genetic Algorithm
HAT	High Astronomical Tide
LAT	Low Astronomical Tide
MSL	Mean Sea Level
NSGA	Non-dominated Sorting Genetic Algorithm
OPEX	Operational Expenditures
RHS	Right Hand Side: decision variable
SA	Simulated Annealing
SEC	SECondary breakwater: decision variable
TEU	Twenty-foot Equivalent Unit

Greek Symbols

α	Breakwater seaward slope angle	°
α_i	Angle of the wave front with respect to the depth contours	°
β	Incident wave angle with respect to breakwater gap axis	°
β_w	Angle of wave attack	°
χ_i	Decision variable for a certain breakwater layout configuration	-
γ_β	Influence factor for oblique wave attack	-
γ_f	Roughness factor	-
Φ	Breakwater material volume ratio	-
$\Phi_{bw,m}$	Ratio of annual breakwater maintenance costs w.r.t. construction	-
θ_0	Wave direction in deep water	°
θ_{ch}	Approach channel orientation with respect to y-axis	°
ξ	Surf similarity parameter = $\tan\alpha / \sqrt{H_s / L_0}$	-
X_i	Vector of decision variables for a certain breakwater layout configuration	-

Roman Symbols

(x_i, y_i)	Coordinates of breakwater node locations	m
(x_{max}, y_{max})	Outermost point defined for the primary breakwater	m
(x_{tc}, y_{tc})	Coordinates of turning circle centre	m
(x_{tm}, y_{tm})	Coordinates of tugboat mooring dock centre	m
$1 : x_b$	Bank slope of the dredged areas in the harbour basin	-
$1 : x_f$	Breakwater slope on the front side	-
$1 : x_r$	Breakwater slope on the rear side	-
A	Area	m^2
B	Breakwater gap width	m
B_s	Beam of the design vessel	m

B_{core}	Width of the top of the breakwater core	m
B_{crest}	Breakwater crest width	m
B_{eq}	Equivalent breakwater gap width	m
BL	Ratio of breakwater gap width to wave length	m
c_0	Wave propagation velocity in deep water	$\mathrm{m\,s^{-1}}$
C_c	Present value of CAPEX and OPEX	€
C_d	Downtime costs	€
c_i	Wave propagation velocity at desired location	$\mathrm{m\,s^{-1}}$
C_{bw}	Breakwater construction costs	€
C_{dr}	Capital dredging costs	€
C_{land}	Land costs related to port construction	€
C_{TEU}	Unit rate per TEU	€/TEU
D	Draught of the design vessel	m
d	Water depth	m
d_b	Depth addition for channel bottom type	m
D_n	Nominal diameter of armour units	m
d_{ch}	Channel depth below MSL	m
d_{dom}	Depth at 2/3 of the length of a breakwater segment	m
F	Average fitness of a single population	-
f	Objective function	-
f_f	Fitness function for a single solution	-
F_{max}	Maximum fitness of all generations	-
F_{min}	Minimum fitness of all generations	-
F_{rel}	Relative fitness of a single population	-
f_{TEU}	TEU-factor	-
g	Gravitational acceleration constant	$9.81\,\mathrm{m\,s^{-2}}$
H	Wave height	m
h_c	Height of the top of the breakwater core above HAT	m
h_f	Average fill-up level above MSL	m
h_l	Level of the armour layer extension on the leeward side below MSL	m
H_s	Significant wave height	m
H_{bq}	Beam and stern quartering wave height	m
k	Wave number	$\mathrm{rad\,m^{-1}}$
K_d	Diffraction coefficient	-
K_R	Refraction coefficient	-
K_r	Reflection coefficient	-
K_S	Shoaling coefficient	-
K_t	Transmission coefficient	-
L	Wave length	m
L_0	Deep water wave length from linear wave theory = $gT^2/(2\pi)$	m
L_B	Harbour basin length	m
L_q	Quay length	m
L_s	Length over all of the design vessel	m
L_{ch}	Length of a channel section	m

L_{fq}	Future quay length, allowing for port expansion	m
L_{max}	Outermost distance in x-direction defined for the secondary breakwater	m
L_{seg}	Breakwater segment length	m
m_b	Berth occupancy factor	-
N_a	Number of armour units per breakwater segment	-
n_b	Number of berths	-
n_d	Amount of downtime per year	$\mathrm{hrs\,yr^{-1}}$
n_v	Porosity of the armour layer	-
Pr	Probability of occurrence	-
q	Mean overtopping discharge	$\mathrm{l\,s^{-1}\,m^{-1}}$
r	Discount rate	-
R_c	Freeboard crest height above HAT	m
s_{max}	Maximum directional concentration parameter	-
T	Wave period	s
t	Time	yr
t_a	Thickness of the armour layer	m
T_L	Design lifetime of the breakwater	yr
T_p	Peak wave period	s
t_s	Average annual siltation thickness of harbour basin	$\mathrm{m\,yr^{-1}}$
t_u	Thickness of the underlayer	m
t_{tug}	Time required for tug fastening	s
u_{cc}	Cross-current speed	$\mathrm{m\,s^{-1}}$
u_{cw}	Cross-wind speed	$\mathrm{m\,s^{-1}}$
u_{lc}	Longitudinal current speed	$\mathrm{m\,s^{-1}}$
V	Volume	$\mathrm{m^3}$
V_f	Terminal fill volume	$\mathrm{m^3}$
v_s	Vessel entrance speed	$\mathrm{m\,s^{-1}}$
V_{ch}	Total channel volume to be dredged	$\mathrm{m^3}$
$v_{s,min}$	Minimum vessel speed	$2.0\,\mathrm{m\,s^{-1}}$
W	Total channel width	m
W_B	Bank clearance	m
W_i	Additional channel width	m
W_{BM}	Basic manoeuvring lane width	m
y_f	Cross-shore sediment fill distance	m
y_m	Distance for manoeuvring, berthing and terminal fill	m
y_{bl}	Distance from shoreline to breaker line	m
z	Bed level w.r.t. MSL	m
z_0	Bed level at the onshore side of the terminal w.r.t. MSL	m
z_q	Bed level at the quay location w.r.t. MSL	m

Subscripts

0	Value corresponding to deep water conditions
a	Breakwater armour layer value
b	Characteristic berth value
bb	Value corresponding to the berthing basin

br	At location of wave breaking
bw	Characteristic breakwater value
c	Breakwater core value
d	Diffracted value for wave conditions
$d1$	Depth value corresponding to the onshore side of a breakwater segment
$d2$	Depth value corresponding to the offshore side of a breakwater segment
dd	Value corresponding to dredging and subsequent disposal
df	Value corresponding to dredging and subsequent filling
dom	Value at the dominant depth of a breakwater segment
i	Incident value for wave conditions
in	Value corresponding to the inner approach channel
n	Value corresponding to navigational downtime
o	Value corresponding to operational expenditures
od	Value corresponding to operational downtime
out	Value corresponding to the outer approach channel
r	Reflected value for wave conditions
$rest$	Value corresponding to remaining harbour basin volume to be dredged
t	Transmitted value for wave conditions
tb	Value corresponding to the turning basin
u	Breakwater underlayer value

1. Introduction

This chapter provides an introduction to the study performed on the optimisation of breakwater layout for ports using a parametric model. At first, some general background information is given considering breakwater layout design and the relevance of this research. A problem statement is provided, after which the research objectives and research questions are stated, including the scope restrictions that are applied in this research. To conclude this chapter, the thesis outline is discussed.

1.1. Research introduction

There have been breakwaters as long as there have been harbours. They can have several functions, of which the most relevant ones (related to harbours) are listed below (Piccoli, 2014):

- Harbour protection against waves and currents
- Prevent siltation of the approach channel and harbour basin
- Provide dock or quay facilities

The main function of a breakwater at a harbour is to provide shelter from waves and currents, as stated in the first bullet point. Preventing siltation can be accomplished by decreasing the wave action in the harbour entrance, cutting off littoral sediment transport supply to the approach channel or by natural scouring processes (as a counterbalance). The result is a decrease in maintenance dredging costs. What may also be of interest, is the ability of breakwaters to provide berths.

Breakwater design forms an integral part in the overall design of a port, as associated costs are relatively high. The process of the entire master plan of a port is schematised in Appendix A.1. Generation of breakwater alternatives is generally performed after the port analysis, which consists of the aspects mentioned in this figure. It can be observed that cargo flow and shipping forecasts are already performed in this stage. Also field data, relating to environmental, geotechnical and coastal conditions have been obtained at this moment. Therefore, a general idea of port planning has already been acquired.

Breakwater design is a complex and time-consuming process, which can be subdivided into several phases. The project phases are related to those stated in The Rock Manual (CIRIA/CUR/CETMEF, 2007), as the process described there is used widely in the engineering world and therefore serves as a solid base point. A concise summary of the project phasing sequence, specifically related to breakwater layout design, is given in Table 1.1.

In the detailed design phase, the elements of the previous phases are used as input. The result of the detailed design phase is the final design, which forms the basis for the implementation and operation phase. Conventionally, many calculations need to be performed in this phase, which require a large amount of time and effort. New technologies and improvements to the design process are needed as time progresses to keep up with higher demands. As a result, external pressure is increasing, which can also be accounted to society and competition between different ports. Since breakwater design depends on many different factors, a fully-automated process would be desirable. This could decrease labour and associated costs, especially when considering the conceptual and preliminary design phases. Ideally, many different options need to be set up and compared in these phases, and because sizes and costs are still estimates at this moment, a specific model could decrease the workload coming along with it significantly. Besides, computers should be able to execute the design process in the future in a more optimal way than humans do, as they should be able to consider all possible alternatives and compare them in a quantitative way. The model to be set up should focus on the key design elements. It should be able to identify the necessary information requirements, so that these can be used as input. In addition, performing analytical studies to set-up a typical breakwater layout is

Project phases	Elements
Problem understanding	• Functional requirements • Performance criteria • Constraints: budget, access, materials, environment, maintenance
Information requirements	• Available materials • Hydraulic conditions (e.g. waves, currents, water levels) • Bathymetry and topography • Ground conditions
Conceptual design	• Structure layouts and types • Identify information requirements • Review project feasibility
Preliminary design	• Analytical studies and modelling • Assess alternatives against performance criteria and constraints • Cost estimates • Compare alternatives (technical, environmental and economic)
Detailed design	• Calculate detailed structure dimensions • Design transitions, end protection, drainage, services, etc.
Implementation	• Specifications • Construction
Operation	• Monitoring • Maintenance • Decommissioning or removal

Table 1.1: Typical project phasing for breakwater design (adapted from CIRIA/CUR/CETMEF (2007))

something the model should be able to execute. If the model is able to develop several design alternatives, a final step could be to estimate resulting costs and compare the alternatives that are developed.

Breakwater design can be split up into the cross-sectional design and the layout design. For the design of a breakwater cross-section and corresponding armourstone sizes, many techniques are available. Performing a reliability analysis or making deterministic calculations are some of the possible options. Arcadis built up a parametric cross-sectional model for breakwaters, calculating required dimensions for any of the mentioned design phases, which can be found in Section 2.4. For breakwater layout however, little research exists at the moment and therefore engineers are destined to rely on their experience and expert judgement. This also means that results are never fully optimised, although they may be close. As the conceptual design phase is an iterative process, many steps are required to truly optimise the breakwater layout. Furthermore, physical and numerical models can take up too much time and investments in early design stages. Therefore, many opportunities remain available to experiment with new strategies, so that more optimal breakwater layouts can be developed.

A breakwater layout model in an early design phase brings along many uncertainties, which are important to identify for a thorough evaluation. The fact that economic uncertainty and recent trends are amplifying the competitive environment in which ports are located only supports this. Examples of recent trends are forecasting future regulations and policies, increasing volatility (e.g. port expansion, allowance for larger vessels, etc.), technological modernisation and environmental concerns (Taneja et al., 2010). These trends can clearly be seen for container ports. Containerised trade more than tripled over the last twenty years and container vessels are continuously increasing in size, whereas they spend less time in ports than other cargo vessels (United Nations Conference on Trade and Development, 2018). To cope with these trends in an efficient manner, the need to design breakwaters in a more flexible manner arises. One of the ways to include for this flexibility in the design process is to adapt to changes adequately and quickly, which could be realised with a model that effectively reduces the required process time. Another way to account for design flexibility in the model is to build it up in such a way, that it does not need to repeat the entire optimisation process when dealing with small changes. Also in later design phases such a model could be valuable, especially when feedback is needed due to a change in project objectives for example. There can be dealt with flexibility by providing a clear structure in the model, by considering a range of plausible futures (including corresponding breakwater layouts) and by helping to increase the speed of decision-making.

Besides flexibility factors, there will be uncertainties related to model robustness. To know to what extent a comparison of breakwater layout alternatives is robust, all relevant uncertainties need to be identified, which is done below (Ligteringen & Velsink, 2012; Rustell, 2016):

- Lack of site specific data, region specific cost data and/or shipping forecasts
- Lack of adequate modelling techniques
- Outdated, incomplete or inaccurate site data
- Random uncertainty in predicting or extrapolating conditions
- Inaccuracy in the determination of the economic optimum
- Uncertainty in effects of breakwater construction phasing and future developments
- Unfamiliarity with or underestimation of nautical requirements and nautical safety

When comparing breakwater layout alternatives, model uncertainty (treated in Section 5.5.3) is unavoidable, however this is inflicted on all layout alternatives, since the same model should be used for all of them. This results in an increased importance of site specific data and cost data to price each option (Rustell, 2016). Uncertainties cause risk, which can be applied in the model as a constraint (by applying a minimum confidence level) or as a comparison method. Cost estimates in the preliminary design typically require an accuracy of about 30% (Ligteringen & Velsink, 2012). Therefore, the uncertainty of a breakwater layout model simulating this design phase should remain below its accuracy limit, while taking into account all other project uncertainties.

1.2. Problem statement

Arcadis has been digitising their way of working over the last couple of years and have built a tool for the automated development of a standardised design of a breakwater cross-section under wave loading. As only the cross-section of a breakwater has been considered until now, this tool does not result in a complete picture when making a conceptual breakwater design. Breakwater layout, like its alignment and length, should ideally also be examined within a comparable tool to come up with the (economically) most optimal breakwater design. As conceptual breakwater layout design relies mostly on experience and engineering judgement at the moment, it is difficult to demonstrate that an optimum has been reached. Assurance of results is becoming more important due to an increase of external pressure, making it doubtful if the current techniques are able to keep up. This emphasises the need to develop a tool that is able to establish an optimal port layout for a certain set of requirements and site-specific data.

1.3. Research objective

Relating to the problem statement, the research objective is built up as follows:

Setting up a flexible, robust, parametric model that optimises breakwater layout alternatives for container ports from an economical point of view to be able to compare them in an efficient manner

It is relevant to state that the model to be developed is intended to serve as a starting point for a decision-making tool. In order to fit within the limitations of an MSc thesis, a proof of concept forms the main focus, as the model may initially be only applicable to a limited amount of cases. Nevertheless, by adding components to this model in the future, more realistic situations can be treated.

1.3.1. Research question

To achieve the research objective, the following research question has been formulated:

How can the optimal breakwater layout for a container port, in the conceptual design phase, be determined using a flexible, robust, parametric model?

To be able to give a complete answer to the research question, some sub-questions are formulated that each treat an integral part of the problem:

- Which optimisation method serves best to compare breakwater layout alternatives in a simple but efficient way?
- How does the parametric model need to be set up to ascertain optimal layout choices?
- How does the parametric model reflect the influence of key parameters on the breakwater layout?
- Why does the proposed model type form an improvement to current breakwater layout design and what are its limitations?

1.3.2. Scope

To create a model that serves as a starting point for a decision-making tool, a simple case is used initially, generating a robust concept. In this way, the proposed method can be successful from the beginning. Focus is laid on producing a breakwater layout configuration that approaches an optimal solution, rather than exactly coming up with it. Only critical parameters are included in the initial model, but room is created to add in second order effects later on. A well-bounded problem is created by narrowing down the scope. In order to do so, some scope restrictions should be applied, which are stated below:

- The considered port is a commercial cargo port, which specialises in container shipment. This choice is based on the need to narrow down the vessel types at this stage, as different vessels react differently on wave loading and require different mooring conditions. Container ships are chosen, as they form the most common form of new commercial transport and experience high demands concerning vessel sizes and time spent at the berth (see Section 1.1).
- A straight, alongshore uniform coastline and a constant bed slope with a homogeneous bed are assumed.
- Only rubble-mound breakwaters (possibly with a crest-element) which are connected to the coast have been treated. These are compatible with the cross-sectional model (see Section 2.4).
- Numerical and physical modelling is left out of the design model, since they are too expensive and time-consuming to incorporate in the preliminary design phase (Rustell, 2013). This results in the exclusion of local flow patterns caused by the breakwaters (including resulting bed changes), water quality related issues and thermal mixing. Sedimentation is treated in a simplified way, using some rough estimations.
- A simplified terminal layout is considered as a starting point. It consists of one quay wall, parallel to the shore, with a number of berths in one line.
- Special conditions, like ice, hurricanes and earthquakes are left out, as these are highly site specific. Separate studies should be performed to assess the effect of these conditions.
- The location of the port is set, as focus is laid on the optimal length and alignment of the breakwaters, rather than on site selection.
- Environmental and social considerations are not within the scope of this research.

1.4. Thesis outline

After the introduction given in the current chapter, a literature review is performed in Chapter 2. Consequently, a basis for the optimisation is provided in Chapter 3. Using this, the methodology adopted in this research (Chapter 4) and the set-up of the parametric model (Chapter 5) are elaborated. In Chapter 6, the sensitivity of the model is assessed. Following that, the influence of certain parameters on the breakwater layout is treated in Chapter 7. Model results are compared to those generated using conventional techniques for a specific case study in Chapter 8. All generated results are evaluated in Chapter 9, to determine model limitations and improvements on the current design process. Ultimately, some conclusions and recommendations are provided in Chapter 10. The outline of this report is visualised in Figure 1.1.

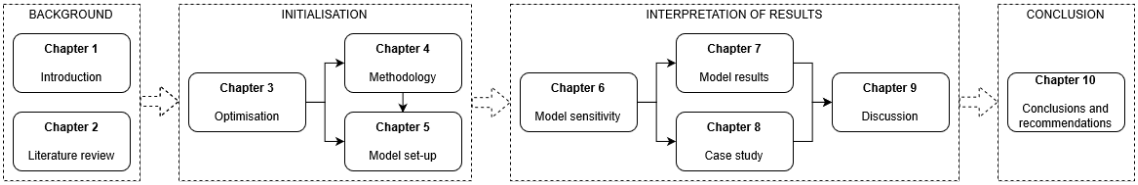

Figure 1.1: Outline of the report

2. Literature review

When looking at the first two sub-questions defined in Section 1.3.1, it has to be assessed what are the key parameters that influence breakwater layout and what are the possible optimisation methods to compare layout alternatives. A literature study is performed to acquire the information that is needed. First of all, the overall port layout is treated in Section 2.1, as this determines to a large extent the breakwater alignment. Then, the breakwater functionality is treated, based on the downtime occurring in the harbour basin (see Section 2.2). To determine the amount of downtime, wave processes and penetration inside the harbour basin are treated in Section 2.3. Some developments within Arcadis regarding cross-sectional design are in Section 2.4. Littoral transport is addressed in Section 2.5. Possible optimisation methods are discussed in Section 2.6.

2.1. Port layout

The overall port layout obviously has a large effect on breakwater layout and the total costs of a port. One of the reasons is that its geometry has a crucial role on the wave agitation within the harbour basin. Besides, the dimensions of the approach channel and manoeuvring basins are an important aspect in breakwater layout design. Not only do they determine dredging volumes (to compare dredging costs to other costs for optimisation), but the breakwater length is also dependent on the length of the approach channel that needs to be sheltered. Furthermore, the length of the breakwater gap depends on the approach channel width. Safety can also be directly related to the dimensions of the manoeuvring areas, as smaller margins induce larger nautical risks. Simplified methods for developing estimations of approach channel depth, length and width are given separately. Some general guidelines for approach channels are that they should be as short as possible, avoiding bends and taking into account prevailing winds, currents and waves (PIANC, 2014). The approach channel can usually be divided into an inner and an outer channel, which are situated respectively within and outside of the breakwater protection.

2.1.1. Channel width

The approach channel is a stretch of waterway connecting the manoeuvring area with the open sea. The channel allows safe passage for design ships, whereas the fairway is defined as the wider waterway navigable for all vessels (PIANC, 2014). A one-way approach channel is assumed, leading to a channel width consisting of the basic manoeuvring lane width (W_{BM}) and a bank clearance (W_B). In addition, cross-winds, currents and waves should be accounted for, since these environmental forces affect the ship's motions. All additional width elements (W_i) should be added to come up with the total channel width (W), which can be seen in Equation 2.1 (PIANC, 2014).

$$W = W_{BM} + \sum W_i + 2W_B \tag{2.1}$$

Container vessels are considered having moderate manoeuvring capacities, making the corresponding width of the basic manoeuvring lane equal to $1.5B_s$, where B_s is the width of the design vessel. Determination of the additional widths is based on PIANC (2014), although some simplifications are made as the influence of W_i on the overall breakwater layout is limited. In Table 2.1, all different additional width components are stated, assuming moderate vessel speeds (2−4 m/s). Some other assumptions that are made in this simplification are the presence of good aids of navigation, no hazardous cargo and a relatively shallow water depth compared to the ship's draught.

Waves coming in at 0° with respect to the longitudinal vessel axis are considered stern. Therefore, cross-winds and cross-currents, have an angle of 30-150° with the longitudinal vessel axis, whereas the angle of

Width (W_i)	**Condition**	**Outer channel**	**Inner channel**
Prevailing cross-wind (u_{cw})			
• Mild	$u_{cw} < 7$ m/s	$0.2B_s$	
• Moderate	$7 \leq u_{cw} < 16$ m/s	$0.4B_s$	
• Strong	$16 \leq u_{cw} < 24$ m/s	$0.7B_s$	
Prevailing cross-current (u_{cc})			
• Negligible	$u_{cc} < 0.1$ m/s	0.0	0.0
• Low	$0.1 \leq u_{cc} < 0.25$ m/s	$0.25B_s$	$0.2B_s$
• Moderate	$0.25 \leq u_{cc} < 0.75$ m/s	$0.7B_s$	$0.6B_s$
• High	$0.75 \leq u_{cc} < 1.0$ m/s	$1.2B_s$	n/a
Prevailing longitudinal current (u_{lc})			
• Low	$u_{lc} < 0.75$ m/s	0.0	
• Moderate	$0.75 \leq u_{lc} < 1.5$ m/s	$0.1B_s$	
• High	$u_{lc} \geq 1.5$ m/s	$0.2B_s$	
Beam and stern quartering wave height (H_{bq})			
• Low	$H_{bq} \leq 1$ m	0.0	
• Moderate	$1 < H_{bq} < 3$ m	$0.2B_s$	
• High	$H_{bq} \geq 3$ m	$0.4B_s$	
Aids to navigation	Good	$0.2B_s$	
Bottom surface			
• Smooth and soft		$0.1B_s$	
• Rough and hard		$0.2B_s$	
Depth of waterway	Relatively small	$0.2B_s$	$0.4B_s$

Table 2.1: Additional width components of the approach channel, adapted from PIANC (2014)

longitudinal currents is in between 0-30°. Beam and stern quartering waves do have an angle of 30-120° with the longitudinal vessel axis.

When considering sloping channel edges, the bank clearance equals $0.5B_s$ for moderate vessel speeds (PIANC, 2014).

2.1.2. Channel depth

When determining an optimal breakwater layout, the approach channel depth (d_{ch}) is only required to compute dredging volumes. Therefore, an estimation of the depth should suffice, which can be based on PIANC (2014). For the inner channel, a basic channel depth of $1.10D$ (where D is the draught of the design vessel) gives a fairly conservative value (corresponding to a vessel speed up to 5 m/s). For the outer channel, this depth can be taken as $1.3D$, which is also fairly conservative (corresponding to a significant wave height of about 2 m for waves with peak periods above 10 s). This basic channel depth is based on ship-related factors, such as ship squat, dynamic heel and wave response allowance. An addition of about $0.015B_s$ is required for container vessels as an estimate for ship sinkage due to dynamic heel (container ships are prone to heeling by strong cross-winds) (PIANC, 2014). A bottom type factor (d_b) should be added, which can be found in Table 2.2.

Bottom type	**Inner channel**	**Outer channel**
Mud	-	-
Sand/clay	0.4 m	0.5 m
Rock/coral	0.6 m	1.0 m

Table 2.2: Channel depth additions for bottom type (PIANC, 2014)

If no tidal windows are applied, ships should always be able to sail into the port and the channel depth as given above has to relate to low astronomical tide (LAT). A dredging tolerance of 0.7 m also needs to be included.

2.1.3. Channel length

The length of the approach channel depends directly on the stopping length of the design vessel. Two cases can be distinguished: a case where vessels can already slow down to the minimum vessel speed ($v_{s,min}$ = 2.0 m/s) outside of the harbour entrance (mild wave climate) and a case where the vessel can start lowering its speed only when it is within the protection of the breakwater (rough wave climate). For both cases, the length of the inner approach channel ($L_{ch,in}$) needs to be determined, since this determines for a large part the corresponding breakwater length. In the first case, this length only depends on the time needed to tie up the tugboats to the vessel and the actual stopping distance (see Equation 2.2a). As for the second case, tug fastening can take place during slowing down of the vessel when the conditions allow to do so. The time required to attach the tugboats to the vessel (t_{tug}) depends on crew expertise and environmental conditions, in average conditions ranging from 5 to 20 minutes (PIANC, 2014). Wave conditions with a significant wave height higher than 1.5 to 3.0 m or a vessel entrance speed (v_s) which is higher than 2.5 to 3.0 m/s results in tugs not able to attach while maintaining acceptable safety standards (PIANC, 2014). Very often, tugs have to wait until the vessel is at an acceptable distance inside the harbour entrance before the wave conditions are such that they can approach the vessel (PIANC, 2014). Therefore, a distance equal to the overall design vessel length is included in the length for tying up the tugboats. It is assumed that in this case, the vessel does enter the port with an acceptable vessel speed for tugs to make fast. For the second case, Equation 2.2b can be used.

$$L_{ch,in} = \begin{cases} L_{mild} + L_{final} & \text{for } H_s < 1.5-3.0 \text{ m and } v_s < 2.5-3.0 \text{m/s} \quad (2.2a) \\ L_{rough} + L_{final} & \text{for } H_s > 1.5-3.0 \text{ m or } v_s > 2.5-3.0 \text{m/s} \quad (2.2b) \end{cases}$$

where:

L_{mild} = length needed to tie up tugboats to design vessel (m)
$= t_{tug} \cdot v_{s,min}$

L_{rough} = length needed to slow down design vessel to a speed of 2 m/s and tie up tugboats (m)
$= \max\left((v_s - v_{s,min})\frac{3}{4}L_s\ ;\ t_{tug} \cdot v_{s,min}\right) + L_s$

L_{final} = final stopping distance from a speed of 2 m/s (m)
$= 1.5 \cdot L_s$

For mild conditions, the fastening time is on average lower than for rough conditions, due to the difference in vessel speed. Therefore, a fastening time of 10 min can be assumed for mild conditions, as opposed to a fastening time of 15 min for rough conditions.

Considering the length of the outer approach channel, only the depth contours need to be taken into account. Dredging should take place until the point where the required channel depth equals the sea bed, since the bed slope is assumed to be constant.

2.1.4. Manoeuvring areas

The approach channel should end in a turning basin, from where vessels are towed by tugboats to the berth. The turning basin can be represented by a circle with a diameter $\geq 2 \cdot L_s$. Assuming that tugboats are available for manoeuvring assistance and no environmental risks of large importance being present, a diameter of $2.5 \cdot L_s$ is considered a reasonably conservative value. The depth of the turning circle is assumed to be equal to the depth in the inner approach channel ($d_{ch,in}$).

For the depth of the other manoeuvring areas, only a bottom type safety margin (see Table 2.2) and a dredging tolerance of 0.7 m are taken into account. These margins need to be added up with the draught of the design vessel to end up with the water depth with respect to LAT (see Equation 2.3). An equal depth is assumed at all berths.

$$d_{bb} = LAT + D + d_b + 0.7 \quad (2.3)$$

As only one quay wall consisting of one or more berths is considered, the width of the manoeuvring basin is estimated by three times the beam of the design vessel and a supplementary 100 m for tugboat assistance (Ligteringen & Velsink, 2012; Puertos del Estado, 2007). In this way, ships can still pass a moored vessel while tugs are fastened, even when towing lines are used. This should be enough to provide the required mooring clearance and manoeuvring space in front of the quay.

2.1.5. Harbour entrance

To avoid that a ship becomes stranded across the harbour entrance in case of an incident, the minimum width of the harbour entrance should be equal to L_s (PIANC, 2014).

2.1.6. Quay

The main variables in the determination of the quay length (L_q) are the amount of berths (n_b) and the design vessel size. Vessel sizes are assumed to be equal for all berths. The quay length can now be computed using Equation 2.4 (Ligteringen & Velsink, 2012).

$$L_q = \begin{cases} L_s + 2 \cdot 15 & \text{for } n_b = 1 \\ 1.1 \cdot n_b \cdot (L_s + 15) + 15 & \text{for } n_b > 1 \end{cases} \tag{2.4}$$

In this way, a gap of 15 m is allowed between the ships moored next to each other and an additional 15 m at the two outer berths (Ligteringen & Velsink, 2012). The quay level for large displacement vessels (> 10.000t) is taken equal to MSL +2.50m (Puertos del Estado, 2007).

2.2. Downtime

Downtime can show up due to several conditions, of which some are related to the wave climate inside the port and others to aspects like wind, shipping or equipment. As the objective of this research is to find an optimal breakwater layout, only downtime due to the wave climate is analysed, since breakwater layout influences this. As wind-related downtime may play a significant role for container handling, some estimations are made to reflect on the effect of wind. Wave-related downtime can be divided into operational and navigational downtime. Operational downtime is the time per year that a ship cannot operate by loading and unloading at the berth due to unsafe conditions. Navigational downtime relates to the time per year that a ship is not able to call at the port or berth safely from the open sea. Both are treated separately, after which some general conclusions are made with respect to acceptable total downtime. Downtime due to the unsafe berthing and unsafe staying at the quay of vessels are not taken into account, as their share is probably minor and environmental limit conditions are likely to show overlap with the definitions as stated before.

2.2.1. Operational downtime

The amount of downtime for loading and unloading in a port is dependent on the wave conditions and resulting ship movements at the berths. These movements can be caused by winds, currents, waves, cargo handling operations, etc. When ship movements are too large, they can result in unsafe working and mooring conditions (PIANC, 1995). To calculate ship movements, it is necessary to have a detailed representation of the wave climate at the berth, meaning that not only wave heights, but also wave periods and directions are needed. These wave conditions should be obtained using a numerical model for wave penetration. As this results in high costs and consumes too much time for the conceptual design phase (Rustell, 2013), approximations in this report are based on allowable wave heights. Consequently, the design vessel is assumed to correspond to the largest vessel operating at the berth, as smaller vessels only can be dominant when taking into account wave periods at the berth. The wave heights that can be tolerated are in the order of 0.5 m (Ligteringen & Velsink, 2012). For waves acting in transverse direction to the quay, the allowable wave heights may even reduce to 0.3 m (Puertos del Estado, 2007). These criteria are quite crude, since wave periods and effects of the mooring system on ship movements are not taken into account (Ligteringen & Velsink, 2012).

Ship motion is only one condition which influences the cargo handling efficiency. Wind effects are likely to play a significant role in many situations and should therefore be thought over. The limiting factor here is the handling equipment, i.e. the ship to shore gantry cranes. According to Liebherr Container Cranes Ltd. (2015), operational wind speed limits are in the order of 20 m/s regardless wind direction. Puertos del Estado (2007) indicates operational wind speed limits for container vessels in the order of 22 m/s regardless wind direction, at 10 m height for a one minute gust.

As downtime estimations in the conceptual design phase are rough, it suffices to account for it by some general considerations with respect to wind and waves as elaborated on above. These estimations include the effect of mooring lines and other equipment. Currents and passing ships are assumed to not play a considerable role when calculating operational downtime and are therefore left out in the conceptual design phase.

2.2.2. Navigational downtime

The approach channel and turning basin are designed in such a way that tug fastening, pilot boarding, towing, stopping and manoeuvring can happen in protected areas (if necessary) during normal conditions. This is done by choosing the alignment of the approach channel such, that minimum cross-currents and cross-winds apply, and by having a small angle with the dominant wave direction. Besides, bends in the approach channel are avoided if possible. Channels should have dimensions that can cope with environmental conditions that prevail commonly, this is treated in Section 2.1. Nevertheless, in extreme cases, even the most favourable layout configuration results in navigational downtime. Tugboat unavailability forms the most important contributor to this. When wave heights are too large, tugboats are not able to fasten to incoming vessels safely, resulting in the inability of vessels to enter or leave the port. The sheltered area that is necessary to be able to fasten the tugboat, stop the vessel and perform manoeuvring procedures such as turning and berthing should be known, so that the breakwater can be extended correspondingly.

Operating limits for all possible environmental conditions should be provided to give reliable navigational downtime estimates. The effect of wind, waves and currents should be assessed and also their direction (transversal or longitudinal) has to be taken into account. Tugboat fastening limits are highly dependent on the type of tugboats that is used. For average tugboat sizes, fastening cannot take place when the significant wave height exceeds approximately 1.5 m (Ligteringen & Velsink, 2012). Wind speed limitations for navigational downtime start playing a role for wind speeds exceeding approximately 12 m/s, when comparing several large container ports (Nederlands Loodswezen, 2018; Sjöberg et al., 2016). These limits however strongly depend on vessel sizes, tugboat sizes and harbour geometry. Also the wind direction has a large influence on the wind speed limits, as under certain combinations of wind speeds and directions (strong stern on winds) vessels require a longer stopping distance than can be guaranteed.

2.2.3. Total acceptable downtime

Acceptable downtime for container vessels is still an important subject of discussion. Comparing several theories and ship motion criteria (Goedhart, 2002; Moes & Terblanche, 2010; PIANC, 1995), it can be stated that acceptable downtime largely depends on the intensity of use of the terminal and the type of cargo that is treated. As a financial analysis of the port and corresponding shipping forecasts are already available in the conceptual design phase of breakwaters, it should be known how much downtime is tolerable for the port to be considered. As an indication, the mean acceptable downtime as defined by Puertos del Estado (2007) is used in this report. It states that container ports may have a total downtime of about 200 hrs/yr (corresponding to about 2% of the time), which holds for both the transit vessel areas (approach channel, manoeuvring areas, etc.) and the staying vessel areas (anchorages, berths, etc.). This estimation is based on a 30% area use by design vessels (Puertos del Estado, 2007). It should be noted that in many conditions navigational and operational downtime happen at the same time, so 'double counting' should be avoided.

Downtime costs associated to downtime are port specific, as these are highly dependent on shipping forecasts and cargo flows. For higher downtime values, port competition starts playing a role, as shipping lines prefer to use competing ports when downtime rates are (too) high. Port competition is a factor that is hard to predict and which depends on numerous parameters, like the distance to the closest competing port, even as the vessel intensity and the port capacity. Apart from this, the logistic chains in which the ports take part, might

even be of larger importance. This means that ports no longer depend solely on their own performance, but on other variables, like their connection with the hinterland, too (Meersman et al., 2003).

2.3. Wave processes

When determining the amount of downtime occurring in a port, the wave climate in the harbour basin forms one of the key components. To get an idea of this, all contributing factors should be assessed. Wave transformation until the port, taking into account shoaling and refraction effects, has to be performed, which is done in Section 2.3.1. In addition, wave penetration into the harbour should be considered. The wave climate in the harbour basin can be divided in wave trains travelling through the harbour entrance, secondary wave trains reflecting from quay walls, breakwaters and other structures, and wave trains that are transmitted through the breakwater. Moving ships in the port and local wind-wave generation cause wave agitation, though they can be considered as secondary effects when considering wave penetration into a harbour. Therefore, these effects can be left out for the conceptual design phase and thus they are not treated in this section.

2.3.1. Shoaling and refraction

When wave conditions at sea are known, they should be transformed towards the port to assess their impact on the wave climate inside the harbour basin. The two processes that play a key role in this wave transformation are shoaling and refraction.

Shoaling is the deformation of waves, starting when the water depth becomes less than about half the wave length. This causes a reduction in wave propagation velocity, as waves start 'feeling' the sea bottom. As a result, waves get shortened and steepened.

As wave propagation velocity decreases with water depth, wave length must also decrease proportionally. Waves that approach the shore on an angle therefore have velocity variations along a wave crest, as the part of the wave in deeper water is moving faster than the part in shallower water. This causes the wave crest to bend towards the alignment of the depth contours. This is called refraction and depends on the relation of water depth to wave length.

For parallel depth contours and a straight shoreline, Snell's law can be used directly to compute the angle of the wave front with respect to the depth contours (α_i), which is given in Equation 2.5.

$$\sin \alpha_i = \left(\frac{c_i}{c_0}\right) \sin \alpha_0 \tag{2.5}$$

where:

- c_i = incident wave propagation velocity at the port location (m/s)
- c_0 = wave propagation velocity in deep water (m/s)
- α_0 = angle of the wave front with respect to the depth contours in deep water (°)

The incident wave propagation velocity (c_i) can be determined by applying the wave dispersion relation. This is described by an implicit formula, however Chen and Thompson (You, 2003) proposed an approximation as an explicit formula for the direct computation of the wave number in any water depth (see Equation 2.6), which is used in this report.

$$kd = (k_0 d)\sqrt{1 + \left[(k_0 d)\left(1 + \sum_{n+1}^{6} D_n (k_0 d)^n\right)\right]^{-1}} \tag{2.6}$$

where:

- k = Wave number (rad/m)
- k_0 = Deep water wave number (rad/m)

$D_1 = 0.6522$, $D_2 = 0.4622$, $D_3 = 0$, $D_4 = 0.0864$, $D_5 = 0.0675$ and $D_6 = 0$

The incident wave height at the port location (H_i) can now be computed by making use of wave energy conservation, taking into account a shoaling coefficient (K_S) and a refraction coefficient (K_R), as is done in Equation 2.7. It is assumed that bed friction and turbulence do not result in significant energy losses.

$$H_i = K_S \cdot K_R \cdot H_0 = \sqrt{\frac{1}{2n}\frac{c_0}{c_i}} \cdot \sqrt{\frac{\cos\alpha_0}{\cos\alpha_i}} \cdot H_0 \tag{2.7}$$

where:

$n = \frac{1}{2}\left(1 + \frac{2kd}{\sinh 2kd}\right)$

In the harbour basin, an equal depth is assumed, as depth-related effects are assumed to be minimal. This leads to absence of both refraction and shoaling in the harbour.

2.3.2. Diffraction

When an otherwise regular wave train is interrupted by a barrier (e.g. breakwater, small island), diffraction occurs. Diffraction can be defined as a phenomenon in which energy is transferred laterally along a wave crest (Coastal Engineering Research Center, 1984). A hypothetical case for which diffraction does not occur is visualised in Figure 2.1a, whereas the actual diffraction phenomenon is visualised in Figure 2.1b. Energy flow from region II to region I takes place (represented by arrows in Figure 2.1a) and in region III a partial standing wave occurs by superposition of incident and reflected waves.

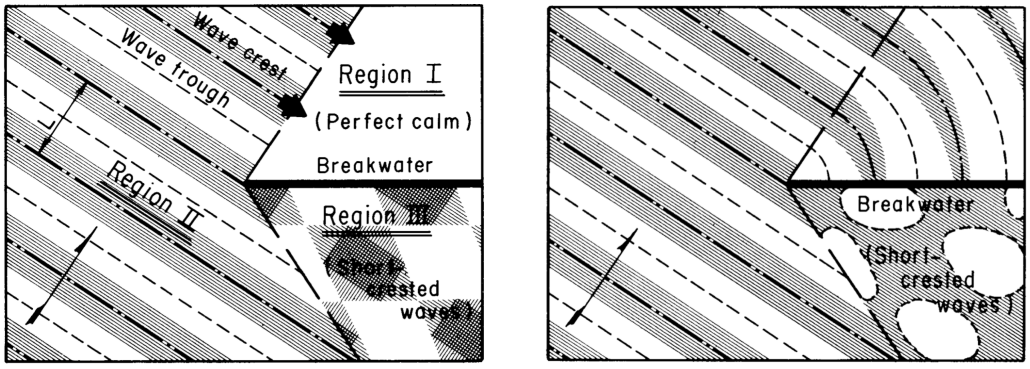

(a) No diffraction

(b) Diffraction effects

Figure 2.1: Straight, long-crested wave incident on a breakwater (Coastal Engineering Research Center, 1984)

To obtain information about the degree of protection of the shadow zone by the breakwater, diffraction effects should be addressed. Diffraction can also be important when assessing harbour siltation or resonance (Coastal Engineering Research Center, 1984). Many studies have been performed to predict the effects of diffraction. Several assumptions have been made to do so:

- Water is an ideal fluid, i.e. inviscid and incompressible
- Waves are of small amplitude and can be described by linear wave theory
- Flow is irrotational and conforms to a potential function satisfying the Laplace equation
- Depth shoreward of the breakwater is constant

When the last condition is not valid, also refraction effects should be analysed. Penny & Price (1952) published a methodology for calculating the diffraction coefficient (K_d) for monochromatic waves due to interaction with a semi-infinite breakwater. It showed that the Sommerfeld's solution (based on the velocity potential theory) was also to apply on water waves. It formed the initiation of wave height estimation behind breakwaters by making use of diffraction diagrams. Goda et al. (1978) presented several diffraction diagrams

for a semi-infinite breakwater and a breakwater gap in the case of normal incidence of directional random waves. This pattern depends on the B/L ratio, which is the ratio of the breakwater gap width over the wave length. In addition, it depends on the maximum directional concentration parameter (s_{max}), indicating the directional spreading of the incoming wave field.

The angle of incidence of a wave train directly affects the diffraction patterns, since the majority of wave energy travels in this direction. An approximate estimation of wave diffraction can now be made by rotating the breakwater axis in the diagrams corresponding to normal incidence while keeping the coordinate axes at their original positions (Goda, 2000). The equivalent breakwater gap width (B_{eq}) should now be computed, which can be done using the method given in Figure 2.2.

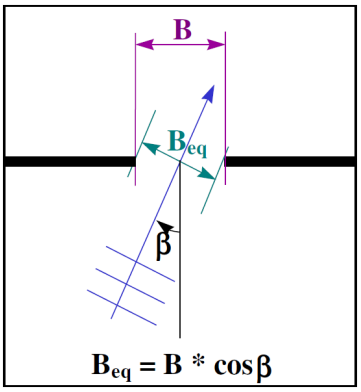

Figure 2.2: Determination equivalent breakwater gap width (Rijksinstituut voor Kust en Zee, 2004)

To give an idea of a diffraction diagram, both a diagram for normal incidence and oblique incidence are given in Figure 2.3. The contours represent lines of equal wave height, where its value represents the diffraction coefficient. The diffraction coefficient (K_d) is defined as the ratio of the diffracted wave height (H_d) to the incident wave height (H_i).

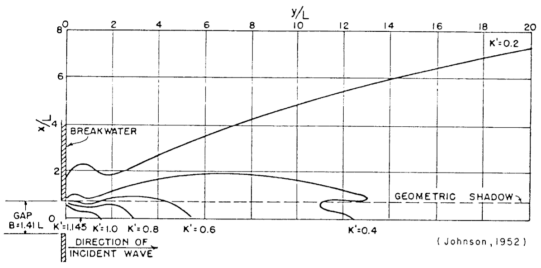

(a) Normal incident waves, $B = 1.41L$

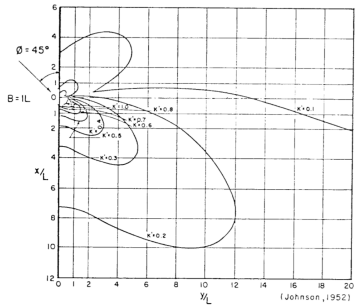

(b) Oblique waves at an angle of 45°, $B = L$

Figure 2.3: Two examples of diffraction diagrams for breakwater gaps (Coastal Engineering Research Center, 1984)

Diffraction tables have been established in Rijksinstituut voor Kust en Zee (2004), based on the diffraction diagrams in the Shore Protection Manual (Coastal Engineering Research Center, 1984). These tables can be found in Appendix B, which are given for both semi-infinite breakwaters as for breakwater gaps, for s_{max}-values of 10 (wind waves) and 75 (swell with medium to long decay distance). Breakwater gap diffraction tables additionally are divided into tables corresponding to different B/L ratios (1, 2, 4 and 8). When diffraction coefficients for other B/L ratios are needed, it is possible to interpolate linearly between two values using Equation 2.8. The subscripts l and g indicate values in the diffraction diagram with a lower B/L ratio and a greater B/L ratio.

$$K_d = K_{d,l} + \frac{BL - BL_l}{BL_g - BL_l} \cdot (K_{d,g} - K_{d,l}) \tag{2.8}$$

When the B/L ratio is lower than 1, the diffraction table for $B/L = 1$ can be used, resulting in a conservative value. When the breakwater gap is larger than five times the wave length, diffraction diagrams for two separate semi-infinite breakwaters may be considered, as diffraction effects resulting from each of the breakwaters are nearly independent of each other (Coastal Engineering Research Center, 1984).

To determine the diffraction coefficient at a specific location, its x- and y-coefficient with respect to the wave length should be known. For a semi-infinite breakwater, the x-y coordinate system has its origin at the breakwater tip. The origin of the x-y coordinate system for a breakwater gap is located in the middle of the gap. The y-axis runs parallel to the incident wave direction and the x-axis is perpendicular to the y-axis. In Figure 2.4, the coordinate system used in the diffraction tables is visualised for both situations. The arrows indicate the positive direction of the respective axis (for a breakwater gap the values are simply mirrored).

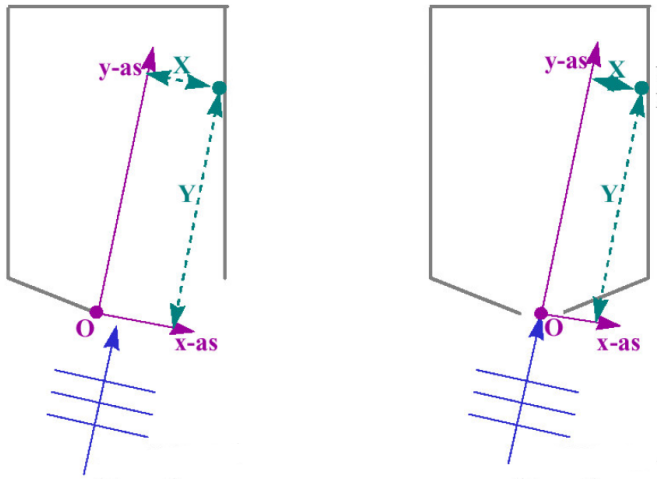

Figure 2.4: Coordinate system definition for a semi-infinite breakwater (left) and a breakwater gap (right) (Rijksinstituut voor Kust en Zee, 2004)

The wave length used to determine diffraction coefficients can assumed to be equal to the deep water wave length at the location of the harbour entrance, since this results in a conservative value (Rijksinstituut voor Kust en Zee, 2004).

2.3.3. Reflection

Water waves can either be reflected totally or partially and can often be as important as diffraction when considering the wave climate in a harbour. When wave reflection occurs, wave energy is reflected instead of dissipated. Many reflections inside a harbour and absence of sufficient energy dissipation may lead to a buildup of energy, appearing as wave agitation or surging inside the harbour (Coastal Engineering Research Center, 1984). Wave agitation in turn may lead to excessive motions of moored vessels and by doing so it also gives rise to operational downtime. It is therefore of importance that quay walls and breakwaters dissipate rather than reflect incident wave energy.

The degree of wave reflection can be expressed by the reflection coefficient (K_r), which is the ratio of the reflected wave height (H_r) to the incident wave height. A reflection coefficient of 1 corresponds to total reflection and 0 to no reflection. The part of the wave energy that is not reflected is not necessarily dissipated by the structure, since wave energy can also be transmitted through the structure (see Section 2.3.4). Wave reflection depends on many factors, such as the relative depth of the structure site, the slope, the permeability of the structure and the wave steepness. In case of a container berth, a berthed vessel can have a large impact on the wave agitation inside the harbour, dependent on the relative depth of the vessel, the type of vessel, a.o.

Some typical ranges of reflection are given in Table 2.3. It can be seen that the effect of reflection against a quay wall is of larger importance than reflection against a rubble-mound breakwater.

As relatively simple harbour geometries can already induce complex wave agitation patterns when accounting for reflection, and since wave height limits for the occurrence of downtime in the conceptual design phase

Type of structure	K_r
Vertical wall with crown above water	0.7~1.0
Vertical wall with submerged crown	0.5~0.7
Slope of rubble stones (slope of 1 on 2 to 3)	0.3~0.6
Slope of energy dissipating concrete blocks	0.3~0.5
Vertical structure of energy dissipating type	0.3~0.8
Natural beach	0.05~0.2

Table 2.3: Typical ranges of reflection coefficients (Helm-Petersen, 1998)

cannot incorporate for this, it is chosen to only consider incoming waves in this report.

2.3.4. Transmission and overtopping

Wave transmission is a phenomenon in which a part of the wave energy of a wave field penetrates through and over a structure, generating waves behind it. Especially when dealing with low-crested breakwaters, wave transmission can have a large impact on the wave climate inside a harbour. The transmission coefficient (K_t) can be defined as the ratio of the transmitted wave height (H_t) to the incident wave height. Briganti et al. (2004) developed a formula for calculating the transmission coefficient, which is given in Equation 2.9.

$$K_t = \begin{cases} -0.4\frac{R_c}{H_{si}} + 0.64\left(\frac{B_{crest}}{H_{si}}\right)^{-0.31}(1-e^{-0.5\xi}) & \text{for } B_{crest}/H_i < 10 \\ -0.35\frac{R_c}{H_{si}} + 0.51\left(\frac{B_{crest}}{H_{si}}\right)^{-0.65}(1-e^{-0.41\xi}) & \text{for } B_{crest}/H_i \geq 10 \end{cases} \tag{2.9}$$

where:

R_c = freeboard crest height (m)

H_s = significant wave height (m)

B_{crest} = crest width (m)

ξ = surf similarity parameter (-) = $\frac{\tan\alpha}{\sqrt{H_s/L_0}}$

The freeboard crest height (R_c) is dependent on the wave climate at the site location. A fairly straightforward way to determine this height is by making use of overtopping criteria for the breakwaters. As a prediction suffices, a mean value approach is applied. The corresponding formula can be found in Equation 2.10 (EurOtop, 2018).

$$\frac{q}{\sqrt{g \cdot H_s^3}} = 0.09 \cdot \exp\left[-\left(1.5\frac{R_c}{H_s \cdot \gamma_f \cdot \gamma_\beta}\right)^{1.3}\right] \tag{2.10}$$

where:

q = mean overtopping discharge (l/s per m)

γ_f = roughness factor (-)

γ_β = influence factor for oblique wave attack (-) = $1 - 0.0063|\beta_w|$ for $0° \leq |\beta_w| \leq 80°$

β_w = angle of wave attack (°)

Tolerable mean overtopping discharges depend on the amount of acceptable damage to the breakwater, facilities located behind the breakwater and the presence of rear-side protection. For significant wave heights larger than 5.0 m, the tolerable mean overtopping discharge is equal to 1 l/s per m, when no damage is allowed. When the rear side of the breakwater is protected, the tolerable mean overtopping discharge can be 5-10 l/s per m (EurOtop, 2018).

To make sure that construction can take place from the land, a minimum freeboard crest height should always be present. This height should ensure that the top of the core layer is located at least 0.5 m above HAT.

2.4. Breakwater cross-sectional design

The model which is in development at Arcadis, works out a cross-sectional design of a breakwater section using a parametric model. To be able to integrate the breakwater layout model with this model, it is relevant to know how the model works and what output it generates that might be of use.

The model focuses on conventional rubble-mound breakwaters and rubble-mound breakwaters with a wave wall or crest element. In Figure 2.5, a conventional rubble-mound breakwater is highlighted including the main dimensions, which are also used in the parametric model.

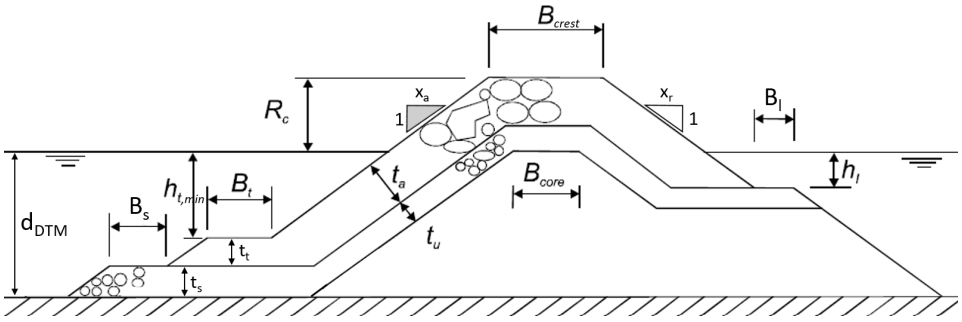

Figure 2.5: Conventional breakwater dimensions (provided by Arcadis)

Cross-sections can be determined at predefined points along the breakwater length. The breakwater alignment needs to be put in using coordinates. The hydrodynamical section within Arcadis provides input data for the model regarding wave and tidal conditions. As the performance of the model is largely dependent on the accuracy of the input conditions, the model could be used in any design phase.

Using the input parameters as illustrated in Figure 2.5, the model calculates several crucial points within the breakwater section to base a technical drawing on. Calculations are based on the failure modes and corresponding limit states. Resulting points are given in Figure 2.6. The top of the core is not always positioned at MSL, as is the case in the figure.

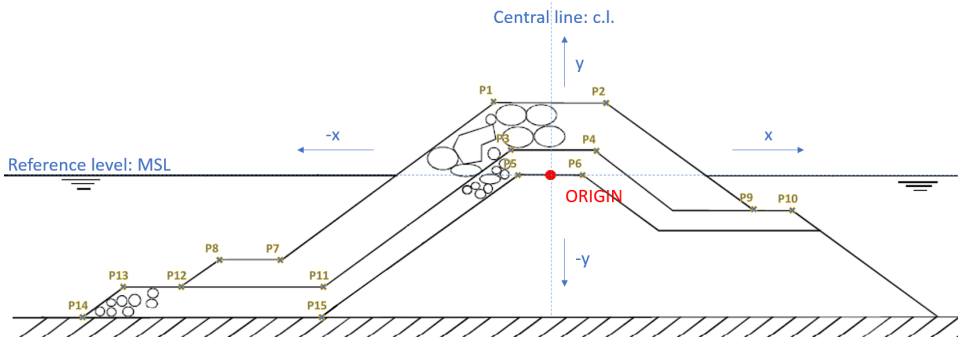

Figure 2.6: Cross-sectional output points (provided by Arcadis)

At this moment, the model can give many relevant design parameters of interest for the breakwater layout, such as the freeboard crest height and crest width of the breakwater. Also transmitted wave heights, by making use of the formula by Briganti et al. (2004), and overtopping rates are computed by the model. Calculating the corresponding costs and material volumes is not possible yet, but will be in the near future. Also the step towards a technical drawing still needs to be made, although all relevant conditions are already present within the model.

2.5. Littoral transport and sedimentation

Littoral transport is defined as the movement of sediments in the nearshore zone by waves and currents (Coastal Engineering Research Center, 1984). Both longshore and cross-shore transport can be discerned. Dominant longshore currents in the surf zone are generated by waves breaking oblique to the shoreline (Sorensen, 1997). Port construction distorts the equilibrium sediment transport of the area, inducing a change in the coastline on the onshore side of the breaker line. In addition, sediment transport may function as a source for harbour siltation and may lead to a decrease in navigability in the approach channel.

The total sediment budget and the character of its distribution across the surf zone largely depend on the grain size distribution and on bed topography (Rytkönen, 1987). Since homogeneous soil conditions and a constant bed slope are considered for this report, the character of the sediment transport distribution is fairly predictable and is mainly determined by the bed slope. In Figure 2.7, a schematic plan view of the nearshore zone is visualised with waves approach at an angle to the shoreline, also including the longshore current velocity distribution (and therewith its corresponding sediment transport distribution).

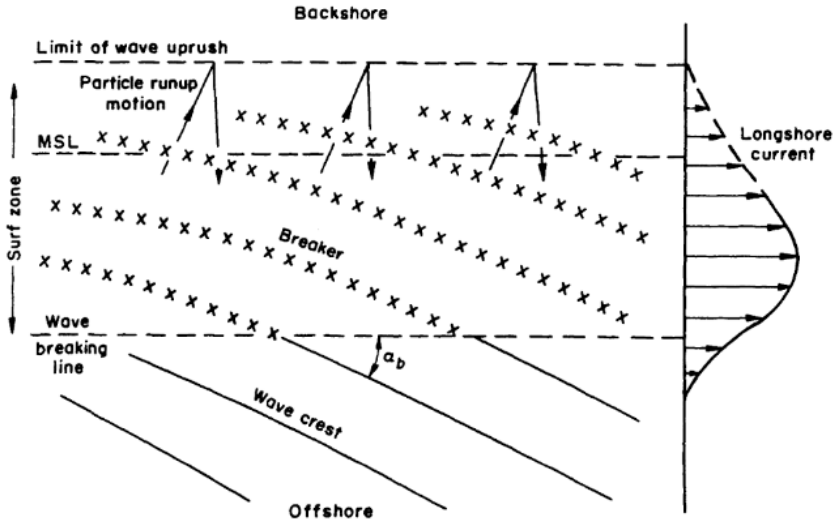

Figure 2.7: Wave-generated longshore current velocity distribution (Sorensen, 1997)

It can be seen from Figure 2.7, that most of the wave-generated longshore sediment transport is confined within the surf zone (on the onshore side of the breaker line). Due to the variability of wave approach, longshore transport direction can vary from time to time, although typically a single direction is dominating. This means that when constructing a breakwater at one side of a port, some form of sediment blocking may also be required on the other side of the port, to prevent sedimentation inside the port.

To avoid sediments passing by the harbour entrance (and therewith enhancing harbour siltation), it is advised to extend the breakwater perpendicularly until the breaker line, indicating the point where waves start breaking. To give an approximation of the required breakwater length in the direction perpendicular to the coastline, the criterion of Miche (1944) is used. Corresponding expressions are given in Equation 2.11.

$$\begin{aligned} \left(\frac{H}{L}\right)_{br} &\approx 0.14 && \text{for } d/L > 0.5 \\ \left(\frac{H}{L}\right)_{br} &= 0.14 \tanh\left(\frac{2\pi d}{L}\right)_{br} && \text{for } 0.04 < d/L < 0.5 \\ \left(\frac{H}{d}\right)_{br} &\approx 0.88 && \text{for } d/L < 0.04 \end{aligned} \tag{2.11}$$

where:

H_b = significant wave height at breaking point (m)

L_b = wave length at breaking point (m)

d_b = water depth at breaking point (m)

As stated in Section 1.3.2, only some rough approximations are made for sedimentation inside the harbour, as sediment-related issues require a large amount of site-specific data and modelling techniques to be able to give reliable estimates. An annual siltation thickness (t_s), defined as the ratio of the yearly siltation volume and the harbour basin area, is used to come up with these approximations. van Rijn (2016) states that siltation thickness is mainly influenced by three parameters: the cross-sectional harbour entrance area below MSL, the yearly-averaged sediment concentration outside of the harbour basin and the density difference between the water contained in the harbour basin and outside of it. As freshwater discharge and thermal mixing are not treated, the main comparison that can be made between layout alternatives at the same location is through its entrance area and through the presence of a secondary breakwater. The latter effect is in this case related to blocking of longshore sediment transport and requires a secondary breakwater that stretches out at least until the breaker line. Following van Rijn (2016), the annual siltation thickness is relatively large in conditions with relatively large density current effects (0.5 to 1 m), and relatively small in conditions with no or minor density currents and low sediment concentrations (0.1 to 0.3 m). As density currents are not considered, it can be stated that siltation thicknesses generally are in the range of 0.1 to 0.5 m, mainly depending on the sediment concentration.

2.6. Optimisation methods

In this section, a selection of possible methodologies for the optimisation problem is treated, so that a well-founded choice can be made on which method is most suitable to use for the existing problem.

2.6.1. General

The objective of optimisation is to find the best solution to a problem within a predetermined set of constraints (Rustell, 2016). This usually is a complex task, since a wide range of inter-related factors needs to be considered (Rustell, 2016). An optimisation problem is solved by minimising a cost or objective function that corresponds to the physical criteria that need to be optimised. Optimisation methods can be divided into deterministic and stochastic approaches. Deterministic refers to variables being uniquely determined by other variables and previous states of these variables, whereas stochastic variables can also be random or being described by a distribution (Renard et al., 2013). In optimisation, the goal can be to find a local optimum, when this is good enough, or to find a global optimum, which is the case for an optimal breakwater layout. Several possible global optimisation methods are shown in Figure 2.8.

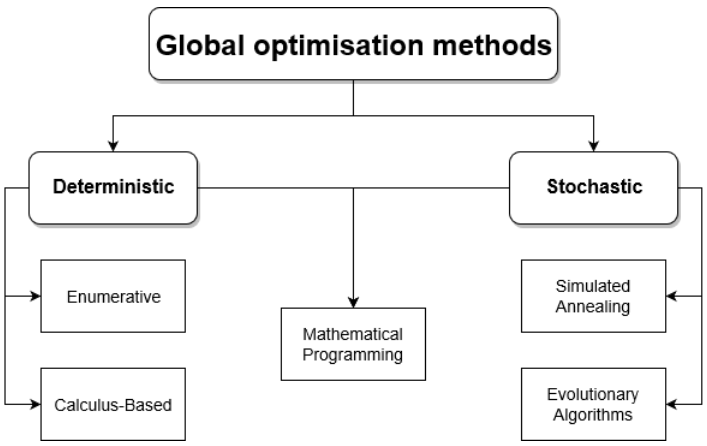

Figure 2.8: Global optimisation methods

2.6.2. Brute force

Probably one of the most straightforward optimisation methods is to use brute force. This method can be considered enumerative, as each possible solution in a defined finite search space is evaluated, after which the best one is selected. For breakwater layout optimisation, this would typically entail a grid of possible locations for each breakwater node and checking all combinations per location. Probabilistic techniques can be included when evaluating all possible alternatives. As many real-world problems are computationally intensive, some means of limiting the search space must be implemented to find 'acceptable' solutions in 'acceptable' time (Coello Coello et al., 2007). The problem needs to remain small, as the number of possible states of the system increases exponentially with the number of dimensions. Also step sizes for each variable describing a solution need to be limited, as a considerable amount of computational power is required otherwise. Nevertheless, for discrete systems, every possible solution is checked.

2.6.3. Calculus-based optimisation

Root-finding algorithms, an example of a calculus-based method, estimate values of x iteratively until $f(x) = 0$ is found. They are easy to implement and their history ranges back thousands of years. Rustell (2013) applied a root-finding algorithm (Brent's algorithm, a combination of several root-finding algorithms) for the optimisation of a detached breakwater layout of an LNG-terminal. The result was a solution within 10% accuracy (in the worst case) and a runtime less than ten seconds (after an hour of preparation). Nevertheless, this was only possible because Rustell defined a one-dimensional problem, only optimising on length to reach the desired level of berth availability.

The problem as defined in Section 1.2 is a multi-dimensional problem, as apart from length also the orientation of the breakwater forms an important optimisation parameter, the water depth varies over the breakwater length and possibly even more parameters need to be optimised. Multivariate calculus-based optimisation algorithms are also available, however they can get very complex, since usually matrices of second order derivatives to the objective function(s) are required. Sometimes analytical expressions to second order derivatives are fairly easy to obtain, but most of the time this is very complicated for real-world problems. Obtaining numerical expressions is another option, however this requires a large amount of computational power. Nevertheless, multivariate calculus-based optimisation methods are deterministic, thus guaranteeing they find the best solution to the problem.

2.6.4. Simulated annealing

Simulated annealing (*SA*) is a probabilistic method for finding the global optimum of a cost function that may possess several local optima (Bertsimas & Tsitsiklis, 1993). The name origins from the simulation of the annealing process of heated solids. It is based on hill-climbing, a deterministic method that searches in the direction of steepest ascent from the current position in an objective function. The difference is that *SA* chooses a random move from the current position, which does not have to be in the direction of steepest ascent. A move which is better than the current position is always accepted, whereas a worse move is accepted based on some probability. Allowing for worse moves sometimes makes it possible to escape from local optima. The probability that an *SA* accepts a worse move decays exponentially over time, leading to the same behaviour as a hill-climbing algorithm and ultimately to a steady state.

Although *SA* tends to escape local optima, finding a global optimum is not that straightforward, as it is difficult to reach the right neighbourhood when only tracking a single solution. This method is however easy to implement for many problems and can lead to little computational costs when compared to other stochastic methods.

2.6.5. Genetic algorithms

A genetic algorithm (*GA*) is a type of evolutionary algorithm, a term for a collection of stochastic search methods computationally simulating the natural evolutionary process (Coello Coello et al., 2007). *GA*'s are based on Darwin's theory of natural selection, that operates on a population of potential solutions to produce better approximations to an optimal solution (Elchahal et al., 2013). New individuals (potential solutions) are

produced by means of natural evolutionary processes, like selection, crossover and mutation. The associated fitness of a certain individual determines which survive into the next generation.

GA's are especially applied in cases when both discrete and continuous domains are involved in the search space, when the objective function(s) or constraints lack regularity or when a large number of local optima can be discerned (Elchahal et al., 2013). Doing so, (nearly) optimal solutions can be found to global optimisation problems. *GA*'s are mostly used in the conceptual design phase and are of good use when constraints are easily defined (Rustell, 2016).

GA's are able to find solutions for all objective functions that can be represented numerically and are therefore highly robust. Besides, they can be easily hybridised with other Machine Learning tools and can produce multiple optimal solutions in a single run (Rustell, 2016). However, there is no guarantee that an optimal solution will be found and the method is computationally expensive. In addition, mutation and crossover parameters are difficult to define, as these parameters are highly problem specific (Rustell, 2016).

2.6.6. Artificial neural networks

The application of artificial neural networks (*ANN*'s) is increasing fast, since computational power is growing exponentially. They consist of an input layer and an output layer, with several hidden layers in between. When both in- and output are known (requiring large, varied and comprehensive data sets), an *ANN* is able to determine the relations in between. The hidden layers can be represented as a 'black box', since the processes that happen here are unknown. Using the retrieved relations between in- and output, an input layer of neurons can be passed through the 'black box' to produce an output. A high degree of accuracy can be reached, often outperforming other modelling processes (Rustell, 2016). The structure of an *ANN* is shown in Figure 2.9.

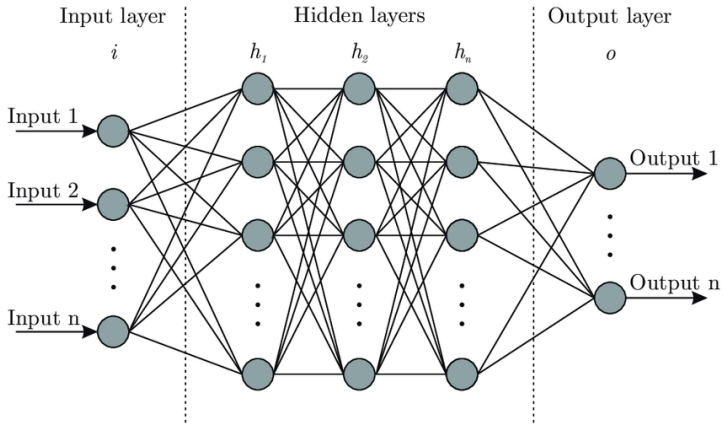

Figure 2.9: Artificial neural network structure (Bre et al., 2017)

An *ANN* consists of many neurons, where each neuron has its own weighted inputs, transfer function and one output. They typically use gradient-based methods to develop the weighting for the neurons. As the weights are adjustable parameters, a neural network is a parameterised system (Agatonovic-Kustrin & Beresford, 2000). The weighted sum of the inputs constitutes the activation of the neuron. As *ANN*'s can be automated, little user involvement is required. Computation times are fast, which makes it an often used method for computationally expensive functions (Rustell, 2016). Data sets are however difficult to obtain in such large and varied amounts. Besides, *ANN*'s are mostly used for pattern recognition rather than for optimisation problems.

3. Optimisation

To be able to choose a suitable optimisation method for breakwater layout comparison from those described in Section 2.6, it should be clear what the model has to do and what characteristics would define a simple and efficient process. Therefore, the results that are required as output from the model need to be determined, which is done in Section 3.1. In addition, optimisation of the breakwater layout requires elaboration, so that the choice of optimisation method matches the desired characteristics of such a method. This is discussed in Section 3.2. Following this, the selection of the optimisation method is performed (Section 3.3). Using this method, both the methodology (Chapter 4) and the set-up of the parametric model (Chapter 5) can be established.

3.1. Required results

Since the primary function of a breakwater for a port is to protect it against currents and waves (see Section 1.1), its performance can be expressed in the downtime resulting from excess wave and current conditions. As local flow patterns are not treated within the research scope (see Section 1.3.2) and since in most cases wave limitations dominate currents inside the port, it is assumed that the breakwaters only affect wave patterns. As treated in Section 2.2, in the conceptual design phase it is possible to make approximations for resulting downtime based on acceptable wave heights only. Consequently, limiting wave heights at several locations in the port should be defined and related to resulting acceptable downtime by the user, so that total downtime can be computed by the probability of exceeding these limits.

The model objective is to find the most economical breakwater layout, resulting in a minimal amount of downtime. To be able to relate to downtime efficiently, it should be quantified in monetary terms. As an economical port analysis is already performed when a breakwater layout model should come into place (see Section 1.1), the user should be able to give the resulting costs per hour of downtime. The breakwater is valued in the capital expenditures (CAPEX) and operational expenditures (OPEX) coming along with it. These can be divided into direct costs (relating to the breakwater itself) and indirect costs (relating to factors influenced by the breakwater layout).

	CAPEX	**OPEX**	**Other**
Direct costs	Breakwater construction	Breakwater maintenance	-
Indirect costs	Capital dredging/filling Land costs	Maintenance dredging	Downtime costs

Table 3.1: Required cost output

Breakwater construction	Material unit prices, influenced by transport, production and construction, multiplied by the breakwater material volumes. These volumes are influenced by main layout parameters as breakwater length and breakwater height per length step.
Breakwater maintenance	Usually only a small part of the breakwater construction costs per year.
Capital dredging/filling	Including approach channel and manoeuvring basins, even as the infill of land and possible disposal of dredged material.
Land costs	Determined by the stretch of coastline that is required for terminal or breakwater construction.
Maintenance dredging	Operational costs related to dredging activities caused by harbour siltation.
Downtime costs	Direct result of operational and navigational downtime occurring in the port.

To compare CAPEX and OPEX with each other, the OPEX have to be capitalised in some way. This can be done by discounting the OPEX with a rate r over the design lifetime of the breakwater (T_L). The result is the present value of the CAPEX and OPEX (C_c). The corresponding equation is given in Equation 3.1.

$$C_c = CAPEX + \sum_{t=1}^{T_L} \frac{OPEX}{(1+r)^t} \tag{3.1}$$

Regarding downtime, resulting costs can be estimated when it is known what are the costs per hour of waiting time if a vessel is unable to either (un)load at one of the berths or sail in/out of the port. Besides waiting costs, also other costs apply, such as those related to port competition, demurrage and legal penalties. These factors are however highly site specific (see Section 2.2.3), making it difficult to incorporate for these in such a generic model. To keep the amount of input parameters to a minimum and to focus on the economical balance rather than the exact computation of downtime costs, it has been chosen to make downtime costs fully dependent on the waiting costs caused by operational and navigational downtime. This is elaborated in Section 4.2.2.

3.2. Output optimisation

The optimal breakwater layout is defined as the layout alternative resulting in an optimal balance between CAPEX and OPEX (C_c) and downtime costs (C_d). To arrive at this balance, the costs can best be visualised in a graph, which is done in Figure 3.1.

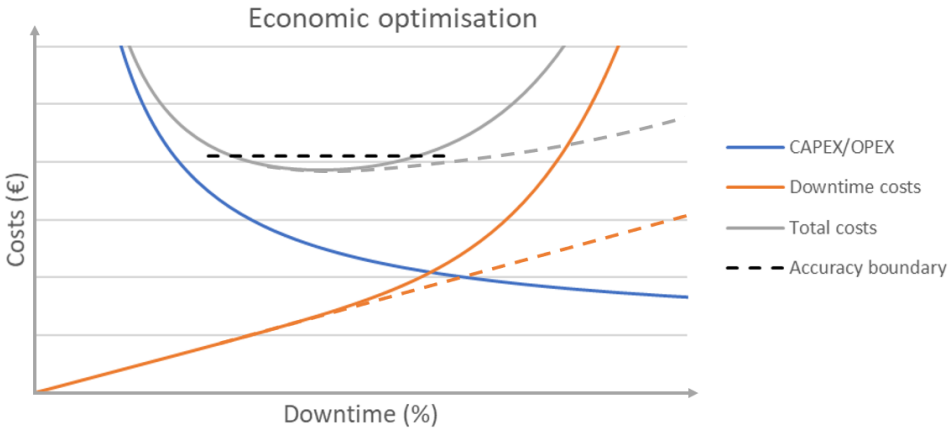

Figure 3.1: Economic breakwater layout optimisation

CAPEX and OPEX are high for lower downtime values, as this would imply a longer breakwater to provide more shelter from waves. Costs for dredging, filling and disposal, which are also included in the CAPEX and OPEX, do not have a considerable dependency on downtime (it only has a minor effect on it). Downtime costs increase linearly, until port competition starts playing a role, resulting in a rapid increase for higher downtime values due to the impact of (frequently) not meeting the tight scheduling requirements (typical for container shipment). The effect of port competition is however not included in this study, as it is highly site specific for a global assessment and likely does not have a large impact on the position of the optimum zone (see Section 2.2.3). The resulting change in the economic optimisation graph when leaving out the effect of port competition is visualised by the dashed lines (grey and orange) in Figure 3.1. Model results are therefore expected to approach the dashed lines. Other costs than the ones mentioned above are assumed to be equal for all layout options. The economic optimum corresponds to the point of lowest total costs and should be approached as closely as possible. It is however not possible to exactly find this point in the conceptual design phase, due to the uncertainties mentioned in Section 1.1. Therefore, all breakwater layout alternatives that are located below the black dashed line in Figure 3.1 suffice. Valid points should generate a breakwater layout that guarantees an accuracy of at most 30% (as defined in Section 1.1) with respect to the exact optimum. The difference between the black dashed line and the economic optimum is however less than 30%, as model uncertainty only forms a part of the total uncertainty that is present in the conceptual design phase. The

exact difference depends on the uncertainties that are present in the specific project. A sensitivity analysis should point out if this accuracy has been reached (see Chapter 8).

Breakwater layout alternatives are optimised based on monetary evaluation, as can be seen in Figure 3.1. This results in an objective type of scoring when compared to a numerical evaluation type such as a multi-criteria analysis. However, it can be more time-consuming and difficult, partly due to the necessity to express qualitative differences in money (Ligteringen & Velsink, 2012). For qualitative evaluation criteria, one can think of aspects like nautical safety, construction time, sustainability and design flexibility. There are several ways to account for these criteria. One of these is to perform a risk analysis, though this can only be integrated within the parametric model when specific probabilities of events (such as ship collisions) and their consequences (in monetary terms) are known. As these parameters are highly site-specific, this option is not chosen. Another way to account for qualitative evaluation criteria is to incorporate them in the boundary conditions of the parametric model. This can be done for nautical safety, by taking a conservative length of the part of the approach channel that needs to be sheltered by a breakwater as a boundary condition. This value is then fully dependent on the input parameters, such as cross-current speeds and tugging time (see Section 2.1.3). Construction time and design flexibility are however harder to grasp within the boundary conditions. These criteria can be included by means of a third alternative, which is to integrate them within the model. The model could be programmed such that it accounts for possible future developments of the port (thus dealing with design flexibility), like the construction of new berths to cope with increased demand. Construction time can be handled by considering construction phasing within the model, which can be done by relating constructed breakwater segments to the corresponding amount of operable berths.

The optimum breakwater layout generates the minimum total costs. Optimisation can take place by defining one or more objective functions and minimising them. For the conceptual design phase, it is advised to use multiple objectives, as they are able to consider a wider range of alternatives and give a more realistic representation of the problem (Rustell, 2016). Representing the design problem as a single objective leads to convergence to a single solution, based on the initial decisions of the user, which can therefore be subjective and does not guarantee optimality of individual objectives (Rustell, 2016). It should therefore be beneficial to separate the total costs into various objectives and possibly add qualitative evaluation objectives to it. To visually see and explore the trade-offs between different objectives, a so-called Pareto front can be established. Alternatives are considered Pareto optimal when they cannot be improved in one objective without compromise in at least one other (Rustell, 2016). Based on Figure 3.1, a Pareto front is established for the objectives 'CAPEX/OPEX' and 'downtime costs'. The result can be seen in Figure 3.2.

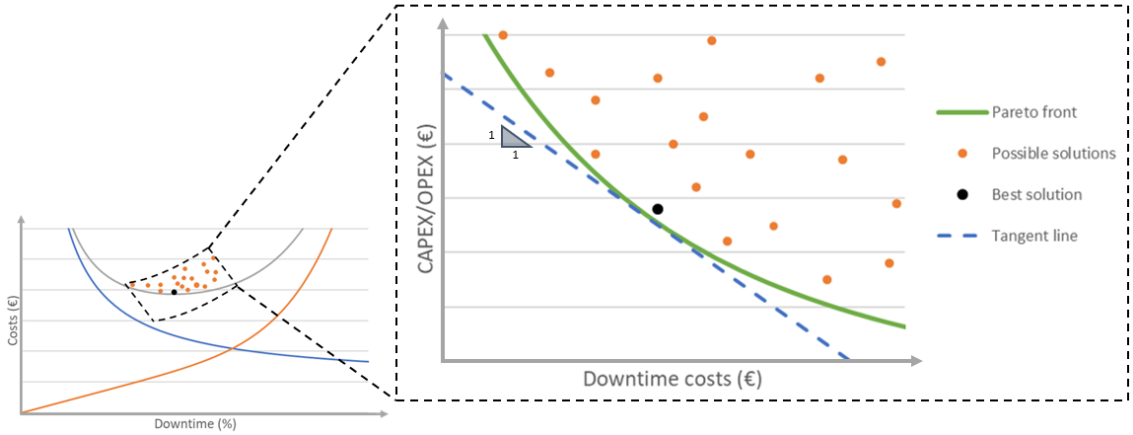

Figure 3.2: Pareto front for the problem with two objective functions

Each solution (possible breakwater layout configuration) associated with a point on the Pareto front is a vector of decision variables whose components represent trade-offs in the Pareto solution space (Coello Coello et al., 2007). On the Pareto front in Figure 3.2, CAPEX/OPEX cannot be decreased without increasing the downtime costs, the same holds the other way around. Solutions that are located on the Pareto front are called Pareto optimal solutions. In case both objectives are weighted equally, the best solution lays on the

Pareto front, at the location having a tangent line at an angle of 45°. The best solution for the set of possible solutions in Figure 3.2 is indicated by the black dot. It must be stated that the comparison of the economic optimisation graph and the Pareto front is only meant to clarify the concept of the Pareto front. The grey line (indicating total costs) is not the same as the green curve representing the Pareto front.

3.3. Method evaluation

In Section 2.6, several possible methods for the economic optimisation of breakwater layouts are discussed. A comparison is made between these methods, based on several aspects, taking into account the criteria resulting from the research question (see Section 1.3.1). Therefore, the chosen method should preferably be simple, computationally inexpensive and feasible. Most importantly, the method should be robust, having low failure rates, converge sufficiently and is able to escape local optima. It is therefore preferential if prior research has been performed successfully.

Brute forcing has a 100% chance of finding the best solution within the defined search space, having an accuracy equal to the applied step size within the decision variables that define the solution. As the problem is quite complex, the brute forcing algorithm however gets highly inefficient, doing more work than necessary, as it calculates all possible solutions which requires a large amount of computational power. This often leads to non-feasible problems.

Multivariate calculus-based optimisation algorithms also guarantee the best solution to a problem and significantly reduce the amount of solutions it has to calculate when compared to brute forcing. They behave well for many variables and smooth objective functions, however they tend to converge to local optima. This can be mitigated partly by choosing several starting points, however it still relies on luck whether to find the global optimum. Second-order derivatives can lead to less iterations within the algorithm, however they require more computational power since they are very complex to obtain. Complex fitness landscapes (due to constraints or choices within the model) are not well suited for calculus-based algorithms.

Simulated annealing has, due to its stochastic nature, the ability to find the global optimum within a search space. It is quite robust, however there still remains uncertainty whether a global optimum is found, as the single solution that is tracked possibly needs to escape many local optima. This uncertainty increases with more complex fitness landscapes.

Genetic algorithms can consider large search spaces and complex fitness landscapes, as solutions can be implemented in parallel to each other. Still, *GA*'s cannot guarantee an optimal solution, but due to the parallel implementation of solutions, the chance of approaching the optimal solution is higher than for *SA*. *GA*'s are fairly easy to program, however tuning the optimisation parameters of the model can be difficult.

Artificial neural networks do have many advantages, since they are fast, automated and can achieve solutions that approach the global optimum closely. It is however difficult or even impossible to obtain the extensive data sets that are necessary to let the network learn from itself, since a substantial amount of breakwater layout project results are necessary to recognise patterns between the in- and output.

All different optimisation methods are evaluated based on several mentioned criteria. Scores are given, where '– –' corresponds to very little agreement with the criterion and '++' corresponds to excellent agreement. All scores are given in comparison to the scores of the other optimisation methods. The scores per optimisation method are given in Table 3.2.

	Brute forcing	**Calculus-based**	**SA**	**GA**	**ANN**
Global optimum	++	–	+/–	+	+
Computational costs	– –	–	+/–	+	++
Feasibility	– –	+/–	++	++	– –
Robustness	+	–	–	+	++
Simplicity	++	–	+	+	+
Rank	*4*	*5*	*3*	*1*	*2*

Table 3.2: Evaluation optimisation methods (– – = very bad; ++ = excellent)

Both brute forcing and *ANN*'s are not feasible enough to use them within this research, as brute forcing requires too much computational power and *ANN*'s require data sets that cannot be obtained in such vast amounts. Calculus-based methods score too low, mainly due to high complexity in comparison to insufficient robustness. *GA*'s outperform *SA*, as *SA* is basically a *GA* with a population of a single individual. The result is that *GA*'s have a higher chance of encountering a global optimum as solutions can be implemented in parallel, leading to higher robustness. Besides, it is likely that a complex fitness landscape is required to obtain a reliable solution, which can be handled very well by a *GA*. In the unlikely case that *ANN*'s would be feasible, its result would just be the optimal breakwater layout. The output would lack for example downtime information, as this is contained in the hidden layers of the network. Therefore, *GA*'s clearly form the most appropriate optimisation method for the current problem.

Challenges for *GA*'s are to tune the optimisation parameters for selection, crossover and mutation correctly, so that reliable results are obtained in a reasonable amount of time. In addition, a *GA* focuses on robustly finding the right neighbourhood (a certain area in the decision space corresponding to a certain breakwater layout alternative) rather than finding an exact solution. This makes *GA*'s actually more suitable for the conceptual design phase, as it is considered more important to discover the entire domain and choose the best layout alternative rather than exactly generating the optimal layout. The main reason for this is that an exact solution cannot be found yet, as for many parameters only estimations are available. It must also be stated that *GA*'s have a well-established link with the Pareto set, making it possible to investigate the trade-offs between the objective functions.

4. Methodology

To arrive at a well-established balance between the costs and performance of a breakwater layout configuration, as elaborated in Section 3.2, a suitable methodology is required. To put this into place, a top-down approach has been applied, starting with the optimisation objectives (CAPEX/OPEX and downtime costs) and working towards a detailed breakdown into smaller segments. The individual segments are treated within the different sections in this chapter. To start off, a basis for schematisation is given in Section 4.1, that complies with the research objective to compare breakwater layout alternatives in a simple and efficient manner. The complete outline of the methodology proposed in this chapter is given in Figure 4.1.

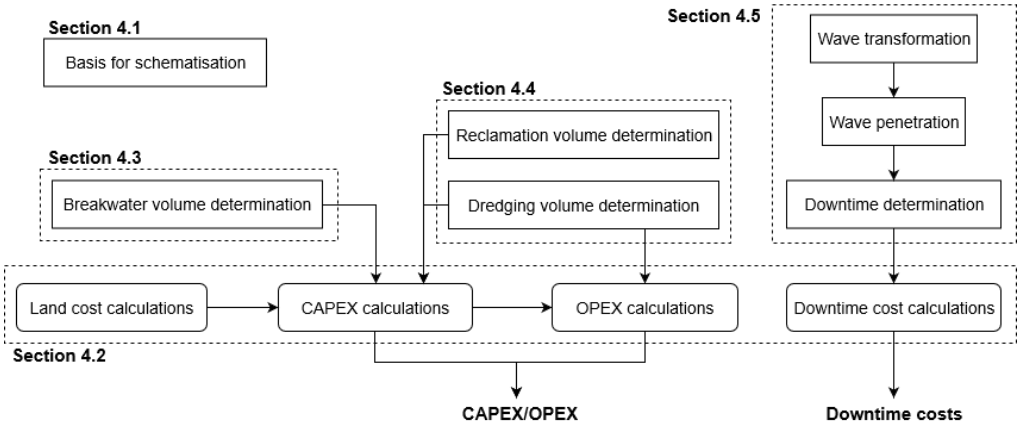

Figure 4.1: Outline of the methodology applied in this research

4.1. Basis for schematisation

Several scope restrictions have been mentioned in Section 1.3.2. To elaborate on these in more detail, some boundary conditions and assumptions are required to obtain a clear and simple model that can serve as a starting point for the problem. In a later stage, these conditions can be modified or even left out, so that more realistic situations can be obtained. Careful attention has been paid to avoiding oversimplification. A schematised breakwater layout has been set up in Figure 4.2, based on both scope restrictions and boundary conditions. As discussed in Section 3.2, there should be accounted for nautical safety within the boundary conditions.

Breakwater configuration

- The principal breakwater is schematised by three segments, of which the first stretches out perpendicularly to the coastline and provides enough space for a berthing basin, as is visualised in Figure 4.2.
- If a secondary breakwater is constructed, it stretches out perpendicularly to the shoreline, minimally until the breaker line (see Section 2.5).

Approach channel

- Vessels approach the port in a straight line with a moderate vessel speed of $2-4$ m/s (see Section 2.1.1).
- The approach channel is to be designed for one-way traffic only (see Section 2.1.1). Vessels cannot pass each other.
- Vessels are assumed to not pose any cargo hazards on the port area or its surroundings (see Section 2.1.1).

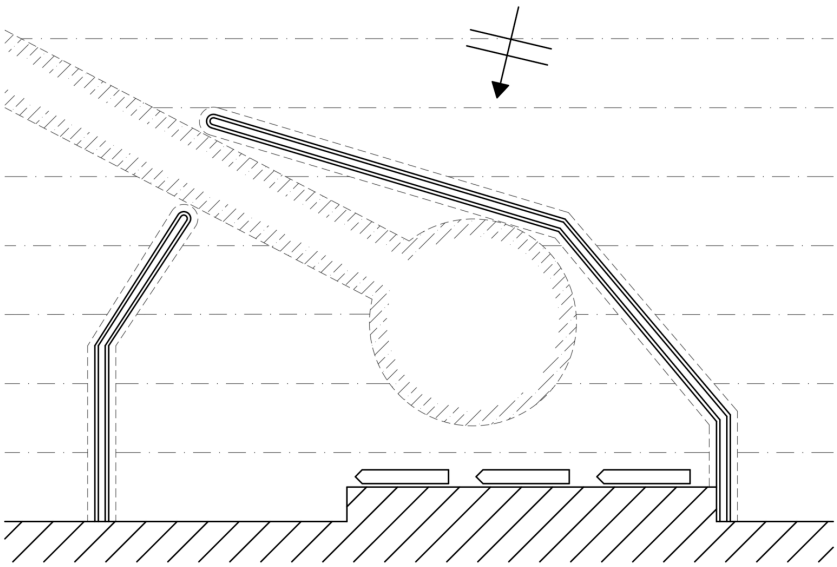

Figure 4.2: Schematisation of breakwater layout applied in this research

- Aids to navigation within and around the port are assumed to be good (see Section 2.1.1).
- There is no tidal window applied for vessels sailing through the approach channel (see Section 2.1.2).
- The sheltered length of the approach channel should be long enough to ensure that vessels can come to a halt safely (see Section 2.1.3).

Harbour basin

- The harbour basin needs to allow space for the required amount of berths, a sheltered approach channel (if necessary), a sheltered turning basin and a small dock for tugboats and pilot boats. It is assumed that a small boat mooring dock can always be located within the sheltered zone, so it is not included in the layout optimisation.
- Tugboats are always used to assist vessels in stopping, turning and mooring.
- Vessels come to a halt within the turning basin.
- Design vessel sizes are equal for all berths (see Section 2.1.6).
- Harbour basin area that needs to be dredged and is not considered as approach channel, turning basin or berthing basin, is schematised by making use of the method described in Section 4.4.2.

Wave penetration

- Regarding wave penetration, the depth in the entire harbour basin is assumed to be equal to the water depth at the harbour entrance. Refraction effects inside the harbour basin are therefore not taken into account (see Section 2.3.1).
- The effect of long waves, local wind-wave generation and passing ships is not considered (see Section 2.3).
- Wave heights at the output locations are based only on the incoming wave field, reflection is not taken into account (see Section 2.3.3).

Downtime

- The design vessel always corresponds to the largest vessel in downtime calculations (see Section 2.2).

- Effects of currents, even as the influence of wave period and direction, are not taken into account (see Section 2.2).
- Downtime is the percentage of time per year that the allowable wave height or wind speed at a certain location within the port is exceeded (see Section 4.5).
- Navigational downtime results in operational downtime at all berths (see Section 4.5).

Breakwater composition

- Breakwaters are schematised as having an armour layer, underlayer and core layer. Toes, crest elements and filter layers are not considered (see Section 4.3). Also excavation activities are not accounted.

Costs

- The only costs that are considered are CAPEX/OPEX and downtime costs, as defined in Section 3.1.
- Downtime costs fully depend on the waiting costs caused by operational and navigational downtime (see Section 3.1), this is elaborated in Section 4.2.2.

4.2. Total cost estimation

As discussed in Section 3.2, breakwater layout is optimised based on CAPEX/OPEX and downtime costs. Both are discussed separately below.

4.2.1. Capital- and operational expenditures

CAPEX/OPEX can be determined using Equation 3.1. The discount rate and the expected lifetime of the breakwater are usually known beforehand. The economic design lifetime of a breakwater is on average approximately fifty years (Secretariat of UNCTAD, 1985). CAPEX can be divided into breakwater construction costs (related to transport, production and construction) and capital dredging costs (related to dredging, filling and disposal). The determination of breakwater construction costs (C_{bw}) is given in Equation 4.1, where material volumes of all layers (armour layer, underlayer and core layer) are multiplied by the corresponding unit rates.

$$C_{bw} = C_{armour} \cdot V_{armour} + C_{under} \cdot V_{under} + C_{core} \cdot V_{core} \tag{4.1}$$

Capital dredging costs (C_{dr}) can be computed using Equation 4.2. Again, this is a multiplication of sediment volumes and corresponding unit costs.

$$C_{dr} = C_{df} \cdot V_{df} + C_{dd} \cdot V_{dd} \tag{4.2}$$

Land costs (C_{land}) are calculated by multiplying the costs per running meter of land by the length of the stretch of land that should be acquired. This length is equal to the distance from the attachment points of both breakwaters to the coast, if two breakwaters are present. If only the primary breakwater exists, this length extends until the other end of the quay wall. The reason to include for land costs is the ability to optimise the position of the secondary breakwater, as this position preferably should be located as close as possible to the terminal to avoid unnecessary costs.

OPEX are approximated by assuming them to be a certain percentage of the corresponding CAPEX. The annual average maintenance costs of a breakwater as a percentage of its current new cost (c_m) can be estimated as a value of 2%, according to Secretariat of UNCTAD (1985).

Section 2.5 gives some directions on the determination of the annual siltation thickness. The user should specify the siltation thickness in case of absence of a secondary breakwater. In addition, siltation thicknesses

should be given for breakwater gap widths larger than 1000 m and for minimum allowable gap width (equal to the length of a design vessel). Consequently, interpolation can take place based on the gap width of the considered layout alternative. Equation 4.3 can be used to compute the corresponding maintenance dredging costs per year ($C_{dr,o}$).

$$C_{dr,o} = t_s \cdot C_{dd} \cdot (A_{ch,in} + A_{tb} + A_{bb} + A_{rest}) \tag{4.3}$$

4.2.2. Downtime costs

The downtime costs can be directly related to the amount of downtime per year per berth, though some more input parameters are required to do so. First of all, it should be known what is the berth occupancy factor (m_b), to be able relate operational hours of a berth to the time that (un)loading activities actually takes place. According to Thoresen (2003), berth occupancy factors are in the order of 0.5 for container terminals (as an average for a terminal having three berths). Nowadays, berth occupancy has increased significantly, leading to average values of 0.6. In addition, the hourly production per berth (P_b) should be known, which is expressed in moves/hr. As costs are usually not given per move, the production units should be transformed to twenty-foot equivalent units (TEU). To do so, the TEU-factor (f_{TEU}) has to be known. Ultimately, the unit rate per TEU (C_{TEU}) should be on hand. The annual downtime costs ($C_{d,o}$) can now be calculated by using Equation 4.4.

$$C_{d,o} = C_{TEU} \cdot m_b \cdot P_b \cdot f_{TEU} \cdot \sum_{b}^{n_b} n_{d,b} \tag{4.4}$$

The effect of port competition, demurrage costs and legal penalties is not included, as stated in Section 3.1. Determination requires many different input parameters, while demurrage costs and legal penalties are independent of the breakwater layout configuration. Furthermore, port competition is expected to induce only small differences between different layout alternatives that are located close to the economic optimum (see Section 3.2). The effect on the location of the optimum itself – within the economic optimisation graph – is therefore envisioned to be minor in comparison to the desired accuracy level.

4.3. Breakwater material volumes

To determine the required volume of the breakwater materials, the cross-section should be schematised firstly. To do so, some general assumptions are made, taking into account the depth-dependency of the cross-section. Figure 4.3 illustrates the schematised cross-section.

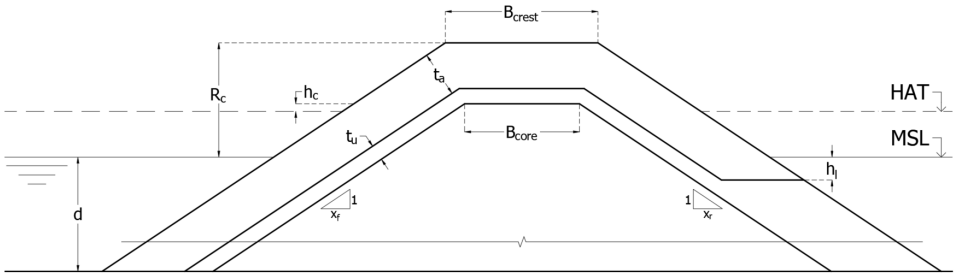

Figure 4.3: Schematic cross-section including dominant parameters and water levels

A conventional multi-layer rubble mound breakwater without superstructure is considered, as defined in PIANC (2016). It can be seen from Figure 4.3 that the amount of dimensions in the cross-section has been drastically decreased when compared to reality, which is the result of some general assumptions. First of all, the cross-section has just been schematised using three layers: a core layer, an underlayer and an armour layer. Other features, like a toe, crest element or filter layer, have been left out for simplicity. This can be done as material volume ratios are only needed to compute the total breakwater costs. A rough approximation

of these volume ratios should therefore suffice for the conceptual design phase. For the same reason, also necessary excavation and replacement activities are excluded. These activities can easily be adopted in the future by accounting for an excavation depth and unit costs for excavation and replacement within the model. Except for the crest height and crest width, which are needed for transmission calculations, cross-sectional parameters are not used for other purposes.

The freeboard crest height (R_c) can be computed using the overtopping criterion that is presented in Equation 2.10 and therefore is dependent on the significant wave height and the angle of wave attack for the considered breakwater segment. All breakwater segments have been indicated in Figure 4.4. As the top of the breakwater core should at least be located 0.5 m above HAT (this vertical distance is indicated by h_c in Figure 4.3), the minimum breakwater crest height can be determined by adding up the thicknesses of the under- and armour layer (t_u and t_a) to this level. Depending on the wave attack and the overtopping criterion, the freeboard crest height may be increased. The core width (B_{core}) is fully dependent on the crest width (B_{crest}) and the layer thicknesses and therefore does not have to be asked as input. As it is not realistic to let the rear armour layer extent all the way to the sea bed, another dimension expressing the leeward armour layer level below MSL (h_l) is specified. The front slope ($1 : x_f$) and the rear slope ($1 : x_r$) should also be given as input.

A feature that cannot be left out for simplicity purposes, is the depth-dependency of the breakwater cross-section. A break line has been inserted within Figure 4.3 to indicate a varying water depth. The breakwater layout is divided into five segments, of which three segments correspond to the primary breakwater and the fourth and fifth depend on whether a secondary breakwater is constructed or not. These segments are indicated in Figure 4.4. The dominant cross-section is assumed to be the one that corresponds to the point that is located at 2/3 of the length of the considered segment (slightly towards the offshore side). This means that material volume ratios are determined within this point, leading to an approach that is too conservative, which is necessary to cope with the cross-sectional assumptions that are made. As the armour layer contains gaps in between the armour units, the armour layer porosity (n_v) - which is defined as the ratio between the void volume and the layer volume - should be considered when determining its volume ratio.

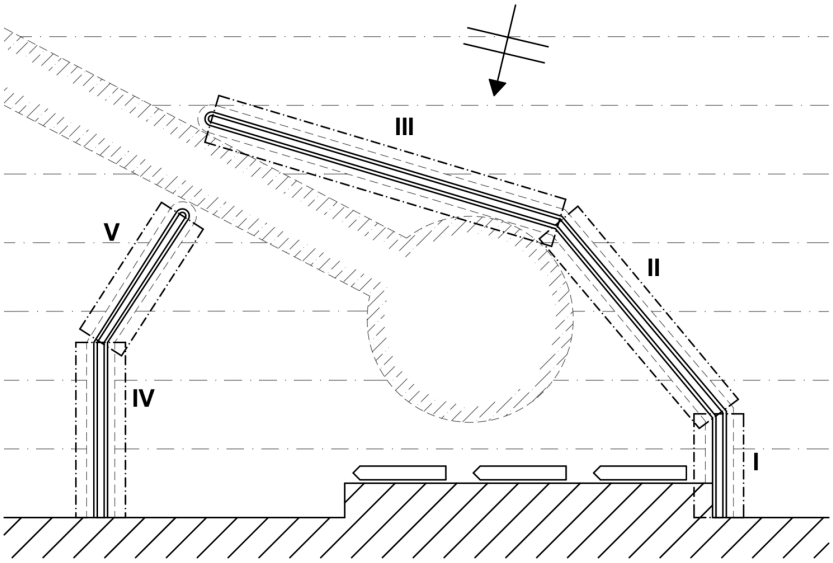

Figure 4.4: Breakwater layout segments

The cross-sectional areas at the dominant depths of each segment (d_{dom}) can be determined by making use of Figure 4.3. From this, the material volume ratios (Φ) can be computed by dividing the area that is occupied by the respective material by the total cross-sectional area of the breakwater. For the armour layer, the resulting value should be multiplied by its porosity, as is done in Equation 4.5.

$$\Phi_a = \frac{A_{a,dom}}{A_{bw,dom}} \cdot n_v \tag{4.5}$$

The next step is to compute the volume of each individual breakwater segment (V_{seg}), which is done in Equa-

tion 4.6. This can simply be done by averaging the areas on both ends of the respective breakwater segment.

$$V_{seg} = 0.5 \cdot (A_{bw,d1} + A_{bw,d2}) \cdot L_{seg} \tag{4.6}$$

where:

$A_{bw,d1}$ = cross-sectional area at the onshore side of the breakwater segment (m^2)
$A_{bw,d2}$ = cross-sectional area at the offshore side of the breakwater segment (m^2)
L_{seg} = breakwater segment length (m)

As cost are usually known for armour units, the total volume of armour units should be divided by the cubed nominal diameter (D_n^3) to obtain the amount of armour units per segment (N_a). This is done in Equation 4.7 (retrieved from CIRIA/CUR/CETMEF (2007)).

$$N_a = \frac{\Phi_a \cdot V_{seg}}{D_n^3} \tag{4.7}$$

The underlayer and core layer costs are expressed in euros per m^3. Corresponding volumes should therefore be multiplied by the volume ratio and the costs per m^3 to arrive at the total material costs per segment.

4.4. Dredging and reclamation

For cost calculations, it is required to know the volume that needs to be dredged and used as filling material afterwards (V_{df}), even as the volume that needs to be dredged and disposed afterwards (V_{dd}). It can be possible that sediment fill needs to be imported if there is a shortfall from dredging, however this is not related to breakwater construction and therefore out of the scope of this research. To come up with the total sediment volumes, the material to be dredged is divided into the approach channel and the rest of the harbour basin. The volume of filling material is discussed separately.

4.4.1. Approach channel

The volume that needs to be dredged to guarantee a safe depth in the approach channel can be computed in a simple manner. The inner and outer channel are computed separately. First of all, the original bed level in the middle of the approach channel should be computed by averaging over both axes (when the approach channel is constructed on an angle with the bed slope direction, there is also a cross-sectional difference in depth). The corresponding level is z_{out} for the outer approach channel and z_{in} for the inner approach channel (their values are negative since they are below MSL). At this point, the cross-sectional area of the channel section that has to be dredged (below the dashed line) can be computed using Figure 4.5, where W and d_{ch} follow from Section 2.1.1 & 2.1.2. The bank slope of the dredged areas ($1 : x_b$) is an input parameter.

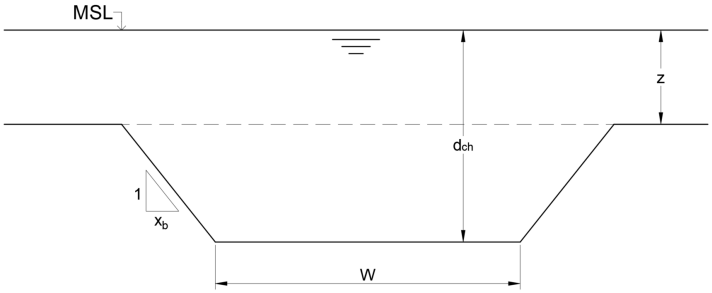

Figure 4.5: Cross-section approach channel

To compute the total dredging volume of the channel section, the cross-sectional area should be multiplied by the length of the respective section (L_{ch}). For clarification, also the longitudinal section of the approach channel is given in Figure 4.6.

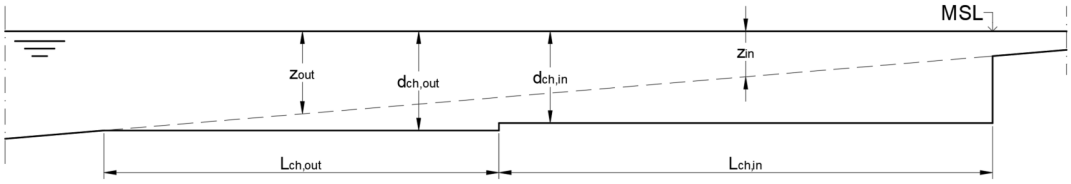

Figure 4.6: Longitudinal section approach channel

4.4.2. Harbour basin

Other manoeuvring areas within the harbour basin should also be dredged. These include mainly the turning basin and the berthing areas. The dredging volume of the turning basin can be computed by multiplying the turning basin area with the dredging depth in the middle of the turning basin. The volume that should be dredged to obtain a proper bank slope for the soil material should also be included. This volume is multiplied with a factor 0.5 as an approximation, since a bank slope is not required at the border with the approach channel and the berthing basin (or the manoeuvring area in between).

The berthing basin is of rectangular shape with a width and depth as defined in Section 2.1.4 and a length as defined in Section 2.1.6. Only at the edges perpendicular to the quay wall a bank slope is assumed.

In most cases, the volume to be dredged is not limited to the approach channel, turning basin and berthing basin. Usually, also other areas should be included, which can be related to anchorages, manoeuvring from the turning basin to the berthing basin, tugboat mooring or other activities. It is however hard to predict these volumes, as they largely depend on the port layout and activities that take place within the harbour basin. The required dredging depth can be taken equal to the average of those in the turning- and berthing basin. For the area to be dredged, a rough approximation should be made. The additional area to be dredged is schematised as a rectangle, as is done in Figure 4.7. Including this area in the dredging volume determination results in an optimal location for the turning basin. The distance from the turning basin to any of the berths should be kept as short as possible, as it leads to reduced dredging costs, but also to less delay when sailing in or out of the harbour. The additional area to be dredged is fully dependent on the distance to the berths at either end and therefore mainly results in a good comparison between layout alternatives, rather than giving an accurate estimation of the dredging volume. When vessels need to sail around a breakwater tip to reach a berth, the resulting distance follows the path around the tip. The width of the rectangle is set equal to a quarter of the quay length. The dotted line gives an indication of the additional area to be dredged at its respective location in the layout.

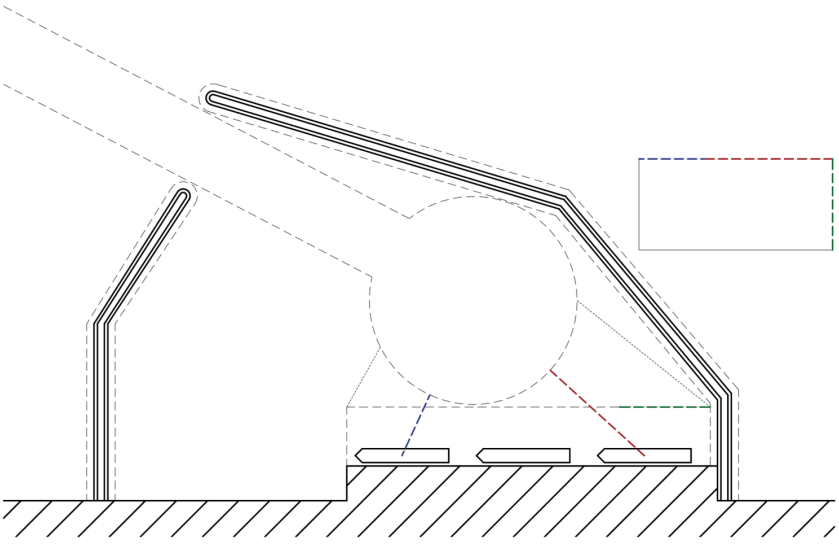

Figure 4.7: Additional harbour basin area to be dredged

4.4.3. Terminal fill

For most harbours, dredged sediment is primarily used for terminal fill. Ideally, a balance between cut and fill is achieved, unless the soil is very hard (high dredging costs) or material that is unsuitable for reclamation (Ligteringen & Velsink, 2012). To determine the required sediment volume for reclamation, its area and level should be known. The reclamation area is the product of the quay length and the cross-shore fill distance (y_f), which is an input parameter that is preferably determined by the cut and fill balance. The fill height is dictated by three parameters: the average fill-up level (h_f, in most cases equal to the level of the hinterland), the bed level at the onshore side of the terminal (z_0) and the bed level at the quay location (z_q). The fill volume (V_f) is given by Equation 4.8.

$$V_f = \left(h_f - 0.5(z_0 + z_q)\right) \cdot L_q \cdot y_f \tag{4.8}$$

4.4.4. Total volumes

The total volumes are now just summations of the volumes mentioned above. If the volume to be dredged is larger than the terminal fill volume, sediment volumes can be computed using Equation 4.9.

$$\begin{aligned} V_{df} &= V_f \\ V_{dd} &= V_{ch,out} + V_{ch,in} + V_{tb} + V_{bb} + V_{rest} - V_f \end{aligned} \tag{4.9}$$

When the volume to be dredged is smaller than the terminal fill volume, sediment needs to be imported, which falls outside this research scope. Other sediment volumes can now be computed with Equation 4.10.

$$\begin{aligned} V_{df} &= V_{ch,out} + V_{ch,in} + V_{tb} + V_{bb} + V_{rest} \\ V_{dd} &= 0 \end{aligned} \tag{4.10}$$

If all dredged sediment material turns out to be unsuitable for reclamation, all the sediment material should be disposed. The user should be able to indicate this.

4.5. Downtime determination

Probably the most challenging part in finding the optimal breakwater layout is the determination of the amount of downtime that is coming along with a certain layout configuration. For accurate downtime determination, dynamic mooring assessments are performed to be able to get an idea of moored vessel motions and the corresponding downtime. In the conceptual design phase, this type of assessments is cost inefficient, which means that an analytical way of determining the amount of downtime should be generated. To do so, first of all the wave and wind conditions should be determined at the locations where output for navigational and operational downtime is required. For navigational downtime, the output location (point N in Figure 4.8) is set at one stopping length away from the turning basin centre, in the middle of the approach channel. This is likely the location within the sheltered approach channel where the wave height is the highest, thus leading to navigational downtime if either wave height or wind speed allowances are exceeded here. The extra wave length that is needed for tugboats to approach the vessel in rough conditions (see Section 2.1.3) is not included. The output locations for operational downtime correspond to the centre point of a moored design vessel at each of the berths (points $O1$ to $O3$ in Figure 4.8). This choice is based on finding a reliable estimate of the wave height and corresponding downtime – rather than finding a conservative downtime value – as locations of maximum wave height may vary for different layout alternatives. The amount of output locations for operational downtime depends on the number of berths that are considered. A schematised port layout with indicators for the locations where downtime output is required is given in Figure 4.8.

Wave transformation is used to determine the wave heights at the output locations. Input parameters are required in deep water. Since the sea bed slope is assumed to be constant (see Section 1.3.2), simple formulas for shoaling and refraction (as proposed in Section 2.3.1) suffice to obtain wave heights at the locations where

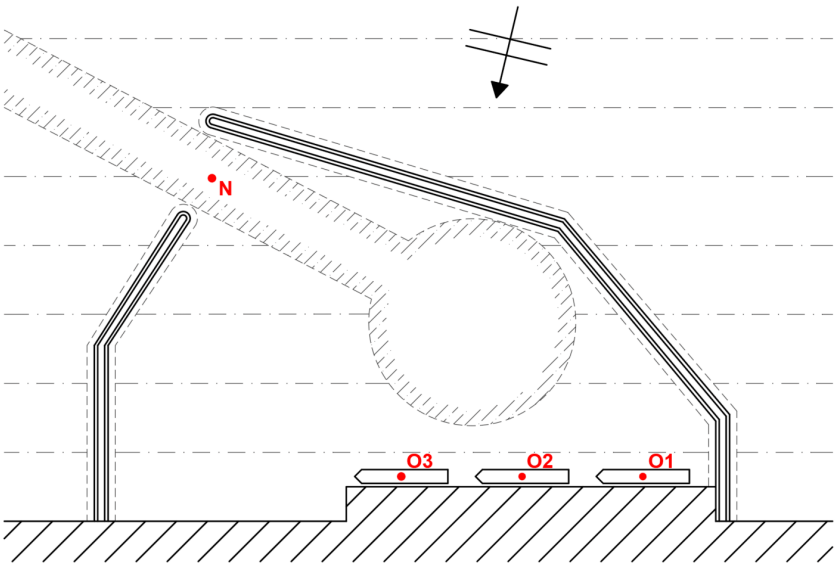

Figure 4.8: Locations for downtime output of a single wave condition (N = navigational downtime; O = operational downtime)

input is required. For diffraction, this location is either the tip of the breakwater (in case of one semi-infinite breakwater, point S in Figure 4.9) or the middle of the breakwater gap (in case a secondary breakwater is also considered, point G in Figure 4.9). For transmission, the desired locations (points $T1$ to $T3$ in Figure 4.9) depend on the wave direction that is considered at that moment. A line can be drawn from the output location (e.g. one of the moored vessels along a berth) in opposite direction of the respective incoming wave direction. The intersection point of this line and the breakwater axis results in the desired input location for wave transmission. For navigational downtime, diffraction is assumed to be dominant, so transmission is not considered. The desired locations are shown in Figure 4.9 for clarification.

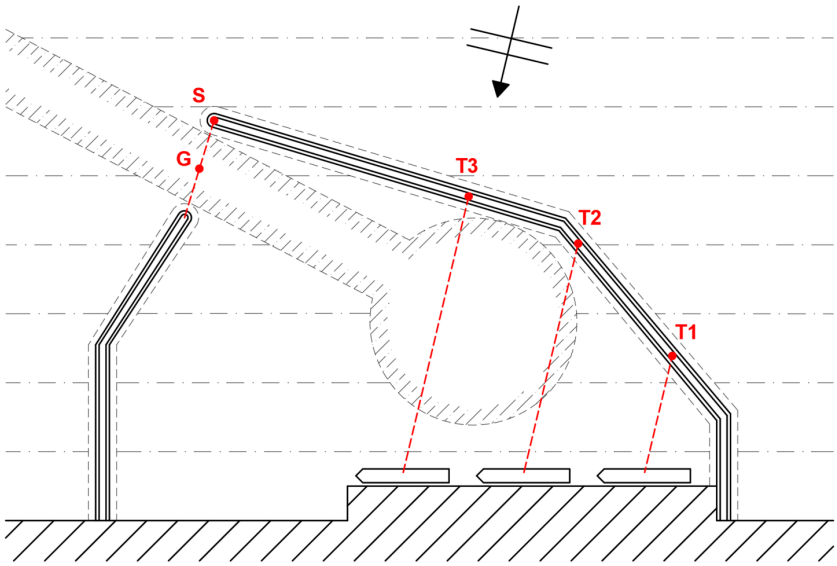

Figure 4.9: Locations for wave penetration input of a single wave condition (G = breakwater gap; S = semi-infinite breakwater; T = transmission)

As mentioned above, the input conditions for the wave climate are considered separately. In this way, each condition can be transformed individually to calculate the corresponding wave height or wind speed at the output locations and therewith if the respective condition generates downtime or not. To do so, each condition should contain a probability of occurrence (Pr), along with a significant wave height (H_s), wave direction (θ_w) and peak wave period (T_p). From the input location, waves are transformed per condition to

the required input locations for wave penetration as given in Figure 4.9. Waves are then diffracted using the diffraction tables in Appendix B. Transmission coefficients are computed with Equation 2.9. It is assumed that the combination of the diffracted and transmitted wave height gives a sufficiently good representation of the problem. The corresponding wave height at a certain output location (H_{out}) can consequently be estimated by superimposing the individual components ($E \sim H^2$) using Equation 4.11.

$$H_{out} = \sqrt{H_{d,out}^2 + H_{t,out}^2} \tag{4.11}$$

where:

$H_{d,out}$ = diffracted wave height at output location (m)

$H_{t,out}$ = transmitted wave height at output location (m)

If the wave height at the respective output location is higher than the allowable wave height, downtime occurs for the considered wave condition. The same holds for the allowable wind speed. In addition, it is assumed that when navigational downtime occurs, all berths are out of operation, as ships cannot enter the port anymore. In reality, a more detailed relationship exists between navigational and operational downtime, as ships that are already moored can usually continue (un)loading procedures while navigational wind/wave limits are exceeded. It is however chosen not to incorporate this into the methodology, as this balance is dependent on the balance of the service and waiting time of the respective port, which is considered too site specific to investigate in the conceptual phase of breakwater layout design. Therefore, downtime occurs for a certain wind/wave condition at a certain berth when EITHER the wind speed or wave height limit is surpassed at location '*N*' OR the allowable wind speed or wave height at the corresponding berth is exceeded. Downtime therefore occurs in every mentioned circumstance, to avoid 'double counting'. An example is given in Table 4.1, where five environmental conditions are considered with there resulting probability of occurrence (Pr). It is only meant for illustration.

Condition	**1**	**2**	**3**	**4**	**5**
Pr	0.1	0.6	0.05	0.15	0.1
Wave height					
O1	–	–	–	–	–
O2	X	–	–	–	X
O3	X	–	–	X	X
N	–	–	X	–	–
Wind speed					
O	–	–	–	–	X
N	–	–	–	–	X
Downtime	**Berth 2 & 3**	**–**	**All berths**	**Berth 3**	**All berths**

Table 4.1: Downtime determination for a set of environmental conditions (X = downtime; – = no downtime)

It can be seen from the lower row in Table 4.1 that for condition 3 and 5, downtime occurs for all berths regardless of exceedance of the limiting wave height at one of the berths. Condition 5 is a typical example where 'double counting' can take place (for berth 2 and 3), as both navigational and operational downtime are now present. This has been overcome by reducing the output to a yes/no value per berth. Combining the input from the upper row and resulting downtime in the lower row, berth 1 results in a value of 0.15 for the probability of occurrence of downtime (downtime only occurs for condition 3 and 5), whereas berth 3 corresponds to a value of 0.4 (downtime for all conditions except condition 2). The probability of occurrence of downtime per berth (Pr_b) can now be multiplied by the amount of hours per year to obtain the total amount of downtime per berth per year ($n_{d,b}$), which is done in Equation 4.12.

$$n_{d,b} = 365 \cdot 24 \cdot Pr_b \tag{4.12}$$

5. Model set-up

Given the methodology as proposed in Chapter 4, it is possible to start setting up the parametric model. This set-up is based on genetic algorithms, as this optimisation method has been considered most appropriate for the current problem, as is discussed in Section 3.3. A model set-up is required to be able to program the parametric model in an adequate, complete and efficient manner. Its structure should be clear, precise and easily adaptable to account for more realistic situations as the model develops. Firstly, an introduction to genetic algorithms is given in Section 5.1. After that, the required variables, constraints and functions are defined in Section 5.2. Subsequently, a complete list of required input parameters is provided, which need to be entered into the model by the user (see Section 5.3). Ultimately, the fitness evaluation is treated, as this forms an integral and complex part within *GA*'s (see Section 5.2.4).

5.1. Genetic algorithm introduction

To get fully familiar with the concept of genetic algorithms, a description of this optimisation method is given, in which the full *GA* process is treated. In addition, the possible operators and *GA* types that can be used in the model are treated.

5.1.1. Terminology

Genetic algorithms borrow the terminology of natural genetics. A full understanding of these terms is necessary to comprehend the *GA* process as described in this section. Therefore, a list of *GA* terms, including their translation to the current problem, is provided in Appendix C.

5.1.2. General

Genetic algorithms represent an adaptive search method, based on the selection of the best elements in a population, similarly to Darwin's theory of evolution (Kureichik et al., 2009). An optimisation problem has many possible solutions, which are defined as chromosomes. For the current problem, these chromosomes represent breakwater layout alternatives that satisfy the model constraints (defined in Section 5.2.2). Each chromosome is a vector of decision variables describing an individual (synonym of a chromosome). Each decision variable is called a gene and its value is called an allele. All decision variables describing a certain breakwater layout alternative are treated in Section 5.2.1. For example, the length of a breakwater could be taken as a decision variable, as it represents a characteristic property of the breakwater, and thus can be called a gene. Its value in metres is the allele. Each gene has a certain position within the string that defines a chromosome. This position is called the locus and the string of genes is referred to as the genotype defining an individual. Its counterpart, the phenotype, is the decoded expression of the string, in this case the breakwater layout that matches the decision variables. A set of chromosomes is called a population. The data that is stored within a chromosome can be encoded in different ways. For the current problem binary encoding and real-value encoding suffice. In this study, binary encoding is only used for decision variables that can be represented by a yes/no value. In Figure 5.1, an example of a population and its terminology for both binary and real-value encoding is given.

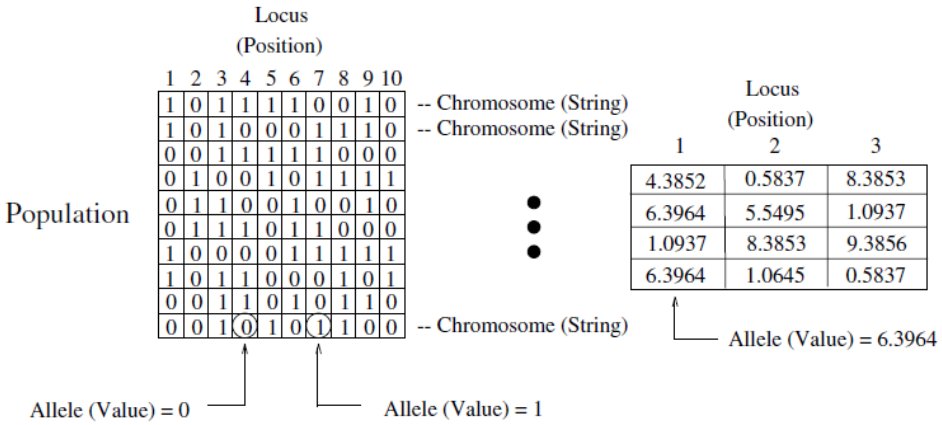

Figure 5.1: Data structure and terminology for binary encoding (left) and real-value encoding (right)

Some typical characteristics of *GA*'s are summed up below (Kureichik et al., 2009):

- They work with a coded set of parameters (as described above).
- They work in parallel, optimising populations instead of single solutions.
- They are able to analyse various areas of the decision space simultaneously, by considering multiple objectives (see Section 5.1.3).
- They make use of probabilistic rules in the optimisation analysis, to include for uncertain hereditary variability.

5.1.3. Process

In genetic algorithms, a population of chromosomes is analysed by assessing each chromosome based on one or more objective functions. By doing so, close attention is paid to the driving forces of evolution. In relation to *GA*'s, as stated in Kureichik et al. (2009), these are the variety of chromosomes in a population, the elimination from replication of the less adapted individuals (struggle for existence) and the survival of the more adapted individuals that in turn lead to new adaptations (survival of the fittest). In this way, evolution takes place by means of continuous adaptation of individuals to environmental conditions, described as a multistage iterative process, while keeping the number of individuals constant (Kureichik et al., 2009). The quality of the solution is defined by their objectives scores, which can be retrieved by decoding the string of decision variables (genotype) of a breakwater layout alternative (phenotype). Environmental conditions can now be applied onto the breakwater layout alternative (like wind and waves, see Section 4.5) to ultimately obtain values for the objective functions, such as cost approximations (see Section 4.2). These values indicate the desirability of the respective solution. A basic *GA* process can be schematised as is done in Figure 5.2.

The first step in the optimisation process is the initialisation of a population. This can be done by random sampling of genes, complying with the model constraints. In this way, a set of chromosomes is generated that corresponds to the population size that is specified by the user. Following this, the objective functions for every individual are computed (indicating their fitness). The next step is to evaluate all chromosomes based on their fitness, and applying genetic operators to form offspring. These operators are formed by selection, crossover and mutation. They are treated separately in

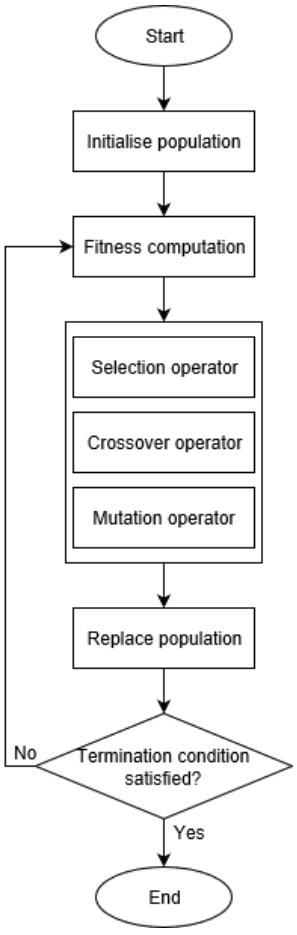

Figure 5.2: Basic *GA* process

Section 5.1.4. After this, the current population can be replaced by the offspring (having the same population size). The next generation is formed, for which the entire process starts over again, unless the termination condition is satisfied. This condition can either be a predefined amount of generations that the evolutionary loop needs to go through, or a certain rate of convergence corresponding to the optimisation process. For the latter condition, the evolutionary process stops if no significant progress is observed anymore.

5.1.4. Genetic operators

Selection Selection can take place at two points within the *GA* process. Firstly, parents need to be selected to form the mating pool from which offspring is generated. Secondly, the best evaluated solutions need to be selected to form the next generation. Chromosomes are selected based on their objective values. In this way, convergence towards optimal solutions is allowed. Selection algorithms often depend on randomness to maintain diversity within the population. The reason to introduce randomness into the selection operator – and therewith maintaining diversity in the population – is to overcome local optima. A good example is formed by proportional selection, also known as roulette wheel selection. This selection operator assigns a probability of selection to a certain solution, which is based on the normalised value of its fitness score. Figure 5.3 illustrates this.

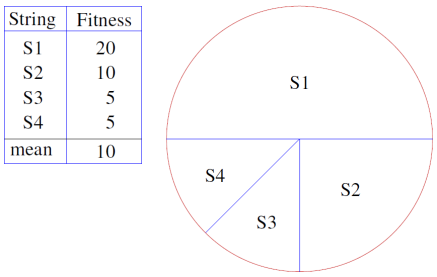

Figure 5.3: Proportional / roulette wheel selection for unequal fitness scores (Coello Coello et al., 2007)

Elitism forms a special type of selection and means that a small proportion of the fittest individuals is selected instantly for the next generation, without applying any changes to them. In this way, the fittest solutions are remembered by the algorithm, however it may lead to increased convergence towards local optima if too many elites are selected.

Crossover In nature, genetic material is passed on from parents to children. This also applies for *GA*'s, where crossover allows the combination of genes of two or more individuals (serving as parents) and inherit it to their children. First of all, the parents to generate offspring are selected. Next, crossover should take place. Many operator options are available, depending mostly on the optimal way to recombine genes for the considered problem. Single-point crossover splits two parent strings at an arbitrary point and recombines them with a piece of the other. This is shown in Figure 5.4, where the strings are split up in the middle, so that the offspring consists of an equal amount of genes from each parent.

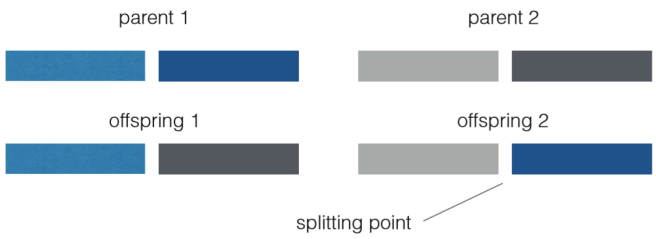

Figure 5.4: Single-point crossover, splitting the parent genotypes into two parts and reassembling them to create offspring (Kramer, 2017)

Other options are to split a string at various locations, to recombine genes in a more random way (for exam-

ple by assigning random probabilities to the inheritance of genes) or to average alleles corresponding to a certain gene from both parents. It is likely that different crossover operators need to be used for binary and real-value alleles. The goal of crossover is to create offspring that generally performs better than its parents, consequently improving the optimisation process.

Mutation To maintain a certain level of guaranteed diversity in a population, the concept of mutation is introduced. This process makes it possible to escape from local optima by disturbing certain solutions randomly. Through mutation, it must be possible to reach each point in the solution space from an arbitrary point (Kramer, 2017). In this way, the chance to reach the optimum remains positive. Mutation should not introduce a search drift in a particular direction and its strength should be adaptable (Kramer, 2017). Mutation based on a probability distribution (such as the Gaussian distribution) is usually appropriate, but when looking at mutations where binary values are flipped, a certain probability must be ascertained to it. This probability is represented by the mutation rate. The other optimisation parameter characterising the mutation operator is the mutation size, which is an indicator for the strength of the disturbance. Both parameters must be tuned as they may have a large effect on the outcomes of the model.

5.1.5. GA type

Until now, only basic *GA*'s have been discussed, however many types exist. The current problem is defined as multi-objective and conflictive, meaning that when improving one objective, the other objective deteriorates (Kramer, 2017). One objective function is formed by the performance of the breakwater (f_1) and the other by its costs (f_2), which forms a typical situation, as both usually contradict each other. As for this case, both objective functions are expressed as a present value (therefore requiring minimisation), leading to equal weights as they can be easily summed up. The Pareto front is set up (treated in Section 3.2) to still be able to constitute a compromise between both objectives. The goal is to find a set of solutions that is not dominated by other solutions, meaning that they are not outperformed on both objectives. To make optimal use of the Pareto front, the solutions can be sorted according to their level of domination. In Figure 5.5, it can be seen that solutions in the lower left quadrant would dominate the solution that is considered, as they outperform it in both objectives. Solutions in the upper right quadrant are dominated by the considered solution and the other two quadrants are non-comparable. The Pareto set is a set of non-dominated solutions with regard to the whole solution space and corresponds to the optimum of the overriding objective function (Kramer, 2017). A certain position on the Pareto front may contain numerous alternative solutions in the objective space, as totally different breakwater layouts may result in an equal value of the objective functions.

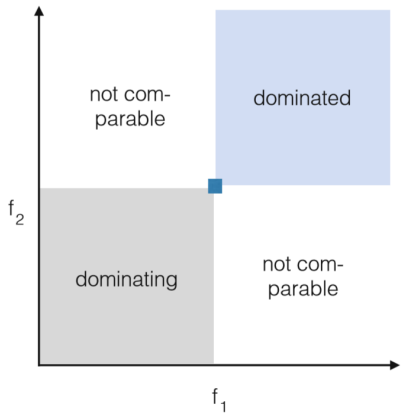

Figure 5.5: Domination for two objectives (Kramer, 2017)

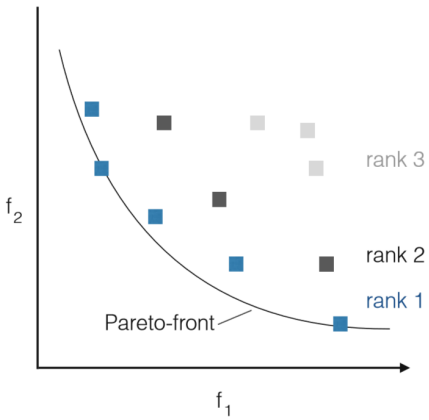

Figure 5.6: Non-dominated sorting (Kramer, 2017)

In Figure 5.6, non-dominated sorting is visualised. It sorts all chromosomes in a population based on their non-domination rank. The first rank consists of solutions that are not dominated by any other solution. The second rank corresponds to all non-dominated solutions in case the first rank has been removed. This continues until the solution set is empty. The non-dominated sorting genetic algorithm (*NSGA*) makes use of

this concept and is therefore suitable for multi-objective problems. Its successor, *NSGA-II* is proven to be even more successful and has also been applied in breakwater layout optimisation in Rustell (2016). The algorithm focuses on three main criteria. It aims to maintain diversity in the population, it enhances convergence to efficiently move towards the Pareto-optimal set and it makes use of elitism to speed up model performance (Deb et al., 2002). A main contributor to these criteria is that the algorithm seeks for a broad coverage among non-dominated solutions (Kramer, 2017). This is achieved by introducing a crowding distance, which is the rectilinear distance of two neighbouring solutions for two objectives, corresponding to the total length of the dotted line in Figure 5.7. *NSGA-II* selects the solutions having the largest crowding distance, therewith stimulating the spread of solutions over the Pareto front. Consequently, a solution scoring very well on one objective, but very low on the other, can have a higher chance of being passed on to the next generation than a solution scoring quite well on both objectives.

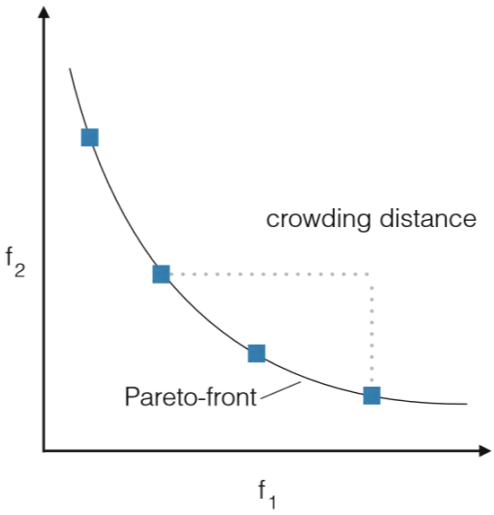

Figure 5.7: Crowding distance of two solutions on the Pareto front for two objectives (Kramer, 2017)

In addition to *NSGA-II*, even more *NSGA*-like algorithms have been developed, which claim to be more efficient. Nevertheless, *NSGA-II* has proven to give satisfactory results for similar problems and is therefore chosen as optimisation algorithm in this study. The corresponding process is shown in Figure 5.8.

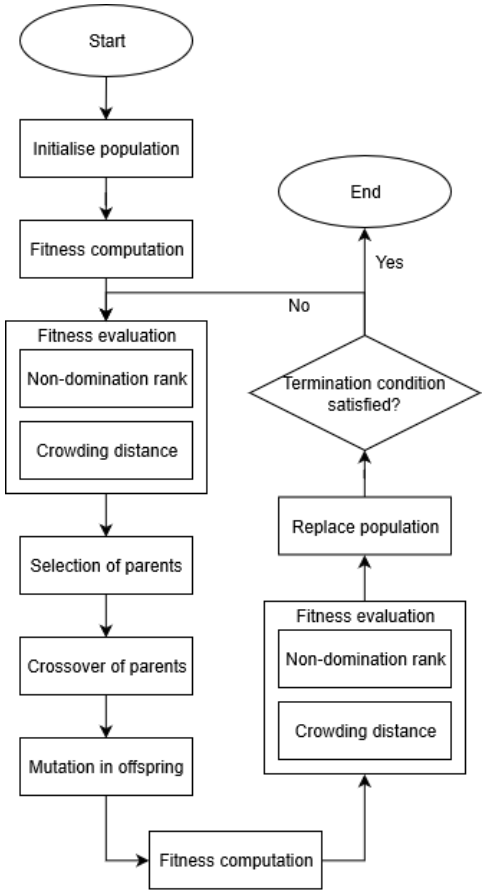

Figure 5.8: *NSGA-II* process

The most important change in the process of Figure 5.8, in comparison to Figure 5.2, is the addition of the fitness evaluation based on non-domination rank and crowding distance. As can be seen from the figure, evaluation is performed to be able to select the parents and to form the next generation of alternatives from the current population and the offspring. During this evaluation, solutions are firstly ranked based on non-dominated sorting. All solutions within the same rank are then compared based on their crowding distance, where solutions having the largest crowding distance are preferred.

Selection of parents takes place based on binary tournament selection. This type of selection randomly picks two solutions and selects the best one, until enough parents are selected. Better evaluated alternatives therefore have a larger chance of getting picked, but every alternative has at least a small chance of getting picked. The crowding distance makes sure that the selected solutions are spread out sufficiently over the solution space. On the other hand, non-dominated sorting and tournament selection make sure that populations keep improving and converging towards an optimum.

The evaluation and selection procedure for the next generation is visualised in Figure 5.9. Firstly, a combined population (R_t) is formed by bundling the current population (P_t) and the offspring population (Q_t), thus having a size of twice the population size. The combined population is sorted based on non-domination. The first front (F_1) contains all elites, which are therefore ascertained to be passed on to the next generation

(P_{t+1}). The first front that exceeds the population size (in this case F_3) is sorted based on crowding distance. Solutions having the lowest crowding distance are eliminated until the remaining amount of chromosomes equals the population size. The next generation is formed by all chromosomes that are left.

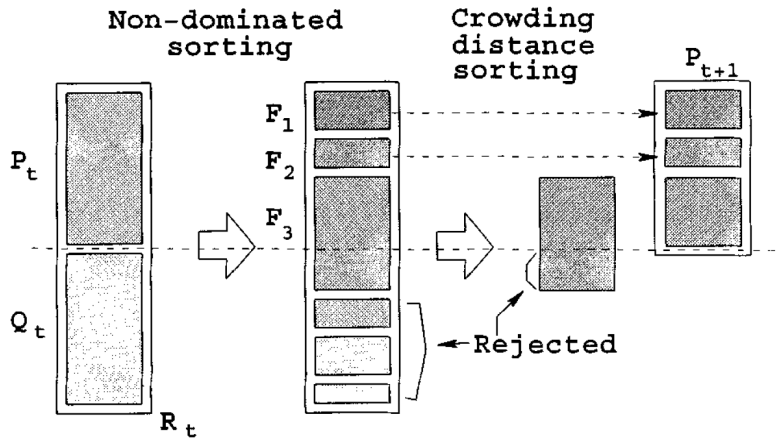

Figure 5.9: Evaluation procedure *NSGA-II* (Deb et al., 2002)

5.2. Optimisation variables and functions

5.2.1. Decision variables

Decision variables are the numerical quantities for which values are to be chosen in an optimisation problem (Coello Coello et al., 2007). With these variables it should therefore be possible to describe the characteristics of a certain breakwater layout alternative. To choose the decision variables, it should be known what information is required to define a breakwater layout. A coordinate system is established, having its origin at the point where the primary breakwater touches the shore. As indicated in Section 1.3.2, the terminal lay-out is schematised with one quay wall, consisting of (several) berths in one line, parallel to the shoreline. The first segment stretches out perpendicularly to the shoreline, with a predefined minimum length (see Section 4.1). Next, the first decision variable comes into place, determining if the breakwater extents towards the left or towards the right (when looking from the shoreline in offshore direction). This determines if the entire port layout is located on the right or left side of the origin and is indicated by RHS with a value of 0 or 1 (binary encoded). A value of 1 indicates that the port is located to the right of the origin, whereas a value of 0 results in a port on the left-hand side of the origin. The x-axis runs along the shoreline and the y-axis runs along the length of the first segment of the primary breakwater. The positive x-axis is always directed to the right (no matter the port orientation) and the positive y-axis in offshore direction. Angles are always defined positive in clockwise direction from the positive y-axis. To illustrate this, examples for both a port with $RHS = 0$ and $RHS = 1$ are given in Figure 5.10.

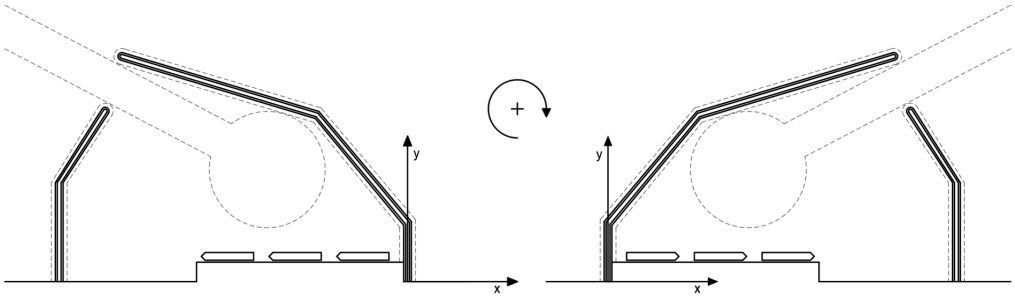

Figure 5.10: Port layout example for $RHS = 0$ (left) and $RHS = 1$ (right)

The most relevant components in the port layout that can be shifted to produce a more optimal breakwater layout are the breakwater nodes, which are indicated in Figure 5.11. Node 0 forms the origin of the coordinate system, node 1 is located along the y-axis at a minimum distance from the origin (dependent on the input parameters) and node 2 and 3 can move freely in positive y-direction and the x-direction corresponding to the port layout orientation. Another binary decision variable determines whether a secondary breakwater is constructed (SEC). When this the case (for $SEC = 1$), three more nodes are added to the decision variables. Node 4 is located at a minimum distance along the x-axis, depending on the quay wall length. Also future expansion potential is included in this minimum distance, so that enough space is reserved for berths that are planned to be constructed in the future. Node 5 is located at a minimum distance from node 4 perpendicularly to the shoreline. This minimum distance is dependent on the breaker depth index. Node 6 can move freely in the x-direction towards the origin and the positive y-direction.

The centre of the turning basin (x_{tb}, y_{tb}) is also taken as a decision variable, as it affects the port layout to a large extent. The turning basin is able to move freely within the harbour basin. The final decision variable is formed by the angle of the approach channel with respect to the y-axis (θ_{ch}). The valid range of this angle is dependent on the coastline and the alignment of the breakwaters. All decision variables are listed in Table 5.1.

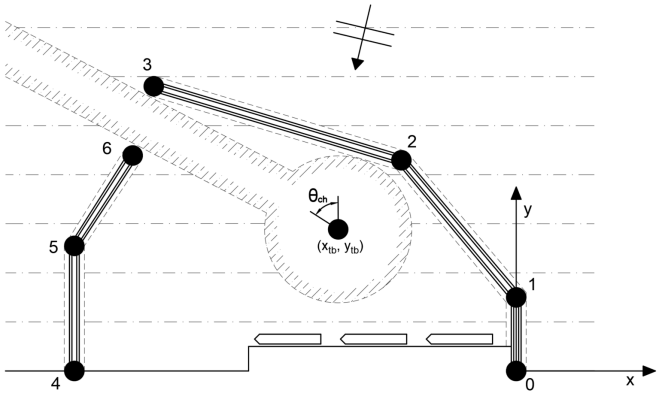

Figure 5.11: Decision variables for $RHS = 0$ and $SEC = 1$

Variable	Description	Units
RHS	Orientation of port location with respect to origin	binary
(x_i, y_i)	Coordinates of breakwater node locations	m
(x_{tb}, y_{tb})	Coordinates of turning basin centre	m
θ_{ch}	Approach channel orientation with respect to y-axis	°
SEC	Whether a second breakwater is constructed	binary

Table 5.1: Model decision variables

A chromosome is defined as a vector of decision variables: $X_i = (\chi_1, \chi_2, \ldots, \chi_n)$. Equation 5.1 gives the representation of a chromosome that corresponds to a certain breakwater layout configuration. In total, fourteen decision variables have to be chosen to define a breakwater layout alternative. The accuracy of all variables is set to zero decimals, meaning that all variables can be defined as integers.

$$X_i = (RHS,\ y_1,\ x_2,\ y_2,\ x_3,\ y_3,\ x_4,\ y_5,\ x_6,\ y_6,\ x_{tb},\ y_{tb},\ \theta_{ch},\ SEC) \tag{5.1}$$

5.2.2. Model constraints

Most optimisation problems have certain restrictions for the solution to be acceptable, due to physical limitations for example. These restrictions are called constraints, which represent dependencies among decision variables and constants involved in the problem (Coello Coello et al., 2007). For the breakwater nodes, these constraints can clearly be defined, which is done in Table 5.2.

Variable	y_1	BW_2	BW_3	x_4	y_5	θ_{ch}
Lower	y_m	$(0, y_1)$	(x_2, y_2)	L_{fq}	y_{bl}	-90
Upper	$3y_m - 2y_f$	(x_{max}, y_{max})	(x_{max}, y_{max})	L_{max}	y_{max}	90

Table 5.2: Breakwater node constraints

where:

y_m = distance for manoeuvring, berthing and terminal fill (m) = $y_f + W_{bb}$

y_{bl} = distance from shoreline to breaker line (m)

(x_{max}, y_{max}) = outermost point defined for the primary breakwater (m)

L_{fq} = future quay length, allowing for port expansion (m)

L_{max} = outermost distance in x-direction defined for the secondary breakwater (m)

The coordinates for the centre of the turning basin are also constrained. The turning basin is located within the protection of the breakwater (if necessary), but outside the berthing area. The distance from its centre to all surrounding breakwaters should be at least equal to the turning radius, with an addition that is enough to provide a bank slope and a breakwater slope. The turning basin should maintain a minimum distance from the future quay wall. Another constraint is formed by the minimum distance between the breakwater tips, which should be at least equal to the design vessel length, with an addition for the breakwater slopes.

One of the most relevant model constraints is formed by the sheltered approach channel length. This length is dependent on the local wave climate, as described in Section 2.1.3. The breakwater entrance marks the begin of the sheltered approach channel. It is located in the middle of the approach channel, where it meets the line from the dominant breakwater node in the dominant wave direction. To illustrate this: when the dominant wave direction comes in from 30° with respect to the positive y-axis, node 3 would probably be the dominant breakwater node for $RHS = 0$, as waves would diffract around this point. Following the dominant wave direction from node 3 to the middle of the approach channel results in the start of the approach channel. Following the approach channel until the turning basin centre results in the sheltered approach channel length. The location of both the dominant breakwater node and the turning basin centre are therefore confined by this constraint.

Other types of model constraints are those related to CAPEX and downtime. It can be that only a certain amount of CAPEX can be spent, which would mean that breakwater alternatives that surpass this limit should automatically be left out. It is however chosen to not take this into account, as optimisation of total costs would automatically lead to an acceptable amount of CAPEX, since its share in the total costs is large. Options resulting in a large amount of downtime can simply be excluded after the simulation. As solutions should have approached the Pareto front by then, the user is able to evaluate the options on this front. If downtime constraints apply, the solution space reduces and only a part of the options on the front remains. The final solution can then be chosen based on the relative importance between CAPEX/OPEX and downtime.

5.2.3. Objective functions

Since the optimal breakwater layout is defined as the layout alternative resulting in an optimal balance between the present values of the CAPEX/OPEX and downtime costs (see Section 3.2), these form the objectives that need to be minimised. The corresponding objective functions are stated in Equation 5.2 & 5.3.

$$f_c(X_i) = C_{bw}(X_i) + C_{dr}(X_i) + \sum_{t=1}^{T_L} \frac{C_{dr,o}(X_i) + \Phi_{bw,m} \cdot C_{bw}(X_i)}{(1+r)^t} \tag{5.2}$$

$$f_d(X_i) = \sum_{t=1}^{T_L} \frac{C_{w,o}(X_i)}{(1+r)^t} \tag{5.3}$$

These equations correspond to the methodology presented in Chapter 4. Both objective functions are dependent on the vector of decision variables and the input parameters that are defined in Section 5.3.

5.2.4. Fitness function

The fitness function measures the quality of the solutions that are generated by the *GA*. Formulating it is often difficult, as the developer has considerable influence on the design choices and therewith also guides the search (Kramer, 2017). As the current problem is defined as multi-objective, it is chosen to evaluate all solutions based on the Pareto front using the principle of non-dominance as explained in Section 5.1.5. Solutions are therefore not evaluated based on their fitness score, shifting the focus away from the formulation of the fitness function. The final choice that the user or client needs to make is therefore restricted to alternatives laying on the Pareto front, which aligns with the conceptual design process. A certain layout alternative having low downtime costs can be compared to another alternative having low CAPEX/OPEX or one that seeks the way in between. This final decision is fully based on the requests of the user or client.

Although the fitness score is not used for evaluation, a fitness function is still established as it bundles all underlying functions that define a breakwater layout alternative (walking through the entire methodology proposed in Section 4.5 - 4.2). It therefore takes significant computational time to run, so fitness function calls should be minimised within the model. In this function, both objectives are weighted equally and its result is meant to give a clear representation of the quality of the corresponding layout alternative and to be able to monitor model convergence. The function is given in Equation 5.4.

$$f_f(X_i) = \frac{1}{f_c(X_i) + f_d(X_i)} \tag{5.4}$$

As can be seen from the fitness function, it is inversely proportional to the sum of the objective functions. A high fitness score thus corresponds to low total costs. As the objective functions are usually expressed in millions of euros, fitness scores become very low. They are therefore normalised with respect to a minimum total cost value, dependent on the project. Fitness scores can be used to compare different layout configurations that are generated using identical input parameters, or as convergence indicator – when using the progress of the average fitness score of the best alternatives in a population (see Section 6.1).

5.3. Input parameters

Input parameters are needed to provide the model with information regarding site data, design parameters and other factors that may be of interest. Without these, no clear values for model constraints and objective functions can be given. They can roughly be divided into the categories stated in Table 5.3, addressing the part of the overall computation where they are required.

Category	Description
Constraints	User-defined model boundaries
Navigation	Limiting wave heights and related influence factors
Vessel	Design vessel characteristics
Costs	Unit rates and other specifications for cost calculations
Terminal	Quay and berth characteristics, port productivity factors
Bathymetry	Ground levels and bed slope (bathymetric data set for [x,y]-coordinates in future)
Coast	Coastline orientation ([x,y]-coordinate representation of coastline in future)
Water levels	Water levels with respect to mean sea level
Breakwater	Parameters relating to the cross-sectional breakwater design
Environment	Joint probability density set of wind, wave and current data
Sedimentation	Harbour siltation parameters and soil conditions
Dredging	Parameters for dredging and reclamation calculations

Table 5.3: Input parameter categories

Based on the method proposed in Chapter 4, the input parameters per category can be determined. The objective functions can be deduced such that only input parameters and decision variables remain. The input parameters per category are given in Appendix D.1, including some default values, which are based on literature research. Using the input parameters, all other parameters that are needed in the model can be

computed (e.g. quay length, channel dimensions, etc.). Table D.9 requires an input file for wind, wave and current data, which is based on a probability density function. This implies that all environmental conditions are normalised with respect to their probability of occurrence. The user of the model can therefore specify as many environmental conditions as desired, given that the sum of all probabilities equals 1. Specific attention should be paid to environmental conditions having low probabilities of occurrence (corresponding to less than approximately 2% of the time), as these conditions are mainly responsible for the occurrence of downtime when approaching the optimal layout alternative. The accuracy of these conditions determines the accuracy of the final layout alternative to a large extent.

5.4. Model flow

As all relevant aspects are treated to set up the parametric model, its structure can be established. The basis is formed by the diagram shown in Figure 5.8, as this is the process it needs to go through. All relevant processes should be divided over the modules that form the parametric model. The resulting flow diagram is visualised in Figure 5.12.

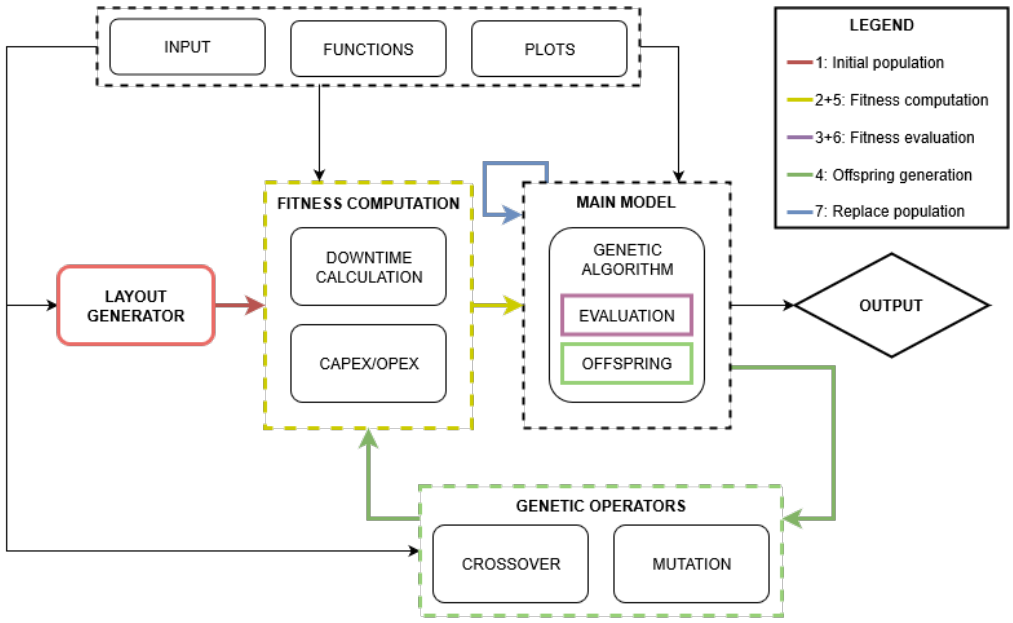

Figure 5.12: Flow diagram for the parametric model

The order to read the diagram is shown in the legend. All modules (nine in total) are indicated by the rounded rectangles. They are briefly elaborated on below:

Input	Import of input parameters and adaptation of these to fit the model language.
Functions	Background functions required for other modules.
Plots	Plot generation required for other modules.
Generator	Initialisation of valid chromosomes to form the initial population.
Downtime	Calculation of downtime due to environmental conditions for an individual alternative.
CAPEX/OPEX	Cost calculations related to dredging, reclamation, breakwater construction, a.o.
Main	This is were the magic happens. Contains the genetic algorithm, including the evaluation of layout alternative, the generation of offspring and the composition of the next generation. Links all other modules together.
Crossover	Separate generator, producing new alternatives by combining two parent chromosomes.
Mutation	Separate generator, producing new alternatives by applying random mutations to generated offspring.

The process starts with the generation of an initial population of chromosomes. The fitness and representative costs of all of these chromosomes are computed individually, after which the population is evaluated using the *NSGA-II* procedure. Based on this evaluation, parents are selected to form a mating pool, from which offspring is generated. This takes place in two steps: a crossover between the two parents and a random mutation to some of the genes in the child chromosomes. Also for the offspring, the fitness and representative costs need to be computed, after which the combined population (equal to twice the population size) is evaluated. The best 50% is then passed on to the next generation. The process now continues from step 3, where the new population is evaluated to be able to select new parents for the mating pool. This process is repeated until the model converged sufficiently. Plots containing all relevant information are produced and model results are compared to those of other runs.

5.5. Model details

Now that the type of *GA*, its decision variables, constraints, functions, process and input parameters have been determined, the parametric model can be completed by making some specific choices to obtain optimal results. Probably, these choices are not optimal initially, which is why the model needs to be tuned based on its results.

5.5.1. Operator choices

A selection operator for both the selection of the parents as for the selection of the chromosomes moving on to the next generation has been chosen in Section 5.1.5. For crossover and mutation however, operator choices still need to be made.

Regarding crossover, it is chosen to remain close to recombination processes in nature. The alleles of child chromosomes are randomly picked in between the alleles corresponding to the respective genes of the parents. This does not always result in valid layout alternatives, which is why a new generator is built that picks values until valid options are obtained. For mutation, a Gaussian distribution is used with a standard deviation that equals the mutation size (see Section 5.5.2). Again, this may lead to invalid layout alternatives, so another generator is built to account for mutations, which picks random alleles for the corresponding gene until a valid value is obtained. Mutations are not restricted to occur to a single gene, so mutations in several genes should still lead to valid layout alternatives.

5.5.2. Optimisation parameters

A genetic algorithm does not uniquely depend on the input by the user. It also needs to be tuned based on its optimisation parameters, which determine the performance of the model. In the tuning process, values for the optimisation parameters are varied until a set is obtained that results in a robust model. Most importantly, the model should produce consistent results (final layouts that are approximately equal over several runs), it should converge to the global optimum in as little time as possible and it should consider enough diversity in the evaluated solutions. The optimal set of optimisation parameters is always related to a specific problem, which is why the values for the optimisation parameters cannot be predefined. In this research, four different optimisation parameters are used, which are stated below:

Mutation rate The probability that a mutation occurs in a certain gene. A low mutation rate may result in getting stuck in local optima, whereas a large mutation rate may hinder the convergence of the model.

Mutation size Standard deviation of the mutation distribution, determining the strength of the resulting disturbance. A low mutation size may not be able to overcome local optima, whereas a large mutation size may prevent the model from improving its results in the final stage of the optimisation process.

Population size The amount of chromosomes forming a single population. Increasing the population size leads to broader coverage of the solution space, however it also significantly increases the runtime of the model.

Convergence rate Indicator for the extent of convergence that needs to be reached before the model stops running. In this way, the model stops running soon when an optimum is found in little time. On the other hand, the model continues running if model results keep improving.

5.5.3. Model uncertainty

To be able to qualify the obtained results through the parametric model, all model uncertainties should be addressed. Attention has been paid to the generic model uncertainties for breakwater layout alternative comparison, as mentioned in Section 1.1. Model uncertainties can roughly be divided into three categories, which are elaborated below.

Standard uncertainties Uncertainties that are inflicted on all layout alternatives within the applied methodology. These uncertainties are by no means influenced by the model performance.

- Outdated, incomplete or inaccurate input data
- Lack of adequate modelling techniques
- Inaccuracy in the determination of downtime and costs
- Uncertainties caused by model simplifications and boundary conditions

Observations are discussed in Section 9.1.

Robustness Uncertainties that can be directly related to the optimisation method, in this case the genetic algorithms. They are fully dependent on model performance and determine the quality of the model results. Two main groups of uncertainties can be discerned:

- Uncertainty in the determination of the optimisation parameters
- Robustness indicators
  - **Consistency**
    Inconsistency in cost estimations and optimal port layout generation over several runs
  - **Convergence**
    Insufficient convergence towards the global optimum
  - **Diversity**
    Only considering solutions in a confined part of the solution space
- Uncertainty inflicted by the random noise generated by the stochastic nature of genetic algorithms

Model tuning may reduce the uncertainty in the determination of the optimisation parameters to a minimum (see Chapter 6). Uncertainties related to the robustness indicators are treated in Chapter 7 and for a specific case in Section 8.3. Outcomes are discussed in Section 9.2.

Flexibility Uncertainties related to the ability of the model to adapt to changing input conditions and its compliance with flexibility in port design. These factors may be influenced by model performance.

- Insufficient adaptability of model results to environmental conditions
- Uncertainty in effects of construction phasing
- Uncertainty in effects of possible future port developments

Adaptability of model results is assessed in general in Chapter 7. Outcomes and observations are discussed in Section 9.4 & 9.5.

6. Model sensitivity

Genetic algorithms do require specific instructions, as simply running the parametric model – using the set-up proposed in Chapter 5 – would result in unrealistic results. As explained in Section 5.5.2, tuning of optimisation parameters should take place to be able to produce consistent results in an efficient manner. For optimisation, four different parameters are used, which are the the mutation rate, the mutation size, the population size and the convergence rate for stopping. Sensitivity of these parameters should be assessed, so that ultimately an optimal set can be established (see Section 6.5).

6.1. Model configuration

Default values apply for all input parameters, as stated in Appendix D.1. Nevertheless, for some parameters default values do not exist, as they generally very widely between different ports and a default value therefore would not result in useful information. For those parameters, some arbitrary values have been chosen to use in this chapter, which are given in Appendix D.2. A wave climate with waves coming from two directions is considered, as accounting only for a single wave direction would result in an oversimplified and therefore unrealistic situation. As it is uncertain if the model can handle more complex wave climates, this is treated separately in a later stage (see Section 7.1.2). The environmental conditions that are used for model tuning are given in Appendix E.1. It is expected that the runtime of the model increases with the number of environmental conditions. Consequently, the amount of conditions is kept to a minimum, while focusing on wave height and direction, as these generally have the largest contribution on breakwater layout. All other environmental conditions are taken to be equal for all conditions, while not exceeding critical values. More complex wave climates likely require more conditions to be represented correctly.

Three out of four optimisation parameters need to be tuned, as their optimal value is unpredictable. No optimal sets exist that are feasible for all problems (Kramer, 2017). The convergence rate for stopping is not optimised, but determined after analysing the behaviour of the model for several runs. The stopping criterion is met when all conditions in Equation 6.1 apply, resulting in a sufficiently low probability that the model would find considerably better solutions in a small amount of time.

$$\begin{aligned} nr\_generations &> 50 \\ avg\_last(15) - avg\_prev(15) &< cvg\_rate \\ best\_fit(-10) &= best\_fit \end{aligned} \tag{6.1}$$

The first condition in Equation 6.1 implies that the number of generations ($nr\_generations$) should have exceeded fifty. The second condition is satisfied when the difference between the average fitness score of the last fifteen generations ($avg\_last(15)$) and that of the previous fifteen ($avg\_prev(15)$) is lower than the convergence rate (cvg_rate). This rate has been set to 0.001. The final condition implies that the best fitness score of ten generations ago ($best\_fit(-10)$) should be equal to the best fitness score of the last generation ($best\_fit$), meaning that no improvements have been made anymore in the best layout alternative.

During the tuning process, three runs are performed for every optimisation parameter value. The reason for this is that every run results in different results as a stochastic search method is applied. This means that every optimisation parameter also should be checked based on consistency. Four values per parameter are analysed, resulting in twelve runs per optimisation parameter. All four values are compared based on the average of the three runs.

6.2. Mutation rate

The main aspects to observe when comparing mutation rates are the model convergence and the ability to escape local optima. An appropriate balance should be found between these criteria. According to Deb et al. (2002), optimal mutation rates are usually in the order of $1/n$, where n represents the number of decision variables in a chromosome. With fourteen decision variables, the mutation rate should therefore approximately equal to 7%. After observing several runs, it was however observed that a large number of mutated layout alternatives did not comply with the boundary conditions and were therefore rejected. Higher mutation rates are therefore required. Runs have been performed for mutation rates of 16%, 18%, 20% and 22%. A population size of 100 chromosomes per generation and a mutation size of 25% have been used as they turned to give acceptable results. Resulting CAPEX/OPEX and downtime are visualised in Figure 6.1.

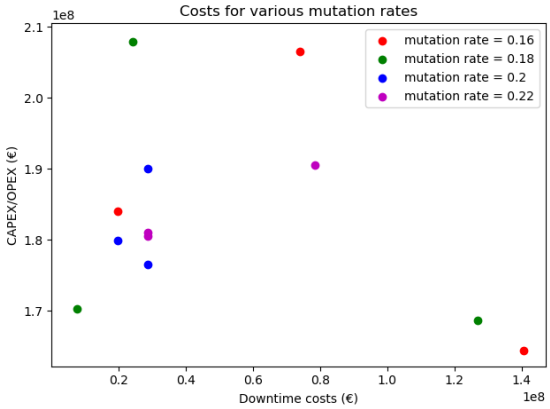

Figure 6.1: Tuning of mutation rate (population size = 100; mutation size = 25%), best layout alternatives per run

Mutation rate	**0.16**	**0.18**	**0.2**	**0.22**
Run 1	0.642	0.609	0.823	0.669
Run 2	0.884	0.775	0.877	0.860
Run 3	0.590	1.012	0.902	0.858
Average	*0.705*	*0.799*	*0.867*	*0.796*

Table 6.1: Fitness scores for various mutation rates (population size = 100; mutation size = 25%)

Several conclusions can be drawn when observing Figure 6.1. First of all, the best layout alternative corresponds to a mutation rate of 18%. The final solution represented in green in the lower left corner dominates almost all other solutions. Only the two alternatives in the lower right corner are not dominated, however they have significantly higher downtime costs. The green solutions however show a large spread. A mutation rate of 20% results in the lowest spread, generating final alternatives having highest fitness scores on average. Mutation rates of 16% and 22% both show an alternative which performs weak on both objectives. It can therefore be concluded that a mutation rate of 20% resulted in the most consistent model performance.

Both for mutation rates of 18% and 20%, the model did converge approximately at an equal amount of generations, ranging from 100 to 160 generations. For a mutation rate of 16%, the model often converged too soon (in less than 100 generations), indicating a local optimum. For a mutation rate of 22%, the model sometimes converged too soon and sometimes took too long to converge (more than 200 generations). In cases were it took too long, this was probably due to the high mutation rate, as diverse alternatives kept getting created.

6.3. Mutation size

For mutation size tuning, values of 15%, 20%, 25% and 30% were used. The product of the mutation size and a characteristic distance varying with the decision variable equals the standard deviation of the mutation. This characteristic distance is for variable $x3$ for example equal to the distance to $x2$. Therefore, the closer $x3$ is located to $x2$, the smaller the mutation generally is. The population size is kept at 100 alternatives. The mutation rate is changed to 19% to check whether it outperforms other mutation rates for a mutation size of 25%. Results are shown in Figure 6.2.

First of all, it can be seen that the scales on the x- and y-axis differ. For CAPEX/OPEX the alternatives are located quite close to each other, whereas for downtime costs the spread is much larger. This results in the green and blue dot in the middle left (CAPEX/OPEX $\approx$ €$180 \cdot 10^6$) showing highest fitness scores. The mutation size of 20% shows the least spread in costs and the highest average fitness score. It also scored better based on CAPEX/OPEX than the mutation size of 25%, but worse on downtime costs. The mutation size of

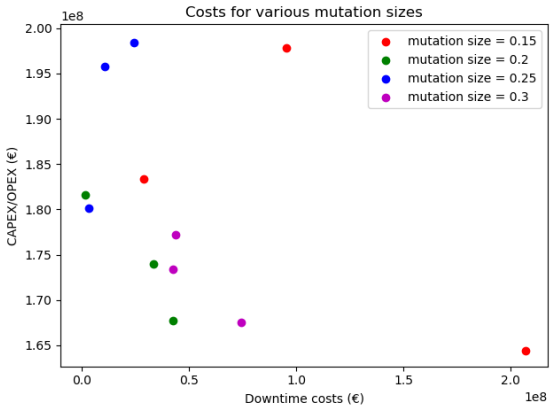

Figure 6.2: Tuning of mutation size (population size = 100; mutation rate = 19%), best layout alternatives per run

Mutation size	0.15	0.2	0.25	0.3
Run 1	0.849	0.983	0.809	0.834
Run 2	0.614	0.857	0.983	0.814
Run 3	0.485	0.868	0.872	0.745
Average	*0.649*	*0.903*	*0.888*	*0.798*

Table 6.2: Fitness scores for various mutation sizes (population size = 100; mutation rate = 19%)

20% showed faster convergence than for 25%, which is not expected, since a smaller mutation size continue making small(er) improvements in the final stage. For the other mutation sizes several runs did result in fast convergence to a local optimum. In general, it can be stated that the differences in outcomes between a mutation size of 20% and 25% are not that large. For the next run, a mutation size of 22% is adopted to observe if it outperforms both mutation sizes used above.

The runs with a mutation size of 25% showed a higher average fitness score with a mutation rate of 19% (see Table 6.2) than for mutation rates of 18% and 20% (see Table 6.1). The optimal mutation rate can therefore be set to 19%.

6.4. Population size

The population size has a large contribution to the model performance. Increasing it results in inclusion of a wider search domain and a higher probability of finding alternatives inducing lower total costs over the course of generations. The downside is that by increasing the population size, the model runtime also increases. A qualified population size can therefore be defined as generating sufficiently good results in a sufficiently short time. Three population sizes are compared to each other: 50, 100 and 150 alternatives per generation. A mutation rate of 19% is used and a mutation size of 22%, as proposed in Section 6.3. Results are shown in Figure 6.3.

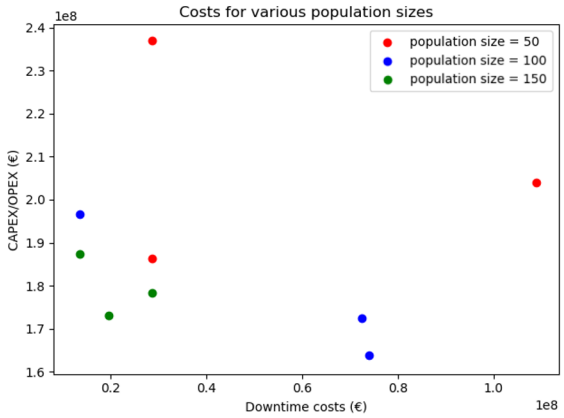

Figure 6.3: Tuning of population size (mutation size = 22%; mutation rate = 19%), best layout alternatives per run

Population size	50	100	150
Run 1	0.575	0.857	0.869
Run 2	0.837	0.757	0.896
Run 3	0.677	0.735	0.934
Average	*0.703*	*0.783*	*0.900*

Table 6.3: Fitness scores for various population sizes (mutation size = 22%; mutation rate = 19%)

It can clearly be seen from Figure 6.3 that an increase in population size leads to improved performance. Runtime however showed to increase proportionally with population size. In Figure 6.3, a population size of 150 clearly outperforms a population size of 100. For a population size of 100, the model was however able to converge in a fewer amount of generations on average. An example has been given in Figure 6.4, where the

progress of the fitness score over the course of generations is illustrated. Two runs with comparable fitness scores, but different population sizes (100 and 150), are compared based on convergence. It can be concluded that the run in Figure 6.4a showed faster convergence. Nevertheless, the many jumps in Figure 6.4b illustrate the ability of the model to escape local optima for a population size of 150. As both properties are desired within the model, it is advised to use a population size between 100 and 150.

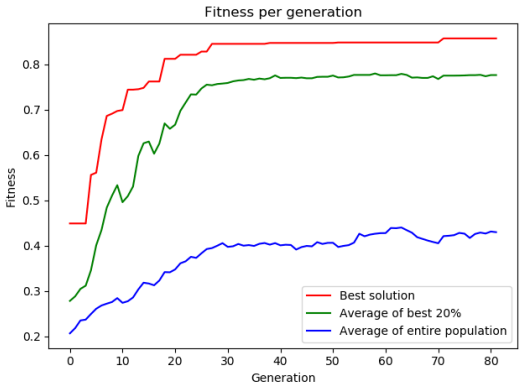

(a) Population size = 100; Run 1 (score: 0.857)

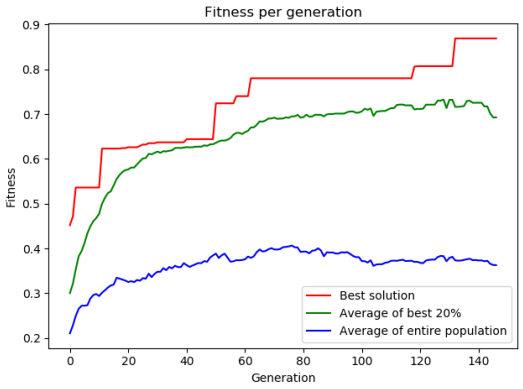

(b) Population size = 150; Run 1 (score: 0.869)

Figure 6.4: Fitness graphs for runs with various population sizes

When comparing the fitness scores of the runs for a population size of 100 in Table 6.3 to the scores in Table 6.2, it can be seen that mutation sizes of 20%, 25% and 30% all showed higher scores than a mutation size of 22%. A mutation rate of 22% is therefore unsuitable to use as optimisation parameter.

6.5. Base case

Based on Sections 6.2 to 6.4, the set of optimisation parameters to be used in the continuation of this report is established as in Table 6.4.

Parameter	Mutation rate	Mutation size	Population size
Value	19%	25%	120

Table 6.4: Set of optimisation parameters after model tuning

Since a mutation size of 22% showed unsatisfactory results, mutation sizes of 20% and 25% were compared once again, using the new set of parameters. A mutation size of 25% now clearly showed the ability to escape local optima, even as a higher average fitness score, and is therefore adopted in Table 6.4. It can however be stated that the results of a certain set of optimisation parameters may vary widely due to the stochastic nature of the parametric model. To be entirely certain about the correct choice of this set, more extensive research would be required, which is considered to be not necessary yet in the current model development stage. This is further elaborated in Section 9.2.

Resulting layouts using the parameters in Table 6.4, for three separate runs, are shown in Figure 6.5. All other input is still defined as described in Section 6.1. The terminal is visualised by the rectangle in the lower right corner. The berthing basin is shown by the dashed blue line. Some observations regarding Figure 6.5 are summed up below.

- The position of the turning basin, the orientation of the approach angle and the position of the primary breakwater tip can be considered consistent.
- The position of the secondary breakwater and the alignment of the primary breakwater around the turning basin still requires improvement.
- Overall consistency is considered as fairly good, as fitness scores and the cost comparison in Table 6.5 are comparable for all runs. Total costs for separate runs differ at maximum about 2%, costs related to the individual objectives differ maximally 4% in relation to the total costs (see Table 6.6).

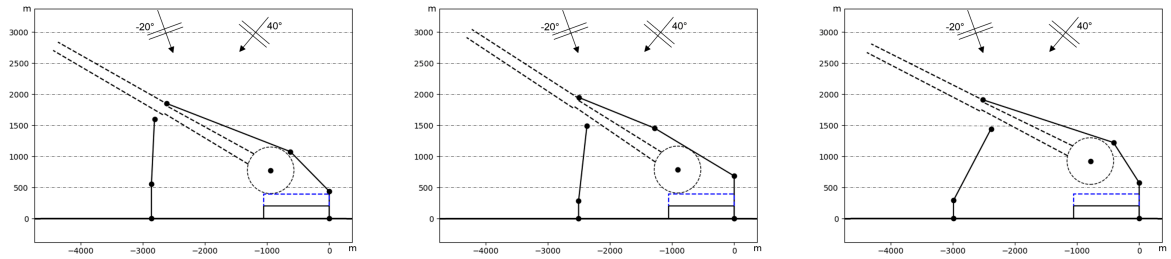

(a) Run 1 (score: 0.906) (b) Run 2 (score: 0.901) (c) Run 3 (score 0.886)

Figure 6.5: Final layouts for base case

Type of costs	Run 1	Run 2	Run 3
CAPEX/OPEX (capitalised)	**€171.6 million**	**€168.1 million**	**€175.9 million**
Breakwater construction	€62.6 million	€61.9 million	€65.3 million
Breakwater maintenance	$€1.3 \cdot 10^6$ per year	$€1.2 \cdot 10^6$ per year	$€1.3 \cdot 10^6$ per year
Capital dredging	€53.2 million	€51.8 million	€51.6 million
Maintenance dredging	$€1.5 \cdot 10^6$ per year	$€1.5 \cdot 10^6$ per year	$€1.6 \cdot 10^6$ per year
Downtime costs (capitalised)	**€27.2 million**	**€31.7 million**	**€27.2 million**
Average downtime per berth	3%	3.5%	3%

Table 6.5: Cost information per run for base case

Type of costs	Maximum difference	Percentage of min. total costs
Total costs	€4.3 million	2%
CAPEX/OPEX	€7.8 million	4%
Downtime costs	€4.5 million	2%

Table 6.6: Cost consistency for base case

Fitness graphs for all three runs are given in Figure 6.6. It can be seen that a good balance has been found between the ability to escape local optima (visualised by the jumps in the red line) and the amount of generations required to converge. The average runtime is equal to approximately one hour.

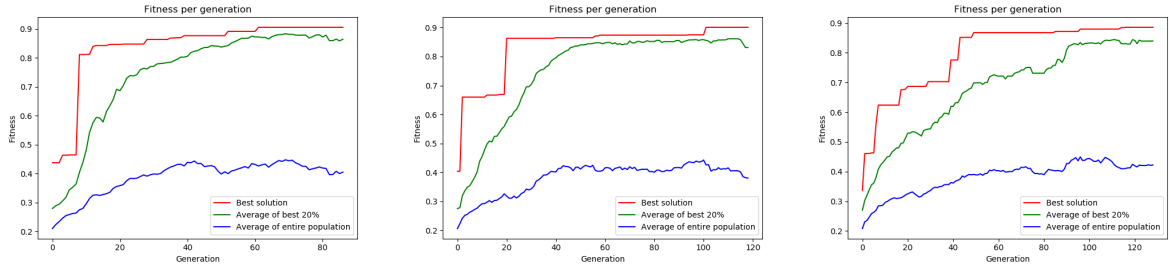

(a) Run 1 (score: 0.906) (b) Run 2 (score: 0.901) (c) Run 3 (score 0.886)

Figure 6.6: Fitness graphs for base case

As run 1 shows best performance (having the largest fitness score and thus lowest total costs), it is used to compare the layout, costs and downtime of the base case to those of other cases (also best out of three runs).

7. Model results

One of the most powerful benefits of a parametric breakwater layout model would be to perform rapid sensitivity analyses on key parameters. It is therefore of crucial importance to assess the effect of changing these parameters on the resulting breakwater layout. In this way, more insight can be obtained in the effect of uncertainties within certain parameters. For other parameters, resulting layout changes can be a reason to make design adjustments.

7.1. Wave conditions

The environmental conditions affect the breakwater layout to a large extent. Wave conditions form the most relevant environmental conditions in most cases, as wave height reduction is usually the main reason a breakwater comes into place. Within this model, breakwater layout is not affected by currents and winds. Several wave climates are considered. First of all, a wave climate with a single wave direction is compared to a double wave direction (which is already treated in Chapter 6). Next, a full wave climate is treated, using both mild and rough wave conditions.

7.1.1. Single wave direction

The response of the model to a single wave direction is tested and compared to that of a double wave direction, which has already been treated in Chapter 6. The environmental conditions for a single wave direction can be found in Appendix E.2. Model consistency is quite comparable to that of a double wave direction, as can be seen in Figure 7.1.

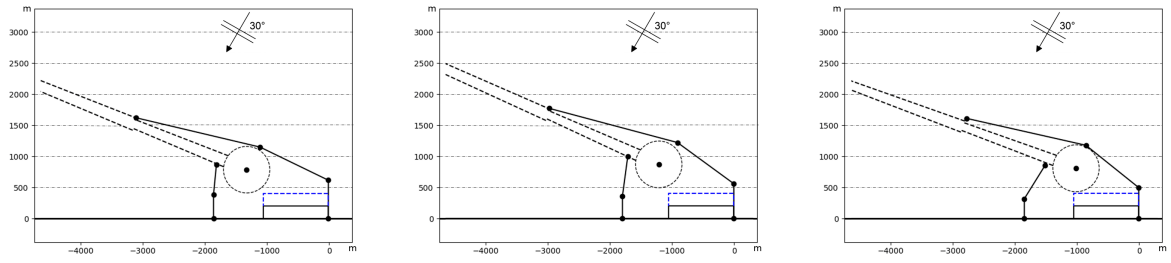

(a) Run 1 (score: 1.003) (b) Run 2 (score: 1.029) (c) Run 3 (score: 1.077)

Figure 7.1: Final layouts for a single wave direction

Type of costs	Run 1	Run 2	Run 3
CAPEX/OPEX (capitalised)	**€176.4 million**	**€172.0 million**	**€164.1 million**
Breakwater construction	€55.8 million	€58.7 million	€51.8 million
Breakwater maintenance	$€1.1 \cdot 10^6$ per year	$€1.2 \cdot 10^6$ per year	$€1.0 \cdot 10^6$ per year
Capital dredging	€63.2 million	€57.0 million	€58.3 million
Maintenance dredging	$€1.8 \cdot 10^6$ per year	$€1.7 \cdot 10^6$ per year	$€1.7 \cdot 10^6$ per year
Downtime costs (capitalised)	**€3.0 million**	**€3.0 million**	**€3.0 million**
Average downtime per berth	0.7%	0.7%	0.7%

Table 7.1: Cost information per run for a single wave direction

Type of costs	Maximum difference	Percentage of min. total costs
Total costs	€12.3 million	7%
CAPEX/OPEX	€12.3 million	7%
Downtime costs	€0	0%

Table 7.2: Cost consistency for a single wave direction

The costs in Table 7.1 are given as comparison between different runs, rather than an attempt to approximate the exact cost values. Run 3 shows best performance as it generates lowest total costs. Regarding model performance, some observations can be made, often based on the differences with the breakwater layout configurations with a double wave direction (see Figure 6.5):

- The model makes a clear choice on the breakwater layout alternative that should be adopted. For a single wave direction, the secondary breakwater clearly has a less significant role in wave reduction when compared to the breakwater layout for a double wave direction, leading to a decrease in breakwater construction costs.
- The parametric model is able to perform a balance between direct and indirect CAPEX/OPEX. When comparing Figure 7.1 to Figure 6.5, a single wave direction seems to allow for higher dredging costs so that the breakwaters can be positioned more favourably.
- Downtime costs are significantly reduced when only a single wave direction is considered. Besides, despite of the stochastic variability in the performed runs, downtime costs can be considered very consistent for a single wave direction.

It is obvious that downtime costs can be reduced when the port only needs to be protected from waves coming from a single direction. Insight in the balance between breakwater construction costs, dredging costs and corresponding downtime costs however clearly shows that the model can have added value in an early design stage.

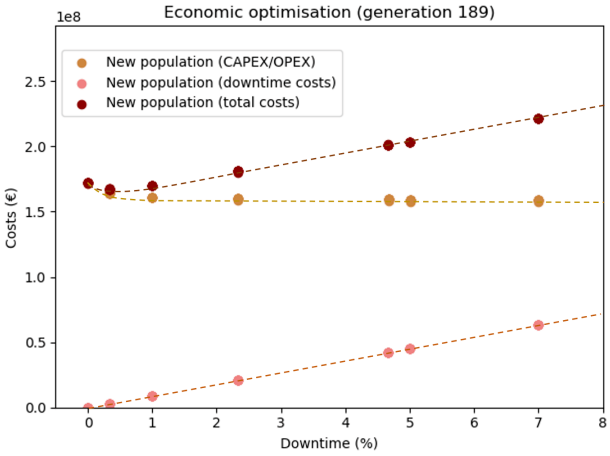

Figure 7.2: Economic optimisation graph for a single wave direction

The economic optimisation graph for a single wave direction is provided in Figure 7.2. Some general remarks are summed up below:

- A parabolic shape of the total costs function can be observed for lower downtime ranges (below approximately 2%). For higher downtime ranges the behaviour of the total costs function is almost linear, which is mostly due to the exclusion of port competition and is therefore expected.
- The optimal downtime range is located in between 0 and 1%. This is relatively low, which can be subscribed to the inclusion of only a single wave direction, making it comparatively easy to offer the required amount of wave protection.
- It is desired to have more results within the lower downtime ranges to be able to determine the optimum more accurately. This however implies that the number of environmental conditions used as

input should increase, which also increases runtime.

7.1.2. Full wave climate

Both a mild and a rough wave climate are analysed, so that conclusions can be drawn regarding the intensity of the waves and its effect on the breakwater layout. All input conditions are equal for both wave climates, except for the wave heights (so wave directions are also equal). For a mild wave climate, the final layout is shown in Figure 7.3a. The final layout for a rough wave climate can be found in Figure 7.3b. The corresponding environmental conditions can be found in Appendix E.3 & E.4. The waves for a rough wave climate are about 2-3 times higher than for a mild wave climate.

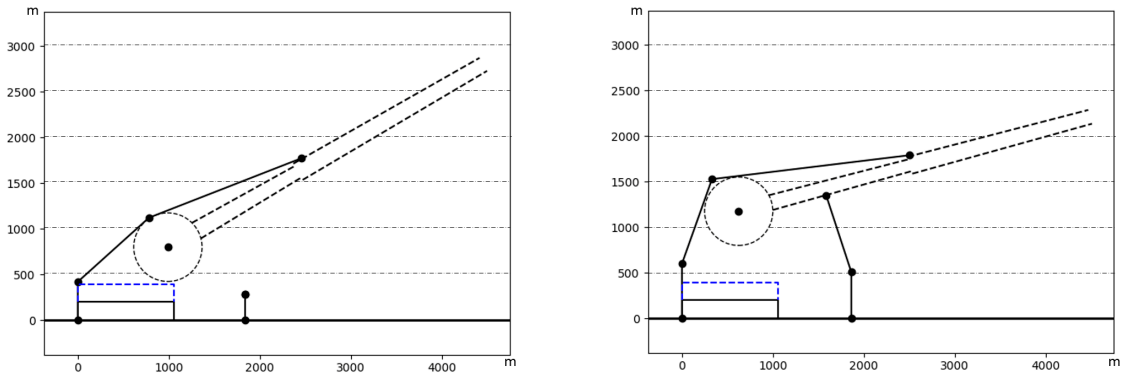

(a) Mild wave climate

(b) Rough wave climate

Figure 7.3: Final layouts for a full wave climate with various intensities

Type of costs	Mild wave climate	Rough wave climate
CAPEX/OPEX (capitalised)	**€149.5 million**	**€185.3 million**
Breakwater construction	€43.0 million	€68.3 million
Breakwater maintenance	$€0.8 \cdot 10^6$ per year	$€1.4 \cdot 10^6$ per year
Capital dredging	€54.3 million	€52.8 million
Maintenance dredging	$€1.8 \cdot 10^6$ per year	$€1.9 \cdot 10^6$ per year
Downtime costs (capitalised)	**€5.4 million**	**€43.5 million**

Table 7.3: Cost information for a mild and rough wave climate

	Maximum difference		Percentage of min. total costs	
Type of costs	Mild wave climate	Rough wave climate	Mild wave climate	Rough wave climate
Total costs	€6.3 million	€11.0 million	4%	5%
CAPEX/OPEX	€11.8 million	€9.1 million	8%	4%
Downtime costs	€6.0 million	€18.2 million	4%	8%

Table 7.4: Cost consistency for a mild and rough wave climate

Some conclusions can be drawn regarding Figure 7.3 and Table 7.3:

- Only the best out of three runs are shown in Figure 7.3. As the other runs did not always show the same breakwater layout alternative, the consistency is considered lower than for a single or double wave direction, although costs are still quite consistent (see Table 7.4). This makes it harder to state that the optimal layout alternative has been found. More runs should be performed to increase the reliability, which requires more time and the process therefore becomes less efficient. Another option is layout validation, which is performed for a case in Chapter 8.
- The way the model deals with the differences in wave heights is as expected, as for a rough wave climate a more extensive amount of protection is applied. This is reflected in Table 7.3 by a larger share of downtime costs.

- The model is able to fully reduce the secondary breakwater to a single segment that extends until the breaker line, therefore functioning only to block the longitudinal sediment transport. Additional maintenance dredging costs (capitalised) coming along with the removal of the secondary breakwater are therefore found to be larger than its construction costs. Exclusion of the secondary breakwater would lead to increased design flexibility with regard to possible future port developments. This is however not incorporated in the optimisation.
- For a rough wave climate, downtime costs become less consistent in relation to CAPEX/OPEX (see Table 7.4). Also, when comparing downtime cost consistency for a full wave climate to that of a single and double wave direction, it appears that this consistency decreases for a more complex wave climate.

For a rough wave climate, almost all waves are higher than two metres and some even reach heights of 6.5 m. Consequently, the parametric model is pushed to its limits. It can be seen that the model has chosen to put the turning basin further offshore to achieve a breakwater gap orientation that diminishes waves coming in from almost all directions. Higher investments are allowed, as the main concern is to keep downtime costs to a minimum (see Table 7.3). Low model consistency indicates that the model struggles in finding the global optimum, which can also be observed from the fitness graph in Figure 7.4.

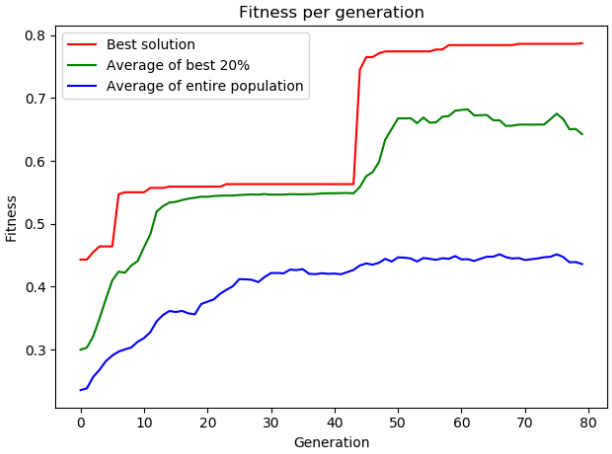

Figure 7.4: Fitness graph for a rough wave climate

In Figure 7.4, a clear jump in the fitness score of the best generated solution can be discerned in generation 44. The model did almost fully converge beforehand, as both the red and the green line did not show any significant improvements anymore. Nonetheless, the model managed to improve the fitness score of the best alternative by more than 30% in a single generation. This indicates the ability of the model to escape local optima, which underlines the power of genetic algorithms and shows why this optimisation method is found to be appropriate for the considered problem. In this case, the jump was the result of a mutation of the RHS gene, which resulted in a flip of the entire port layout around the y-axis. From the graph it can also be seen that model performance has been picked up again after the jump, therewith starting the search towards a better optimum.

7.2. Number of berths

The amount of berths to be constructed in a terminal forms one of the main parameters to be optimised. It is often difficult to immediately make a decision on the amount of berths that is optimal, as downtime occurring at a berth largely varies with the breakwater layout. In some cases, the highest waves occur at the berth located closest to the primary breakwater, while in other cases the opposite is true. When it is uncertain how many berths should be constructed or how many berths should still be constructed in the future, the resulting costs and downtime can be analysed by making use of the parametric model.

In the base case (see Figure 7.5b), three berths are present, with the possibility to expand to five berths in the future. Two alternatives are treated in this section, of which the first is a single berth with the possibility to expand to two berths (see Figure 7.5a). The other alternative is eight berths without expansion potential (see Figure 7.5c).

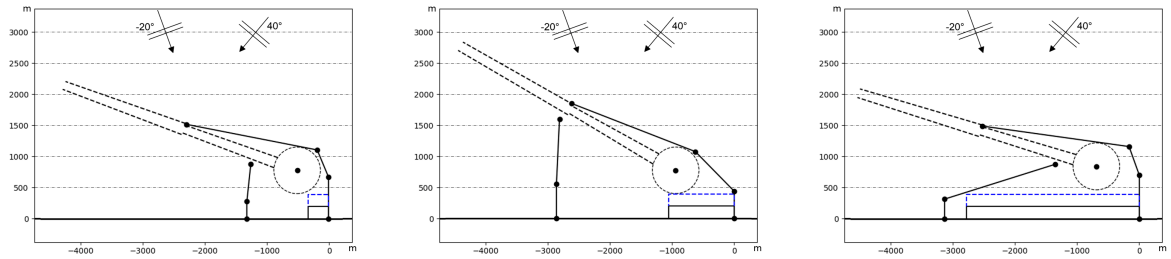

(a) Single berth (future: 2 berths) (b) Three berths (future: 5 berths) (c) Eight berths (no expansion)

Figure 7.5: Final layouts for a varying amount of berths

Type of costs	Single berth	Three berths	Eight berths
CAPEX/OPEX (capitalised)	**€140.2 million**	**€171.6 million**	**€256.7 million**
Breakwater construction	€48.3 million	€62.6 million	€63.8 million
Breakwater maintenance	$€1.0 \cdot 10^6$ per year	$€1.3 \cdot 10^6$ per year	$€1.3 \cdot 10^6$ per year
Capital dredging	€45.4 million	€53.2 million	€110.5 million
Maintenance dredging	$€1.4 \cdot 10^6$ per year	$€1.5 \cdot 10^6$ per year	$€2.9 \cdot 10^6$ per year
Downtime costs (capitalised)	**€25.7 million**	**€27.2 million**	**€74.1 million**
Average downtime per berth	8%	3%	3%

Table 7.5: Cost information for a varying amount of berths

Regarding Figure 7.5 and Table 7.5, some conclusions can be drawn:

- The model is capable of assessing the profitability of a breakwater gap. For the alternative with three berths, the presence of a breakwater gap resulted in less downtime than for a single berth (allowing for higher investments, see Table 7.5). For eight berths, the model prefers to offer increased protection to a limited amount of berths. This seems logical, as in this way a larger reduction in average downtime per berth can be obtained for an increasing amount of berths.
- From Figure 7.5c, it can be observed that the model seems to struggle in finding the optimal location of the attachment point of the secondary breakwater to the coast, as some unnecessary space is left open. Besides, the primary breakwater is not aligned optimally around the turning basin.

7.3. Limiting wave heights

It is not always possible to choose what limiting wave height to apply in a harbour, as this largely depends on the type of vessels calling at the port and on the type of tugboats that is used. Nevertheless, it is interesting to see what effects these changes have on the breakwater layout. It might give a reason to invest in better tugboats or to reconsider nautical safety standards.

When looking at the base case, it can be seen that the primary breakwater extends until the point of minimum sheltered channel length that is required to comply with the boundary conditions. Therefore, increasing the limiting wave height for navigation is likely not to change anything to the breakwater layout. It is however interesting to assess the effect of a decrease in limiting wave height for navigation. In Figure 7.6a, the limiting wave height has been decreased to 0.8 m and the final layout for the base case (Figure 7.6b) is again provided to compare them to each other.

Type of costs	0.8 m	1.5 m
CAPEX/OPEX (capitalised)	€170.8 million	€171.6 million
Downtime costs (capitalised)	€96.7 million	€27.2 million
Average downtime per berth	*8%*	*3%*

Table 7.6: Cost and downtime information for several limiting wave heights for navigation

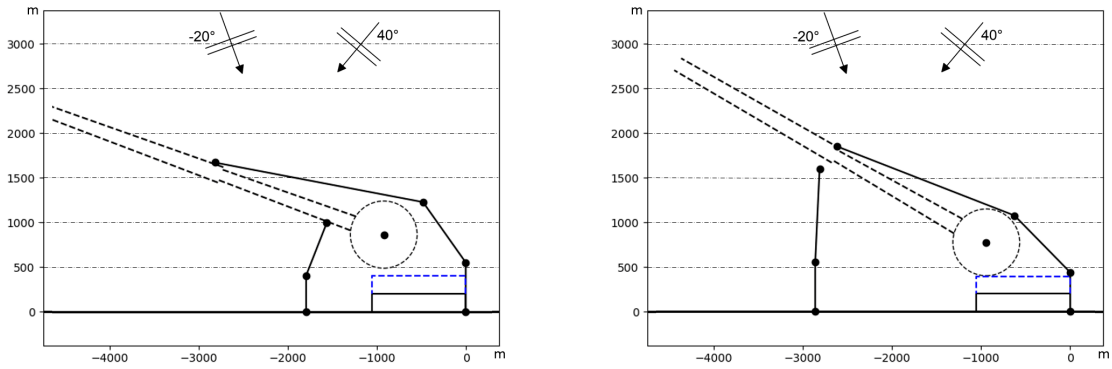

(a) Limiting wave height for navigation: 0.8 m (b) Limiting wave height for navigation: 1.5 m

Figure 7.6: Final layouts for several limiting wave heights for navigation

The resulting port layout for a limiting wave height of 0.8 m is remarkable. Some comments are given below:

- Increased protection should be present for point N when the limiting wave height is lowered. The model did not do so, since the investments for increased protection are too high. It is therefore chosen to accept more navigational downtime (8%).
- The boundary condition that navigational downtime causes operational downtime at all berths (as vessels cannot sail in/out anymore) results in 8% downtime at all berths. This is not realistic, as operational downtime usually dominates navigational downtime. It is therefore recommended not to realise a certain port layout when a limiting wave height of 0.8 m should be respected.
- As navigational downtime dominates operational downtime in Figure 7.6a, less attention has to be paid to reducing wave heights at the berth. This is not the case in reality, which is why the relation between navigational and operational downtime should be treated in more detail within the model (see Section 10.2.2). The result is a lower CAPEX/OPEX in Figure 7.6a than in Figure 7.6b, which realistically should be the other way around.

A model result as the one in Figure 7.6a could be a reason to invest in larger tugboats or to reconsider nautical safety standards.

Operational downtime due to excessive wave heights at the berth forms one of the main contributors to total port downtime. To analyse its sensitivity, three different limiting wave heights for operations have been studied. Final layouts are presented in Figure 7.7.

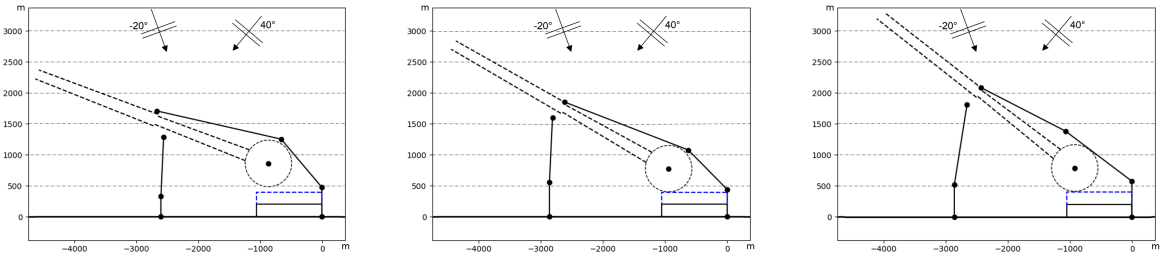

(a) Limiting wave height: 0.3 m (b) Limiting wave height: 0.5 m (c) Limiting wave height: 0.7 m

Figure 7.7: Final layouts for several limiting wave heights for operations

Type of costs	**0.3 m**	**0.5 m**	**0.7 m**
CAPEX/OPEX (capitalised)	€173.9 million	€171.6 million	€174.4 million
Downtime costs (capitalised)	€136.0 million	€27.2 million	€6.0 million
Average downtime per berth	*15%*	*3%*	*0.5%*

Table 7.7: Cost and downtime information for several limiting wave heights for operations

Some conclusions are summed up below:

- The model manages to give increased importance to downtime reduction when the limiting wave height for operations is lowered. Downtime costs still increase considerably, but the breakwater gap orientation is changed such that it becomes harder for waves to propogate into the harbour for lower limiting wave heights.
- The layout in Figure 7.7c should result in the lowest CAPEX/OPEX, as wave heights do not have to be reduced as much as in the other cases. The opposite is true, which can be subscribed to a less optimal layout. This can be affirmed by looking at the position of the secondary breakwater (an unnecessary bend is present) and the enclosure of the turning basin by the primary breakwater.
- Downtime costs are clearly affected by the change in limiting wave height, but layout changes are minimal and mostly related to gap orientation and approach channel orientation.

7.4. Bathymetry

Bathymetry is incorporated into the model by means of a constant bed slope. Since both breakwater construction costs and capital dredging costs are depth dependent, the bed slope has a large influence on the breakwater layout. For steep bed slopes, the most important concern is that the breakwaters do not reach large water depths, as this results in a significant rise in costs. For mild bed slopes, the main goal is to reduce dredging costs to a minimum, as dredging should take place until a significant distance in cross-shore direction. The final layouts are generated for various bed slopes, which are visualised in Figure 7.8.

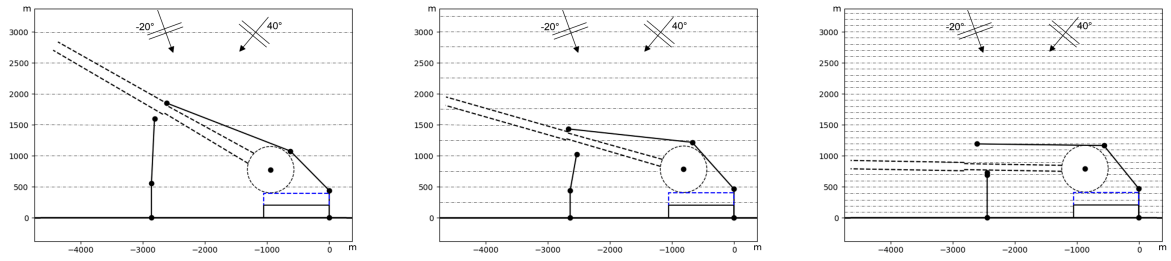

(a) Bed slope: 1:100 (b) Bed slope: 1:50 (c) Bed slope: 1:20

Figure 7.8: Final layouts for various bed slopes

Type of costs	1:100	1:50	1:20
CAPEX/OPEX (capitalised)	**€171.6 million**	**€160.8 million**	**€236.4 million**
Breakwater construction	€62.6 million	€86.5 million	€162.4 million
Breakwater maintenance	$€1.3 \cdot 10^6$ per year	$€1.7 \cdot 10^6$ per year	$€3.2 \cdot 10^6$ per year
Capital dredging	€53.2 million	€22.4 million	€2.3 million
Maintenance dredging	$€1.5 \cdot 10^6$ per year	$€0.8 \cdot 10^6$ per year	$€0.4 \cdot 10^6$ per year
Downtime costs (capitalised)	**€27.2 million**	**€4.5 million**	**€10.6 million**

Table 7.8: Cost information for various bed slopes

Bed slope effects are clearly reflected in the generated layouts. A clear balance is visible between dredging and breakwater construction costs. With increasing bed slope, the primary breakwater tip is located closer to the shore and the approach channel is oriented more in parallel to the shoreline.

7.5. Downtime costs

Downtime costs are computed using the methodology provided in Section 4.2.2. Apart from downtime itself, the main parameter that changes in Equation 4.4 for different terminals likely is the berth productivity. As ports are modernising rapidly these days, berth productivity increases. In Figure 7.9, the productivity of the berths is therefore varied to assess the sensitivity of the model to productivity changes.

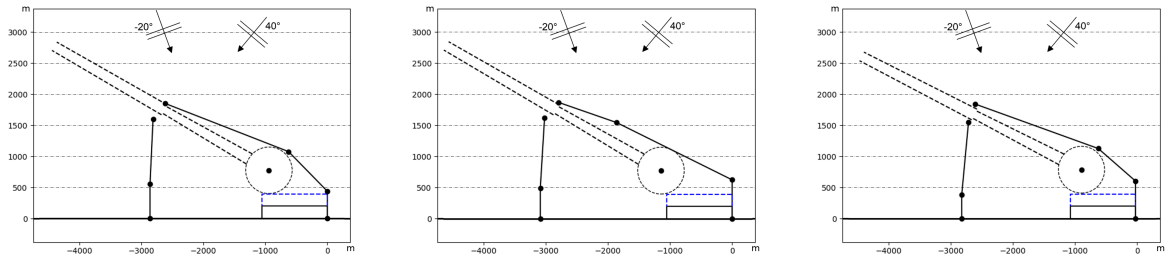

(a) Berth productivity: 35 MPH (b) Berth productivity: 45 MPH (c) Berth productivity: 55 MPH

Figure 7.9: Final layouts for various levels of berth productivity

Type of costs	**35 MPH**	**45 MPH**	**55 MPH**
CAPEX/OPEX (capitalised)	€171.6 million	€179.0 million	€173.7 million
Downtime costs (capitalised)	€27.2 million	€13.6 million	€52.2 million
Average downtime per berth	*3%*	*1%*	*3.5%*

Table 7.9: Cost information for various levels of berth productivity

It can be observed that the port layout stays approximately the same when berth productivity changes. For an equal breakwater layout, downtime costs increase when berth productivity increases (when more turnover is generated, downtime costs increase too), but CAPEX/OPEX stay the same. The resulting Pareto front is consequently spread out more in x-direction. The optimal breakwater layout now should focus more on downtime reduction, which leads to a slightly higher CAPEX/OPEX in the most optimal case. In the economic optimisation graph, the line representing the downtime costs grows faster for an increase in downtime. The optimum is thus shifted to the left and upwards, leading to higher total costs in which the share of CAPEX/OPEX is larger. In general, it can be stated that the effect of berth productivity on the breakwater layout is minimal, as it does not stimulate a trade-off between the CAPEX/OPEX and downtime costs for a certain breakwater layout alternative. The magnitude of the changes applied in Figure 7.9 do not have a visible effect within the current model, as the model accuracy at the moment is still insufficient to consistently take such minor changes into account.

7.6. Harbour siltation

Ultimately, the effect of changes in sediment import on the breakwater layout is investigated. Several combinations of annual siltation thicknesses are treated, of which the respective layouts are given in Figure 7.10.

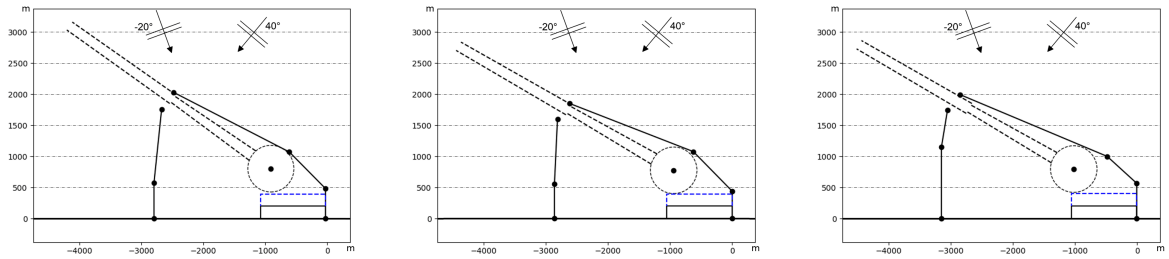

(a) $t_{s,0} = 0.2$; $t_{s,max} = 0.15$; $t_{s,min} = 0.1$ (b) $t_{s,0} = 0.4$; $t_{s,max} = 0.3$; $t_{s,min} = 0.25$ (c) $t_{s,0} = 0.5$; $t_{s,max} = 0.4$; $t_{s,min} = 0.4$

Figure 7.10: Final layouts for various siltation thicknesses in metres per year

Type of costs	a)	b)	c)
CAPEX/OPEX (capitalised)	**€157.9 million**	**€171.6 million**	**€199.5 million**
Breakwater construction	€66.3 million	€62.6 million	€71.2 million
Breakwater maintenance	$€1.3 \cdot 10^6$ per year	$€1.3 \cdot 10^6$ per year	$€1.4 \cdot 10^6$ per year
Capital dredging	€50.9 million	€53.2 million	€53.4 million
Maintenance dredging	$€0.6 \cdot 10^6$ per year	$€1.5 \cdot 10^6$ per year	$€2.3 \cdot 10^6$ per year
Downtime costs (capitalised)	**€33.2 million**	**€27.2 million**	**€9.1 million**
Average downtime per berth	3.5%	3%	1%

Table 7.10: Cost information for various siltation thicknesses

No significant changes can be observed in the breakwater layouts in Figure 7.10. This can mainly be related to the layout configuration of the base case, as it turned out to be most optimal to realise a breakwater gap to effectively reduce downtime. The secondary breakwater is therefore mainly constructed for wave reduction, instead of the reduction in sediment import. The breakwater gap width has already reached its minimum (equal to the length over all of a design vessel), so any increase in the annual siltation thickness would have likely not resulted in breakwater layout changes. It would however been possible that the choice to realise a breakwater gap was not that obvious. As this choice is related both to downtime reduction and to sediment import reduction, a reduction in the annual siltation thickness could in that case have lead to the preference of another breakwater layout alternative. A significant reduction in the difference between $t_{s,0}$ and $t_{s,max}$ could have lead to exclusion of the secondary breakwater. A significant reduction in the difference between $t_{s,max}$ and $t_{s,min}$ could have lead to an alternative having a larger distance between the secondary breakwater tip and the primary breakwater. The generation of an equal breakwater layout alternative for a lower annual siltation thickness therefore indicates that wave reduction has a larger impact on the total costs than sediment import in this case. Besides, it shows once again that the model is able to robustly find the right neighbourhood.

8. Case study

Results have been evaluated based on performance indicators in Chapter 7, however the questions remains if the model is able to find the actual optimum. Therefore, the model results need to be validated in some kind of way. It is chosen to compare the results to a case study to check for similarities and to observe what improvements still need to be made to represent a realistic situation.

8.1. Case introduction

The case that is used to validate the model is the port complex of Tanger Mediterranée (Tanger Med), located in Morocco at the Strait of Gibraltar, which forms the connection between the Atlantic Ocean and the Mediterranean Sea. It therefore has a strategic position, as it forms a crossing point for 20% of global trade. Both North/South and East/West maritime routes cross here, as can be seen in Figure 8.1. The port complex is the largest for containers in Africa, while the Spanish mainland is located only 17 kilometres away. The port complex consists of two container ports, Tanger Med 1 and Tanger Med 2, and a passengers and trucks port. The container ports each consist of two terminals. Tanger Med 1 went into service in 2007 and Tanger Med 2 has been inaugurated by the end of June this year, which marks the completion of the first phase.

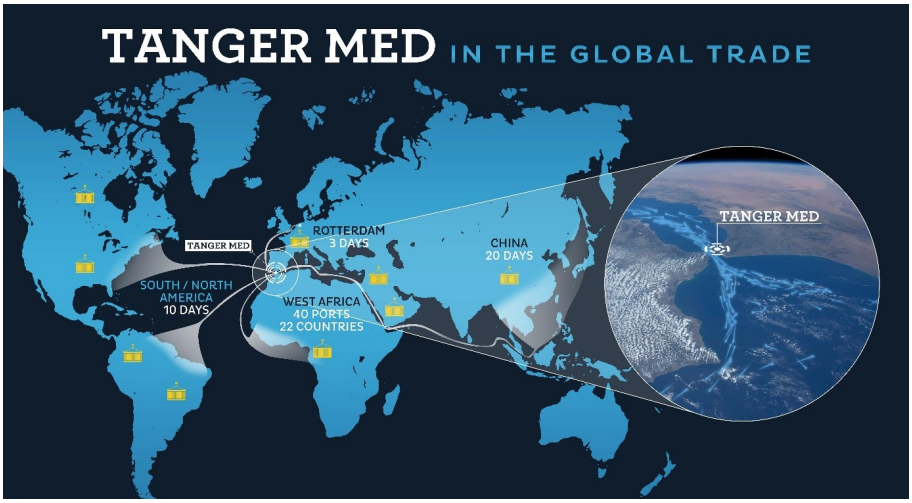

Figure 8.1: Global trade position of the Tanger Med port complex (Tanger Med Port Authority, 2017)

The choice to perform a case study at the Tanger Med port complex is based on several aspects, of which the most important are formed by the simple terminal layout and close to parallel depth contours. The quay wall of both ports is located parallel to the coastline. The port therefore complies with the simplifications and scope restrictions applied in this research (see Section 1.3.2 & 4.1). The most interesting port is formed by Tanger Med 2, as it purely focuses on container shipment. Six berths are to be located here, all in one line. The project consists of several phases, however the breakwaters are constructed in the first phase. Phasing therefore does not have to be included in the breakwater design. The breakwaters are of a composite type, consisting partly out of 35 m high caissons and partly out of rubble-mound with Accropodes^{TM}, which has mainly been chosen due to the steep bed slope at the port location. The breakwater type is not in line with the scope restrictions (see Section 1.3.2), however it is expected to have little effect on the final layout, as it likely does not result in large differences between different alternatives. Cost details are not available, so only the breakwater layout can be compared. Figure 8.2 shows an illustration of what the port of Tanger Med 2 should look like when it is fully operational. The point of view is towards the East and in the upper left part of the figure it is possible to see the port of Tanger Med 1, with the passengers and trucks port located in between.

Figure 8.2: Animation of the port of Tanger Med 2 (Tanger Med Port Authority, 2017)

The environmental conditions are quite difficult to model at this location, but fortunately a simplification of these conditions suffices. The average bed slope is approximately 1:45, as the port is located in a somewhat flatter part in the Strait. The reclamation for the terminal stretches out about 500 m into the sea, which is possibly due to the use of caissons for breakwater construction. Waves from the Atlantic Ocean dominate, as the port is located relatively unsheltered for these (see Figure 8.3). Waves from the Mediterranean Sea are lower and partly blocked by the Moroccan coastline. The tidal range equals approximately 1.0 m. Strong currents are present in the Strait of Gibraltar, mainly flowing from the Atlantic Ocean into the Mediterranean Sea. Figure 8.4 shows the principal current flow, which is from the East, approximately following the curve of the coastline. The location of Tanger Med is indicated with a green circle and the legend on the right shows current velocities in knots.

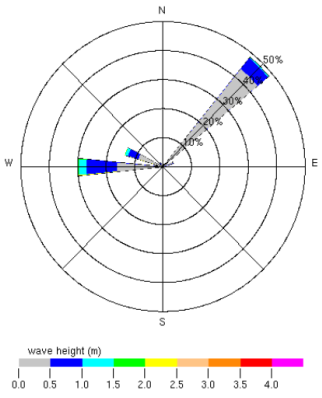

Figure 8.3: Wave rose Tanger Med 2

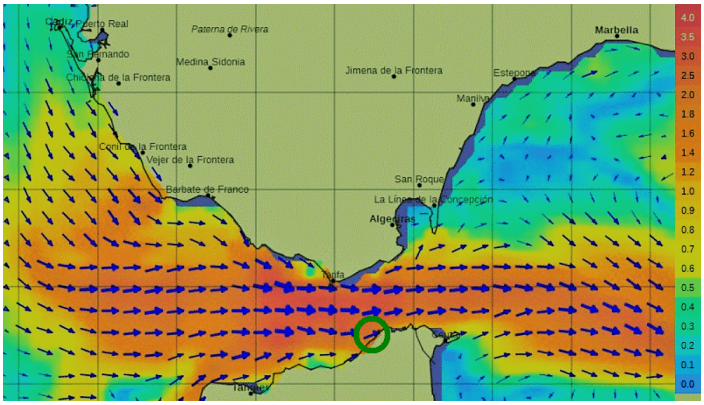

Figure 8.4: Principal current flow in Strait of Gibraltar (source: `https://giphy.com/`)

8.2. Model configuration

The port layout of the entire Tanger Med port complex is given in Figure 8.5, Tanger Med 2 is located in the top left. It is bounded on the right by the passengers and trucks port. The total quay length is approximately 2800 m, which suffices for the mooring of six design vessels. The port is designed such that it can receive the largest container ships in the world, like the Maersk Triple-E class. A design vessel has a length overall of 400 m, a beam of 59 m and a draught of 16 m. The coastline normal at the port location has an angle of $-50°$ with respect to the North and the approach channel is oriented $30°$ with respect to the North.

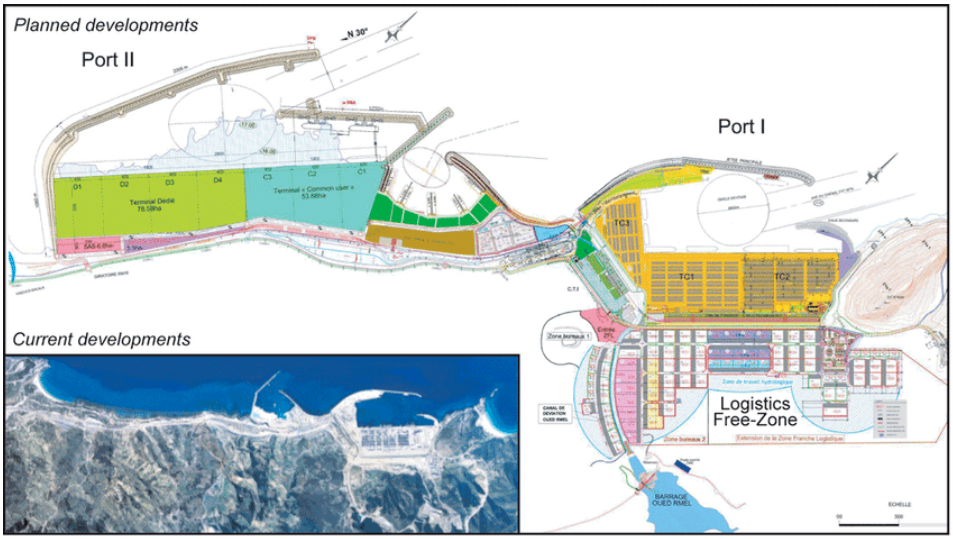

Figure 8.5: Port layout of Tanger Med port complex (Ducruet et al., 2011)

The harbour basin in Figure 8.5 does not meet the boundary conditions as defined in Section 4.1. First of all, the turning basin diameter at the narrowest part is only $1.5 \cdot L_s$, which is significantly smaller than the diameter defined in Section 2.1.4. Besides, the turning basin and the berthing basin overlap each other, which has not been integrated into the model yet. It forms a clear example of the differences between design guidelines and reality, as safety risks can often be mitigated in several ways. The port layout in Figure 8.5 does show a relatively small turning basin, but behind the basin a large empty space exists which can function as a safety margin for vessels that are not able to stop in time. Furthermore, the terminal is entirely located on an area that has been reclaimed from the sea. The relatively steep foreshore results in very high costs when extending the breakwaters further into the sea, so alternative ways to reach the required safety level are preferred. In the model, the diameter of the turning basin is adapted in the advanced input sheet (relating to changes in design guidelines). To include the overlapping turning and berthing basin, major changes in the model code should be made. Instead, it has been chosen to keep the model as it is and discuss the differences between both layouts. Furthermore, it can be seen from Figure 8.5 that the sheltered approach channel length is not as large as is prescribed by the current model, although a high degree of shelter is present for waves coming from the Atlantic Ocean. It has therefore be chosen to let the model come up with a suitable sheltered approach channel length by itself.

The new port makes use of state of the art ship-to-shore cranes. In 2013, the Tanger Med port complex was able to reach an average berth productivity of 46 moves/hour (JOC Group Inc., 2013). It is expected that this number increases due to the opening of the new port. Demands are likely to increase in the future, which is why the berth productivity is estimated to reach an average of 55 moves/hour. Berth occupancy is estimated at 65%, which may be a little low, since a modernised terminal is treated. Since berth occupancy only affects downtime costs, a small change in berth occupancy is however not expected to have a large effect on the resulting port layout. Since caissons have been used and no cost details are available, unit rates are kept equal to the default values as stated in Appendix D.1. An overview of all parameters that have been changed related to the case can be found in Appendix D.3.

For the determination of the environmental conditions, data has been retrieved from ARGOSS (`http://www.waveclimate.com/`). As output points are only available on either the Atlantic Ocean or the Mediterranean Sea, sets of wave conditions have been retrieved for both locations. Using the ray model integrated in the website, an approximate wave climate in front of the port has been obtained. This wave climate has been simplified to the table in Appendix E.5, which also includes wind and current conditions. Attention has been paid to the following aspects:

- Only ten environmental conditions are considered, as this suffices for the conceptual design phase, and runtime is consequently kept low.

- The principal wave, wind and current directions, including their magnitude, are represented by two conditions, as two main directions can be distinguished. The main reason to include for these is a realistic orientation of the approach channel.
- The two most unfavourable wave directions and their corresponding wave heights are included to make sure that these waves get blocked sufficiently. In this case, these are represented by the wave directions coming in as perpendicular to the coastline as possible.
- Most of the environmental conditions are formed by the extreme wave heights and their corresponding directions. Their probabilities of occurrence should be lower than 5%, as these are the conditions that probably are going to cause port downtime. They should be represented as accurately as possible.
- Excessive winds and currents should form the remainder of the conditions. As wind and current speed limits are defined by the user, it can be estimated what the probability of exceeding these limits is. These conditions therefore always cause port downtime.

Two main wave directions have been considered, of which one originates from the Atlantic Ocean and the other one from the Mediterranean Sea (partly sheltered by the Moroccan mainland, see Figure 8.3). In Appendix E.2, also a bathymetry plot and a wave ray plot have been included.

8.3. Case results

8.3.1. Model consistency

Three runs have been performed to assess the consistency of the model for the case study. The resulting breakwater layout configurations are shown in Figure 8.6. The layout configuration generating lowest total costs is shown in Figure 8.6a.

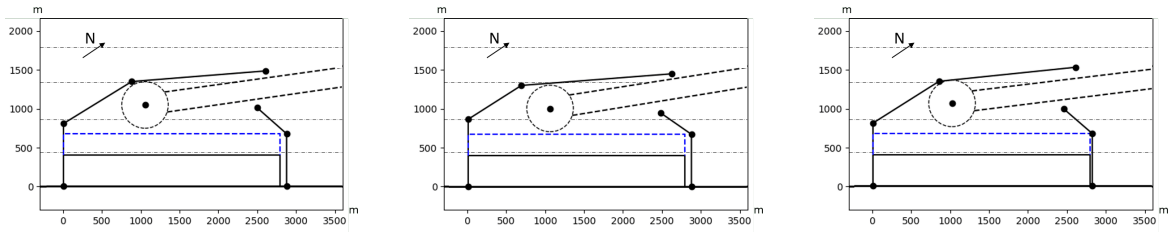

(a) Run 1 (score: 0.683) (b) Run 2 (score: 0.674) (c) Run 3 (score: 0.681)

Figure 8.6: Final breakwater layout configurations for several runs

Type of costs	Run 1	Run 2	Run 3
CAPEX/OPEX (capitalised)	**€252.9 million**	**€256.4 million**	**€253.4 million**
Breakwater construction	€102.6 million	€103.0 million	€103.3 million
Breakwater maintenance	$€2.1 \cdot 10^6$ per year	$€2.1 \cdot 10^6$ per year	$€2.1 \cdot 10^6$ per year
Capital dredging	€52.6 million	€54.2 million	€52.0 million
Maintenance dredging	$€3.0 \cdot 10^6$ per year	$€3.1 \cdot 10^6$ per year	$€3.0 \cdot 10^6$ per year
Downtime costs (capitalised)	**€10.8 million**	**€10.8 million**	**€10.8 million**
Average downtime per berth	0.3%	0.3%	0.3%

Table 8.1: Cost information of Tanger Med case for various runs

Type of costs	Maximum difference	Percentage of min. total costs
Total costs	€3.5 million	1.3%
CAPEX/OPEX	€3.5 million	1.4%
Downtime costs	€0	0%

Table 8.2: Cost consistency for the Tanger Med case

Some general observations regarding Figure 8.6 are summed up below:

- Only minor layout changes are visible. The turning basin location varies slightly, but the orientation of the approach channel is comparable for all layouts.
- A high consistency is achieved, since both total costs and costs related to the individual objectives vary maximally 1.4% (see Table 8.2). The largest differences are present in the dredging costs, which can be related to the slight differences in turning basin locations.
- An equal amount of downtime is generated for all generated layouts.

The share of the generated cost accuracy (1.4%) in the total allowable accuracy for the conceptual design phase (30%, see Section 1.1) is small. Most certainly however, cost differences between the generated optimum and the actual optimum are much larger. In Section 8.3.3, it is therefore investigated to what extent the economic optimum has been reached.

8.3.2. Model convergence

To assess the convergence of the model with respect to the case of Tanger Med 2, the fitness graphs for all three runs are shown in Figure 8.7.

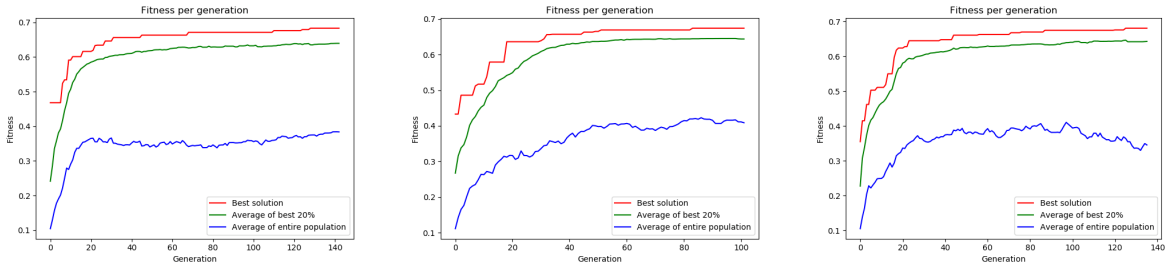

(a) Run 1 (142 generations) (b) Run 2 (101 generations) (c) Run 3 (135 generations)

Figure 8.7: Fitness graphs for several runs

All three runs gradually converged within 100 to 150 generations, while improving the best solution regularly, which are indicators of good model performance. Especially run 1 and 3 show very comparable convergence patterns, which also resulted in similar fitness scores and layout configurations.

8.3.3. Economic optimum

To get more insight in the optimisation process, the economic optimisation graph (Figure 8.8a) and the Pareto front (Figure 8.8b) are visualised for the optimal configuration (run 1).

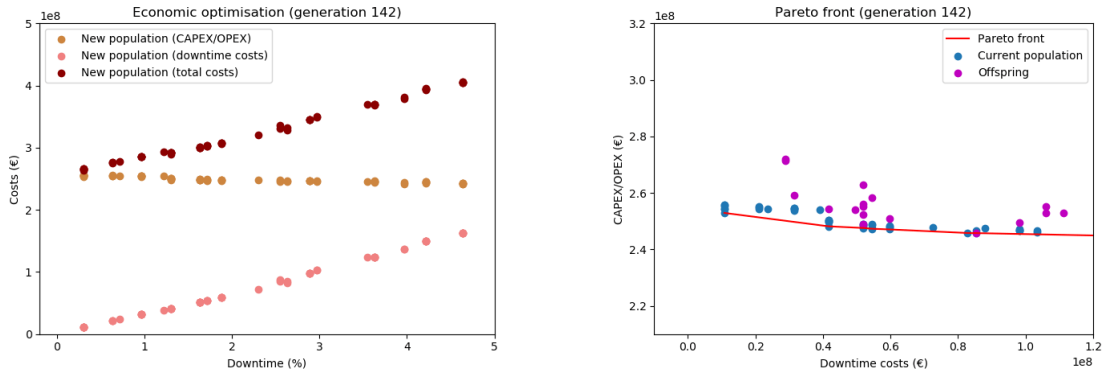

(a) Economic optimisation graph (b) Pareto front

Figure 8.8: Optimisation graphs for the optimal configuration

A list with general conclusions regarding Figure 8.8 is given below:

- A linear shape of the downtime costs over the amount of downtime, even as (slight) exponential behaviour for CAPEX/OPEX over the amount of downtime, can be distinguished in Figure 8.8a. This conforms with Figure 3.1.
- The characteristic parabola representing total costs, even as a steep incline of CAPEX/OPEX for lower downtime ranges, are not visible in Figure 8.8a.
- The economic optimum is located at 0.3% downtime, which means that only the excessive winds cause downtime for the optimal configuration. This is most likely related to the combination of a mild wave climate at the site and a highly modernised port, having a high berth productivity. Protection can therefore be offered relatively cheap, while downtime costs increase rapidly.
- From the Pareto front in Figure 8.8b, it can be observed that the point having a tangent line with a slope of 1:1 has not been reached. To reach this, even higher wave heights should be included, although the corresponding probabilities of occurrence get very small in that case. The result is an asymptote at 0.3% downtime, which likely does not affect the final layout to a large extent.

8.4. Comparison

The optimal breakwater layout configuration corresponding to run 1 in Section 8.3 should be compared to the actual breakwater layout configuration at Tanger Med 2. To do so, a top view from Google Earth is used, as this represents the actual breakwater layout that has been constructed. Both layout configurations are given in Figure 8.9.

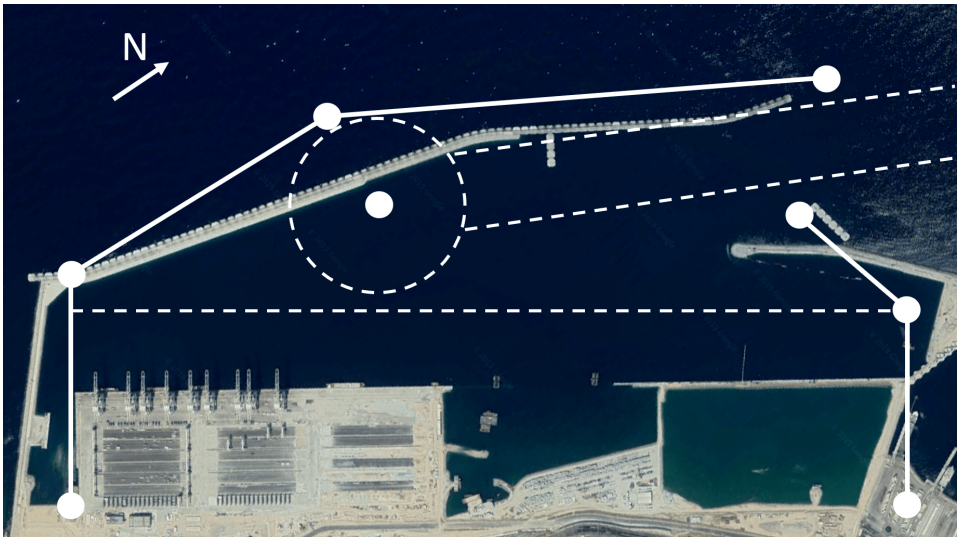

Figure 8.9: Comparison of breakwater layout configurations (background picture retrieved from Google Earth)

It can be seen that a limited portion of the terminal has been constructed, but the outline of the full terminal is clearly visible. Differences between the port layout generated by the model and the actual port layout, visualised in Figure 8.9, are explained below:

- In reality, the secondary breakwater is split up into two parts. The breakwater segment generated by the model does a good job in approaching this.
- For both layouts, the primary breakwater tip extends a little further to the right from the secondary breakwater tip, so that both breakwaters overlap each other. In this way, waves coming in from the North can also be reduced.
- Breakwater node 2 and 3 are located somewhat further offshore for the layout generated by the model. The main reason seems to be that the applied boundary condition requires this amount of space inside

the harbour basin. For the actual layout this has been overcome by letting the turning basin overlap with the berthing basin.

- The change in turning basin location also induced a change in the orientation of the approach channel. The sheltered approach channel length is approached relatively well, especially since no boundary condition has been used for this. The model therefore seems to be able to determine the required sheltered approach channel length by itself, based on the amount of downtime that is generated.

Due to the change in turning basin location and approach channel, another interesting layout option has been created by the model. Though higher safety standards may have been achieved, costs are probably higher due to breakwater construction at larger water depths.

To summarise, the generated breakwater layout configuration differs in some aspects from the actual breakwater layout configuration that has been realised at the port location. These differences can however all be subscribed to the applied model simplifications. Therefore, no signs pf model limitations have been found that would question its quality in the current development stage.

9. Discussion

The development of a parametric model for breakwater layout design has resulted in the ability to assess breakwater layout in an analytic way. It is relevant to clearly specify what implications the model – using the methodology provided in Chapter 4 – has on the design process. Its strengths should be highlighted to make sure its added value can be adopted. In addition, its limitations also require specific attention, to prevent that the model is used in inappropriate situations and to analyse what improvements need to be included in the model in the future. The most suitable way to do so, is to compare the parametric model to the conventional design process. Model criteria are analysed, consisting of factors that either contribute to an improved design process or that evaluate the quality of the solutions generated by the model. These criteria show compliance with the characteristics mentioned in the research objective (see Section 1.3). Besides, they can be related to the model uncertainties elaborated in Section 5.5.3. Ultimately, model applicability is discussed based on the provided scope restrictions, assumptions and boundary conditions to place this research in a bigger picture.

9.1. Basis

The basis of the parametric model is formed by the applied methodology for the determination of downtime and costs per breakwater layout alternative, together with the general model set-up. Uncertainties within this basis are mostly related to inaccuracies in cost and downtime determination and to the applied model simplifications and boundary conditions (see Section 5.5.3). Compared to conventional techniques, it is expected that the parametric model shows a similar amount of uncertainty, because of the following reasons:

- The applied methodology for cost and downtime determination conforms with conventional techniques used in the conceptual design phase.
- Extensive literature research has pointed out that the *NSGA-II* algorithm forms the most suitable optimisation method for the current problem.
- The parametric model has been built up from scratch in full accordance with the chosen algorithm and adaptations to set-up and methodology can easily be made when necessary.

9.2. Robustness

To consider model results as reliable, the parametric model should be able to robustly find an economic optimum. Where uncertainties related to robustness are hardly quantifiable for conventional techniques, this is possible for the parametric model by making use of the robustness indicators, which are defined below:

Consistency	The ability of the parametric model to consistently come up with comparable layouts and resulting costs for every run.
Convergence	The ability of the parametric model to show convergence within a considerable amount of generations for every run.
Diversity	The ability of the parametric model to include breakwater layout alternatives throughout the entire solution space in the optimisation process.

Uncertainties are always present, as we are dealing with a stochastic search technique that cannot guarantee convergence towards an exact optimum. They may be magnified when tuning inaccuracy is present, as the objective of model tuning is to keep model uncertainties to a minimum. From Chapter 6, several conclusions can be made:

- Model results for a certain set of optimisation parameters may vary widely due to the stochastic nature of genetic algorithms, introducing uncertainty in the retrieved optimal set.

- Model runtime in combination with a vast amount of possible combinations of optimisation parameters limit the amount of sets that can be investigated.

The main problem in finding the optimal set of optimisation parameters is therefore formed by the noise which is imposed on the economic optimum by the stochastic search method. When approaching the optimal set, uncertainties related to the optimisation parameters become smaller than this random noise and thus become unnoticeable. A way to overcome this could be to determine all random parameters once and then fixate them to use the same random values over different runs. Parameters are determined randomly within the breakwater layout generator (gene determination) and within the genetic operators (see Section 5.1.4). Model sensitivity should then be executed for several sets of randomly fixated parameters and compared to each other, which should lead to increased insight in the optimal optimisation parameters. For the current development stage of the model (proof of concept) this is considered to be redundant, as related uncertainties already have to be relatively small for these measures to have effect. Nevertheless, in a future development stage, when accuracy issues become more dominant, a certain method may be of added value (see Section 10.2.2).

Strengths, limitations and points of discussion resulting from Chapter 7 & 8, for every robustness indicator, are summed up below:

Consistency

- The base case (double wave direction), introduced in Section 6.5, shows sufficient consistency, as similar breakwater layout configurations are found and costs related to the individual objectives (CAPEX/OPEX and downtime costs) differ maximally 4% with respect to total costs.
- Downtime cost consistency appears to drop for more complex wave climates, even as for larger wave heights.
- Consistency of breakwater layout configurations appears to drop for more complex wave climates, as different layout alternatives are found for different runs.
- The case of Tanger Med shows high cost consistency (1.4%), breakwater layout configurations only show minor variations.

Convergence

- Most of the runs converged within a reasonable amount of generations. This was generally in the order of 80 to 130 generations in Chapter 7 and in the order of 100 to 150 generations in Chapter 8.
- Runs that did converge sooner usually resulted in convergence to a local optimum and were therefore unsuccessful. This happened mostly for unrealistic sets of input parameters.
- Runs that took longer to converge generally showed satisfactory results, though being too inefficient as they did result in large model runtime.

Diversity

- For all runs, the breakwater layout alternatives in the final generation approached the Pareto front. A large spread was observed for both objectives, indicating high diversity.
- Diversity is primarily included to overcome local optima. Escaping these optima has been observed several times (even close to full model convergence), such as in Figure 7.4, indicating that diversity is high enough to fulfil its purpose.

As model strengths and limitations for all robustness indicators have now been identified, it is possible to comment on the ability of the parametric model to robustly find an economic optimum. Some robustness remarks and resulting advises for model use are therefore stated below:

- The parametric model results consistently showed sufficient conformity with actual breakwater layout design, for the conceptual design phase, during validation with a realistic case.
- Cost accuracy between various runs generally turned out to be within a 5% range for model results in Chapter 7. For the case study, this accuracy was reduced to only 1.4%.

- Model accuracy in cost estimates remains hard to predict, but it appears to stay well below the required level for the conceptual design phase (30%, see Section 1.1).

It is advised to keep the amount of environmental conditions to be defined as input to a minimum, as a higher level of consistency can be achieved for less complex wave climates. While doing so, increased attention should be paid to wave conditions within the lower downtime ranges, as in this way the model has a larger amount of potential to find the economic optimum more accurately. These wave conditions correspond to wave heights having a low probability of exceedance. Since the optimal amount of downtime is usually lower than 2%, wave heights having a probability of exceedance lower than this value do have the largest impact on the shape of the parabola representing the total costs and therewith also on the location of the economic optimum. About five to seven points seem to be enough to draw a sufficiently accurate parabola for the conceptual design phase. Nevertheless, this does not always mean that this amount of wave conditions within the lower downtime ranges is required. The amount of berths may increase the amount of points on the parabola, as it is possible that downtime only occurs at some of the berths, therewith reducing the average downtime per berth. For example, a wave condition occurring 2% of the time, can induce port downtime in steps of 0.4% for a port having five berths, as downtime can occur at each berth independently. This is visualised in Figure 9.1 (an adaption of Figure 3.1), where the left marker represents downtime occurring at a single berth and the right marker at all berths for the considered wave condition. The case of Tanger Med 2 showed that the wave conditions provided in Appendix E.5 were still insufficient to accurately determine the economic optimum, although downtime could be spread out over six berths.

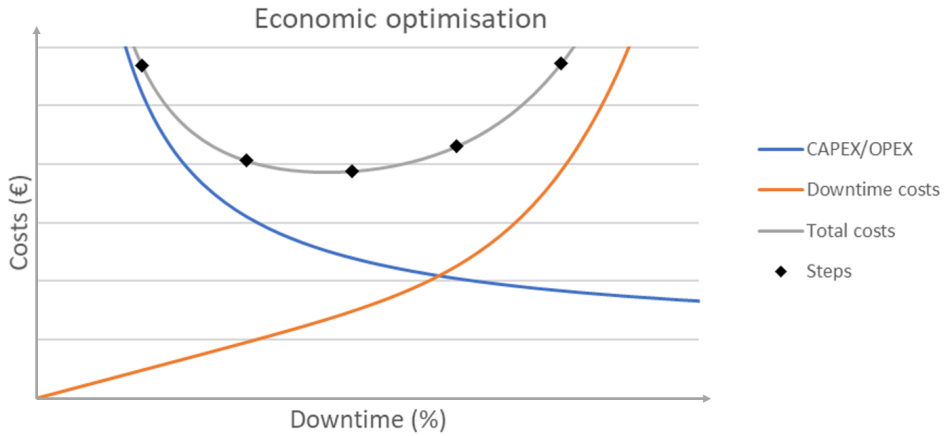

Figure 9.1: Downtime steps for a single wave condition over five berths

9.3. Efficiency

The parametric model can be called efficient when it generally comes up with a more economic layout in a shorter amount of time than by using conventional techniques. The conceptual design phase can be seen as an iterative process, using trial and error to come up with a breakwater layout that is within the desired accuracy range. Conventionally, the steps in this process are performed by hand, drawing possible layouts which are improved gradually until a sufficiently good solution is present. The parametric model is able to perform many more steps, as in total more than ten thousand possible alternatives are generated in a single run. The majority of these alternatives is not nearly optimal, however they are used to bring the best alternative to a higher level. The model especially becomes powerful when also the effect of changes in input parameters or boundary conditions can be assessed, that is to perform various runs while reducing the time that is needed for the entire conceptual design process.

At the moment, a single run takes approximately one hour to run. To get an idea of how the layout should look like, a single run suffices. However, since there is always a probability that the model does not find the optimal breakwater layout alternative during the first run, it is advised to perform as many runs as needed to find two equal breakwater layout alternatives. As the model generally leads to consistent solutions, usually two runs suffice, though sometimes three (or maybe even four) runs are required. The average model

runtime is therefore somewhat over two hours. Nonetheless, the actual labour time is much shorter, as the model can run while the responsible engineer is working on other projects and the model can even be run overnight. Consequently, it can be stated that model runtime is short enough to satisfy the main objective of this research. When comparing the parametric model to conventional techniques, some comments can be given that underline this:

- Preparatory work, such as the retrieval of input data, is required for both methods. It is therefore not expected that this generates differences in the duration of the conceptual design process.
- An average model runtime that is somewhat larger than two hours is fairly short when the retrieval of a breakwater layout configuration that meets the requirements for the conceptual design phase can be guaranteed.
- The ability to run the parametric model in the background reduces the actual labour time to a minimum.

It is expected that model runtime can still be improved significantly with the proper Python expertise and a relatively low amount of effort. As the desired model runtime for this research was already achieved, it has been chosen to focus on other aspects, therewith leaving out some space for model runtime improvements.

9.4. Design flexibility

Breakwaters are rigid structures. Making layout changes when the breakwater has already been constructed leads to very high costs, which therefore needs to be prevented. This can only be done by considering possible layout changes in the design phase, the earlier the better. This sometimes means that a breakwater layout alternative should be chosen that initially is not optimal, but pays off in the long run. Examples of port layout changes are phasing, expansion and other future developments, like growing vessel sizes leading to an increased approach channel depth. The parametric model should be able to account for these. Port expansion has been included by means of an input parameter that specifies the future amount of berths. When the future amount of berths is larger than the initial amount of berths, the model reserves space to locate these berths in a later stage, therewith limiting the location of the secondary breakwater.

Project phasing is harder to include, as optimisation should take place twice. Usually, the primary breakwater is extended in the second phase to be able to provide shelter for (an) additional berth(s). This can be done by performing several runs, using a different amount of berths as input. Comparing both resulting solutions gives an idea of how a final breakwater layout configuration that accounts for project phasing should look like. Since separate runs are used to construct this, the resulting primary breakwater layout can even be built up out of more nodes. In the future, the model should be able to account for project phasing in a single run, as there can always be found some degree of interaction between the separate project phases. For example, it is preferred to initially locate the approach channel such that it already suffices for the final project phase, to avoid unnecessary dredging costs. To do so, the primary breakwater should be schematised by using at least one additional node to guarantee the same level of design accuracy. Ultimately, a continuous breakwater layout (consisting out of an infinite amount of nodes) would be desired.

Other future developments are likely to be very specific or to have a relatively small effect on breakwater layout. They can generally be included by applying another input parameter (e.g. future design vessel size). As this research serves as a proof of concept, it is however not essential to go into further detail on this.

9.5. Adaptability

One of the main strengths of a parametric breakwater layout model is the possibility to assess layout changes based on adaptations within the input or boundary conditions. Therefore, it is of crucial importance that the model reacts appropriately on these adaptations. The first step in verifying this, is to analyse model response to different environmental conditions and other input parameters, which has been done in Chapter 7. It was found that the model behaved well, as most layout changes could be easily explained based on literature. Others did not result in the expected layout representation, but could clearly be subscribed to the assumptions made in this research, as was the case for the limiting wave height for navigation (see Section 7.3). The

interaction between navigational and operational downtime is therefore an important factor to analyse when expanding the model in the future (see Section 10.2.2).

The second step in this verification is to perform sensitivity analyses on key parameters using the parametric model. This can be related to small changes in input parameters, based on expected inaccuracies within the acquired data. Resulting layout changes should remain within acceptable limits to guarantee a robust design. Another option is the assessment of changes in input or boundary conditions based on design considerations. To give an example, the stopping length can be varied to assess the response of the generated optimal breakwater layout configuration. In this way, it can be investigated whether additional research on channel alignment (e.g. by performing a fast-time simulation) or nautical safety levels could positively affect total costs. Furthermore, one could think of a possible investment in larger tugboats, when the resulting breakwater layout would benefit from an increase in the limiting wave height in the channel. These analyses can all be performed in a similar fashion as is done for the results in Chapter 7, only this time for a specific case, by using expected inaccuracies or relevant design considerations to make changes in input and boundary conditions. Relevant analysis options are likely to vary for each case, but the tools provided in this study suffice when dealing with changes that are within the applied scope.

9.6. Applicability

In Section 1.3.2, scope restrictions are presented to generate a robust concept version of a breakwater layout design tool. To make the model applicable in real-life projects, the model should be expanded. As the basis is already here, it can be built out quite easily when assessing the defined scope restrictions. Some model expansion options are given below (additional information can be found in Section 10.2):

- Other types of terminals can be included by changing the guidelines specifically related to container vessels (e.g. wave loading).
- Other types of breakwaters can be included by reconsidering the breakwater cross-section and materials.
- Inclusion of variations in bathymetry, more complex terminal layouts, go/no-go areas and improved OPEX estimations requires additional research.

Section 4.1 treats the assumptions and boundary conditions that are defined to create a simple model. Many of these can be changed conveniently to meet project requirements or to create a more realistic situation. Some of them however require some explanation to be able to make changes to them, which is provided below:

- As boundary conditions do not always comply with design guidelines, it should be possible to change these depending on the case. Some examples are the diameter of the turning basin and the safety tolerances between moored vessels. These adaptations can be applied directly in the Python code, but an advanced input sheet results in fast and user-friendly changes when necessary.
- When including the possibility for vessels to come to a halt at the berth, the approach channel length may be significantly reduced. This is however strongly related to the type of tugboats that are used and the rotation angle of the vessel when it is still moving. Some more literature research can give clearance on this.
- In Chapter 8, the boundary condition related to the minimum sheltered approach channel length has been left out, which has led to more realistic results. It is therefore desired to account for an option to leave out certain boundary conditions when necessary. Resulting optimal breakwater layout configurations can be compared to examine the effect. This option can also be considered as advanced, since it should always be verified if nautical safety requirements are still met.
- Approach channel bends may be required due to no-go areas or unfavourable wind/wave directions. Additional research should be performed to provide a suitable way to include for them when necessary, as they usually should be avoided whenever possible (see Section 10.2.1).
- Other wave processes (e.g. reflection, long waves, local wind-wave generation, passing ships) can be included by expanding the downtime module in the parametric model. Further research should first

be performed to include for these in a simplified way (see Section 10.2.2).

- Interaction between navigational and operational downtime should be investigated in more detail to provide more accurate downtime estimations (see Section 10.2.2).
- More accurate breakwater volume estimations can be achieved when accounting for toes, crest elements and filter layers. Resulting changes in volume calculations can easily be applied within the Python code.
- Cost simplifications (e.g. exclusion of port competition) can easily be avoided when additional research has been performed (see Section 10.2.2).

In its current state, the model functions as a starting point for a decision support tool. Even after expansion, the model is not meant to take over the work of an engineer in the conceptual design phase. It should always be used with proper knowledge of port layout design. Experience and expert judgement will always be required to validate and possibly make changes to the generated breakwater layout.

10. Conclusions and recommendations

In Section 10.1, the conclusions that can be drawn based on the research objective (Section 1.3) and research question (Section 1.3.1) are elaborated. Recommendations relating to the parametric model, its applicability and to further research are given in Section 10.2.

10.1. Conclusions

A parametric model for breakwater layout optimisation has been set up, in which around ten thousand alternatives are compared in a single run with a duration of about one hour. This has been realised by expressing all design criteria in cost terms, to arrive at a balance between costs and performance. The result is a successful proof of concept for a generative breakwater design tool, as final layouts complying with conceptual design standards were consistently obtained. When expanding the model in the future – by discarding the applied simplifications – it is able to provide support to port layout design projects all around the world. This does not only accelerate the conceptual design process, but also makes it possible to efficiently deal with future port developments and changes in design requirements, making it easier to live up to client expectations.

10.1.1. Key findings

The model objective is to find the most economical breakwater layout for a specific case, resulting in a minimal amount of downtime. The main findings of this research are stated below, divided into several subjects that have a close connection to the research questions defined in Section 1.3.1.

Robustness Robustly encountering an economic optimum for a specific case forms one of the main requirements for a successful model. Model consistency has found to be sufficient for the conceptual design phase. During validation with a real case, cost consistency rates of only 1.4% were encountered. Also layouts appeared to be consistent, as only minor changes were observed. Total costs are expected to be well within the typical accuracy limit of 30% for the conceptual design phase, when performing at least two runs generating comparable final layouts. The performed runs in Chapter 7 & 8 showed good signs of convergence, requiring approximately one hour per run. The model performed very well based on diversity, as a large spread over the Pareto front was observed and the model was able to overcome local optima when necessary. In relation to conceptual breakwater layout design 'by hand', optimisation techniques make it possible to consider a much wider range of alternatives in a shorter amount of time.

Flexibility The other main requirement of the parametric model is formed by its flexibility. The model is able to successfully take port design changes and project phasing into consideration. By assessing optimum layouts for each phase, a robust development plan can be generated. Besides, the model is capable of adequately reacting to changes in input parameters and boundary conditions, and even new parameters can easily be implemented in the optimisation process. It is therefore possible to perform rapid sensitivity analyses on key parameters to make informed decisions on relevant design considerations.

Optimisation method Genetic algorithms (*GA*'s) have shown to be the most suitable optimisation method for breakwater layout optimisation.

- *GA*'s are highly robust, as alternatives are implemented in parallel, improving the chances of encountering a global optimum.

- *GA*'s require a limited amount of computational power, as evolutionary processes – such as selection and crossover – ensure fast model convergence.
- *GA*'s are able to maintain a diverse range of alternatives, which diminishes the chance to get stuck in local optima and enables the model to encompass the entire solution space.
- *GA*'s can deal with multi-objective optimisation, enabling the model to investigate the trade-off between costs and performance and therewith stimulating the optimality of both objectives.
- *GA*'s focus on finding a solution that is located within the desired cost accuracy range rather than finding the exact optimum, which matches well with the objective of the conceptual design phase.
- No other optimisation method is as robust and flexible as *GA*'s are for the current problem.

Model set-up The model set-up has been mainly focused on a clear simplification of both the port layout and the optimisation process, while maintaining a realistic representation of the problem.

- The simplified methodology proposed in Chapter 4, relating to the determination of costs and downtime of a breakwater layout alternative, has resulted in realistic layout changes coming along with variations in the input parameters that are treated in Chapter 7.
- The model requires proper knowledge of port layout by the user to produce realistic results. Unrealistic input generates unrealistic output.
- An optimal set of optimisation parameters was generated for the problem, which has been approached sufficiently to comply with conceptual design standards.
- The model set-up is highly flexible, as the model contains all relevant variables, which can easily be added, changed or removed. The model also allows for changes in advanced variables, such as boundary conditions and standard port layout dimensions.

Parameters and sensitivity In Chapter 7, the influence of certain parameters on breakwater layout has been investigated by making use of the parametric model.

- Generally, changes in breakwater layouts generated by the model, based on adaptations in key parameters, can easily be explained based on existing literature.
- Parameters influencing both objectives (costs and performance) affect the breakwater layout generally to a larger extent than those that only influence a single objective.
- As layout changes based on variations in input parameters are reflected by the model as expected, it becomes possible to use the parametric model to perform sensitivity analyses on these parameters.

10.1.2. Advances

The successful development and validation of a parametric model for breakwater layout optimisation has resulted in several innovations and novelties within the field, which are summed up below:

- The robust model consistently generates the economically most attractive breakwater layout configuration.
- The efficient model generates validated optimal breakwater layouts rapidly and is able to run in the background. Therewith, it increases the speed of the decision making process, leading to fast mutual agreement with the client.
- The flexible model is able to adequately react on changes in design requirements and prevailing conditions.
- The model is able to include a large amount of different variables. New parameters, or even entirely new modules, can easily be included into the optimisation.
- Using the model, rapid sensitivity analyses can be carried out on input parameters, boundary conditions and port strategy aspects.

- The model visualisation techniques form an attractive means of layout discussions with the client.
- The ability of the model to robustly generate a suggested breakwater layout may lead to increased trust of investors.

10.1.3. Limitations

Some limitations of this research have been addressed and elaborated in Chapter 9. In summary, the main limitations are:

- The current model is highly simplified and therefore requires expansion to realistically model all port conditions.
- Downtime cost consistency appears to decrease for more complex wave climates (more wave conditions defined as input), even as for higher waves.
- The current model lacks validation of cost estimates for the generated breakwater layouts.
- The current model has only been validated for a single port location.
- Implementation of parameter sensitivity analyses has not yet been tested for a specific case.
- The applied methodology for the determination of downtime and costs, even as the model set-up, are likely to change significantly when the model is extended.
- Expertise is needed in model tuning to avoid adverse effects on the quality of the results.

10.2. Recommendations

The proof of concept for a parametric breakwater layout tool has been performed. It is possible to extend the model, so that it becomes genuinely applicable for breakwater design projects. Some model applicability recommendations are proposed – relating to changes to be made to the applied methodology and model set-up – to overcome simplifications implemented in the initial model. Besides, some recommendations regarding future research are given, which require additional literature studies to determine how they can improve the model.

10.2.1. Model applicability

The parametric model can be improved in many different ways in the future. The most important improvements generating the largest impact on breakwater design are summed up below.

Project requirements During this study, attention has been paid to the economical point of view within breakwater layout optimisation. Apart from cost factors, many other requirements apply when dealing with breakwater design such as nautical safety, construction time, sustainability, social considerations, dredging strategies, etc. These can be converted to monetary terms and included within the cost optimisation.

One of the most important themes is nautical safety, as can be seen from the findings presented in Section 8.4. It is advised to perform a risk analysis, by assessing the probabilities and consequences for the occurrence of a certain event, like a ship collision. Including associated costs in the model makes it possible to compare breakwater layout configurations that adopt different design guidelines or safety requirements. Ultimately, this may also lead to a more robust basis for setting up guidelines.

Integration with cross-sectional design tool As breakwater design also comprises cross-sectional considerations, it is relevant to think about a way to integrate these with a generic breakwater design tool. It is advised to keep both optimisation processes separated from each other for now, as their interaction is expected to result in a decrease in model performance, since they deal with genuinely different optimisation strategies. Instead, it is recommended to couple both design tools by providing the breakwater layout configuration from the layout tool to the cross-sectional tool as input for the parametric design. Consequently,

the breakwater alignment can be split up in sections for which the optimal cross-sectional design can be determined. The resulting model has the potential to achieve considerable improvements in time, costs and design quality.

Inclusion of breakwater types and maintenance plan As discussed in Section 9.6, other breakwater types can be incorporated into the model in a relatively straightforward fashion. The model would benefit from their inclusion, as they make it more generally applicable. As this brings up the need to investigate different breakwater materials, a well-suited addition would be to also include breakwater maintenance planning into the model. This would result in more accurate cost estimates.

Realistic bathymetry and coastline On Earth, no natural foreshore with perfectly aligned depth contours is present and no natural coastline is exactly straight. The parametric model would therefore benefit from the inclusion of realistic bathymetry data sets and coastlines, especially when the model is able to generate a coastline based on the bathymetric data set. Not only does this increase the accuracy of dredging and breakwater material volumes, but the model could also take into account the effect on the breakwater alignment of submerged canyons and shoals.

Increased layout complexity The methodology proposed in Chapter 4 should be adapted to comply with other terminal geometries, like separate basins or opposing quay walls. Also the effect of berths along a breakwater on the model set-up should be investigated. This results in more pronounced waves and current patterns within the harbour basin, as complicated reflection patterns and resonance phenomena may occur. It can be a challenge to incorporate these into the model in a simplified way.

Also breakwater layout complexity could be extended. By applying additional breakwater nodes, more detailed alignments can be achieved. It creates more possibilities for the inclusion of project phasing into a single model.

Variations in vessels and tugboat types Most ports are multi-purpose, so many different vessel types need to call here. Also tugboats may vary widely and as each tugboat/vessel type has its own boundary conditions for navigational requirements.

Approach channel Approach channel dimensions are very site specific. In some cases, vessels come to a halt within the turning basin, while in other cases they come to a halt at the berth. This is dependent on aspects like the applied tugboat types and the nautical safety standards. The model would greatly benefit from this input, so that it can make its own decision for the exact channel orientation and length. Also bends would form an important addition.

Penalty factors For factors that rely on subjective input or other aspects that are hardly quantifiable, penalties could offer an option. An example for this could be the orientation of the approach channel for steep foreshores. Usually unfavourable channel orientations are downgraded by additional dredging costs, but when the approach channel is located in deeper water, this width addition does not influence the final layout. Pilots may however still experience difficulties while manoeuvring, so penalties for channel width and orientation – leading to adverse effects for pilots – could be included.

10.2.2. Further research

Implementation of the aforementioned recommendations into the model may take some time, but methodologies are generally at hand. Other factors, like the recommendations stated below, require additional research. Nevertheless, inclusion would lead to improved model results.

Harbour siltation Sedimentation is one of the most difficult aspects to tackle within the conceptual design phase, as it is hard to predict the magnitude of sediment import into a harbour basin, especially since the effect of the breakwater on current patterns is not yet known. Defining a simple method to give reliable estimates of harbour siltation may therefore form a big challenge. Possibly, the use of a simple sedimentation model would be required. It is therefore advised to firstly assess all relevant parameters that may influence this process, after which it can be investigated how the effect of all these parameters can be implemented in a simplified way. Rustell (2016) has proposed such a methodology, so it could be worthwhile to examine if this would also be applicable to the proposed parametric model.

Determination of downtime costs Downtime costs are highly port specific, as stated in Section 2.2.3. Some influence factors are shipping forecasts, cargo flows, hinterland connections, distances to closest competing ports and delays. Extensive research is needed to assess the effect of these parameters on breakwater layout and include them as input parameters in the model. As only downtime costs are affected, the impact on breakwater layout is likely to be minimal. Therefore, performing research in this field is most suitable when attention should be paid to increased accuracy in cost estimations.

Wave processes Wave transformation and penetration have been simplified in this study, as this sufficed to obtain the required amount of accuracy. However, when terminal layout becomes more complex, wave patterns also become more complex. Reflection patterns may be present to such an extent that they cannot be omitted in the conceptual design phase. Besides, long waves have the potential to cause substantial downtime in areas that are highly susceptible to swell. The interaction of harbour geometry and prevailing wave lengths is something that cannot be ignored. More research on this topic is therefore recommended, possibly requiring more complex input. After realisation, performing a sensitivity analysis on certain wave parameters may result in many new insights, as the interaction between certain wave processes and breakwater layout is still unknown.

Downtime interaction Section 7.3 showed that the assumption that navigational downtime always leads to operational downtime at all berths may result in unrealistic results. To solve this, the interaction between navigational and operational downtime should be investigated further. Service and waiting times at the considered port should be addressed to come up with an amount of time that operations can continue while vessels cannot enter or leave the harbour. It should also be verified what the average duration of navigational downtime is. Implementation of these details leads to improved downtime determination, which has a significant impact on breakwater layout optimisation in certain situations.

Model tuning As has been discussed in Section 9.2, the parametric model would benefit from additional research regarding the optimal set of optimisation parameters applicable to the problem. As a large uncertainty is still present in this set, model results are affected to a large extent. Correctly tuning the model requires time, as a large number of possible sets should be investigated and the stochastic search techniques could be eliminated to improve results.

Bibliography

Agatonovic-Kustrin, S. & Beresford, R. (2000). Basic concepts of artificial neural network (ANN) modeling and its application in pharmaceutical research. *Journal of Pharmaceutical and Biomedical Analysis*, 22(5), 717–727.

Bertsimas, D. & Tsitsiklis, J. (1993). Simulated Annealing. *Statistical Science*, 8(1), 10–15.

Bre, F., Gimenez, J. M., & Fachinotti, V. D. (2017). Prediction of wind pressure coefficients on building surfaces using artificial neural networks. *Energy and Buildings*, 158, 1429–1441.

Briganti, R., van der Meer, J., Buccino, M., & Calabrese, M. (2004). Wave Transmission Behind Low-Crested Structures. In *Coastal Structures 2003* (pp. 580–592). Reston, VA: American Society of Civil Engineers.

CIRIA/CUR/CETMEF (2007). *The rock manual : the use of rock in hydraulic engineering*. London: CIRIA, 2nd edition.

Coastal Engineering Research Center (1984). *Shore Protection Manual, Volume I*. Washington D.C.: US Army Engineer Waterways Experiment Station, 4th edition.

Coello Coello, C. A., Lamont, G. B., & Van Veldhuizen, D. A. (2007). *Evolutionary algorithms for solving multi-objective problems*. Springer.

Deb, K., Pratap, A., Agarwal, S., & Meyarivan, T. (2002). *A Fast and Elitist Multiobjective Genetic Algorithm: NSGA-II*. Technical Report 2.

Ducruet, C., Mohamed-Chérif, F. Z., & Cherfaoui, N. (2011). *Maghreb port cities in transition : the case of Tangier*. Technical report, Centre National de la Recherche Scientifique (CNRS), Paris, France.

Elchahal, G., Younes, R., & Lafon, P. (2013). Optimization of coastal structures: Application on detached breakwaters in ports. *Ocean Engineering*, 63, 35–43.

EurOtop (2018). *Manual on wave overtopping of sea defences and related structures: An overtopping manual largely based on European research, but for worldwide application*. 2nd edition.

Goda, Y. (2000). *Random Seas and Design of Maritime Structures*, volume 15 of *Advanced Series on Ocean Engineering*. World Scientific, 2nd edition.

Goda, Y., Takayama, T., & Suzuki, Y. (1978). *Diffraction Diagrams for Directional Random Waves*. Technical report, Port and Harbour Research Institute, Yokosuka, Japan.

Goedhart, G. (2002). Criteria for (un)-loading Container ships.

Helm-Petersen, J. (1998). Estimation of Wave Disturbance in Harbours.

JOC Group Inc. (2013). *JOC Port Productivity: Key Findings On Terminal Productivity Performance Across Ports, Countries And Regions*. Technical report.

Kramer, O. (2017). *Genetic Algorithm Essentials*. Cham, Switzerland: Springer.

Kureichik, V. M., Malioukov, S. P., Kureichik, V. V., & Malioukov, A. (2009). *Genetic Algorithms for Applied CAD Problems*. Berlin: Springer-Verlag.

Liebherr Container Cranes Ltd. (2015). Technical Description Ship to Shore Gantry Cranes. Retrieved February 8, 2019, from https://www.liebherr.com/shared/media/maritime-cranes/downloads-and-brochures/brochures/lcc/liebherr-sts-cranes-technical-description.pdf.

Ligteringen, H. & Velsink, H. (2012). *Ports and terminals*. Delft Academic Press.

Meersman, H., Van De Voorde, E., & Vanelslander, T. (2003). *Port Pricing. Considerations on Economic Principles and Marginal Costs*. Technical Report 4.

Miche, M. (1944). Mouvements ondulatoires de la mer en profondeur constante ou décroissante. *Annales de Ponts et Chaussées, 1944, pp(1) 26-78, (2)270-292, (3) 369-406*.

Moes, H. & Terblanche, L. (2010). Motion criteria for the efficient (un)loading of container vessels. In *Port Infrastructure Seminar 2010*.

Nederlands Loodswezen (2018). Pilotage Tariffs 2018 - Region Rotterdam-Rijnmond.

Penny, W. G. & Price, A. T. (1952). Diffraction of sea waves by breakwater.

PIANC (1995). *Criteria for movements of moored ships in harbours: A practical guide: Report of Working Group no. 24, of the Permanent Technical Committee II*. Brussels, Belgium: PIANC General Secretariat.

PIANC (2014). *Harbour approach channels design guidelines*. Technical report, The World Association for Waterborne Transport Infrastructure, Brussels, Belgium.

PIANC (2016). *Criteria for the selection of breakwater types and their related optimum safety levels*. Technical report, The World Association for Waterborne Transport Infrastructure, Brussels, Belgium.

Piccoli, C. (2014). Economic optimization of breakwaters-Case study: Maintenance of Port of Constantza's Northern Breakwater.

Puertos del Estado (2007). *Recommendations for maritime works: Planning, management and operation in port areas*. Madrid, Spain: Puertos del Estado.

Renard, P., Alcolea, A., & Ginsbourger, D. (2013). Stochastic versus Deterministic Approaches. In J. Wainwright & M. Mulligan (Eds.), *Environmental Modelling: Finding Simplicity in Complexity* chapter 8, (pp. 133–149). John Wiley & Sons, Ltd., 2nd edition.

Rijksinstituut voor Kust en Zee (2004). *Golfbelastingen in havens en afgeschermde gebieden: een gedetailleerde methode voor het bepalen van golfbelastingen voor het toetsen van waterkeringen*. Technical report, Rijksinstituut voor Kust en Zee, Delft.

Rustell, M. (2013). Breakwater Layout Optimisation Using A Root-Finding Algorithm. In *Ports 2013*, number August 2013 (pp. 1929–1938).

Rustell, M. (2016). *Knowledge extraction and the development of a decision support system for the conceptual design of liquefied natural gas terminals under risk and uncertainty*. PhD thesis, University of Surrey.

Rytkönen, J. (1987). Littoral drift as a source of harbour siltation. *Rakenteiden Mekaniikka*, 20.

Secretariat of UNCTAD (1985). Port development: A handbook for planners in developing countries. In *United Nations Conference on Trade and Development* New York, USA: United Nations.

Sjöberg, H., Roos, H., Edvall, A., & Hallbjörner, F. (2016). *Safe handling of ultra large container ships in strong wind*. Technical report, Swedish Maritime Administration, Gothenburg, Sweden.

Sorensen, R. M. (1997). *Basic Coastal Engineering*. Dordrecht: Springer-Science+Business Media, B.V., 2nd edition.

Taneja, P., Ligteringen, H., & Walker, W. (2010). *Flexibility in Port Planning and Design*. Technical report, Delft University of Technology.

Tanger Med Port Authority (2017). Tanger Med [Brochure]. Retrieved June 16, 2019, from http://www.tmpa.ma/en/.

Thoresen, C. A. (2003). *Port designer's handbook: Recommendations and guidelines*. London: Thomas Telford.

United Nations Conference on Trade and Development (2018). *Review of maritime transport 2018*. New York and Geneva: United Nations Publications.

van Rijn, L. C. (2016). Harbour siltation and control measures. Retrieved January 28, 2019, http://www.leovanrijn-sediment.com.

You, Z.-J. (2003). A close approximation of wave dispersion relation for direct calculation of wavelength in any coastal water depth. *Coastal Engineering*, 48(2), 133–135.

A. Port design

When looking at the overall design process of a port, the master plan can be illustrated as is done in Figure A.1.

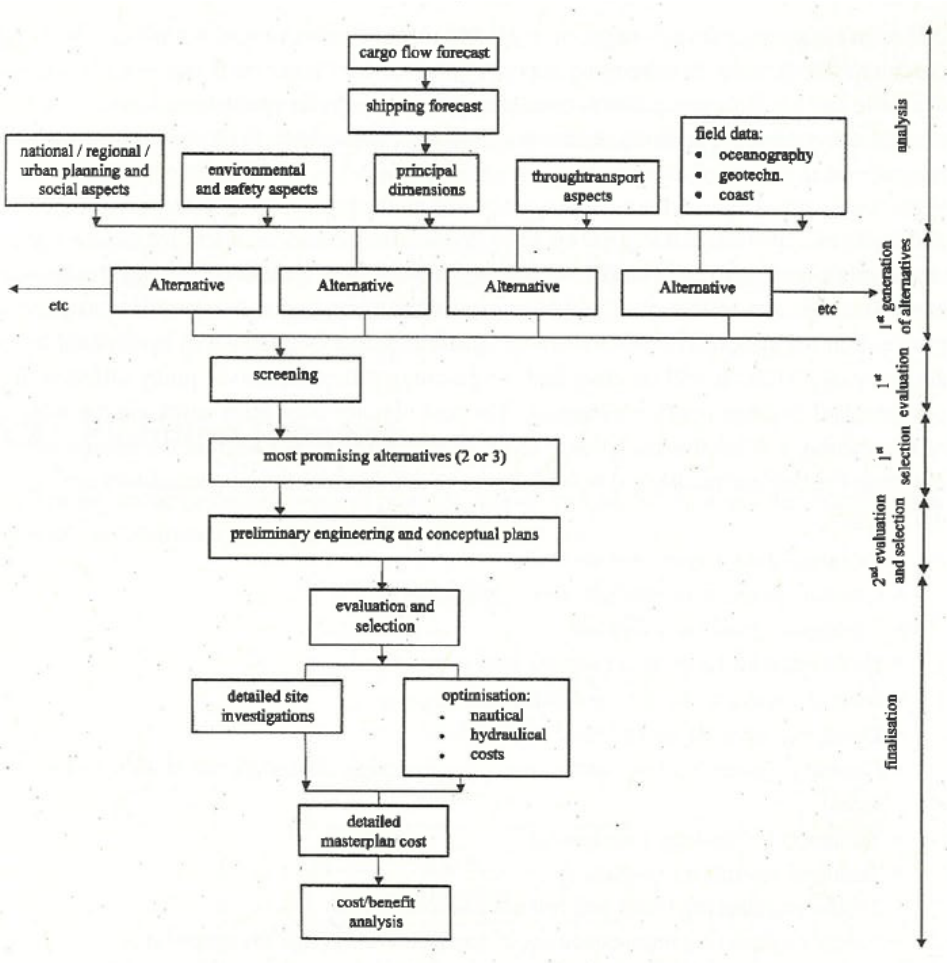

Figure A.1: Process of port master plan (Ligteringen & Velsink, 2012)

The conceptual design of a breakwater is performed during the generation of alternatives and their evaluation/selection. This means that all activities listed under analysis are already performed, which are discussed in Section 1.1.

B. Diffraction tables

Y/L	10	9	8	7	6	5	4	3	2	1	-1	-2	-3	-4	-5	-6	-7	-8	-9	-10
20	0.9	0.9	0.9	0.9	0.9	0.8	0.8	0.8	0.8	0.8	0.7	0.7	0.7	0.7	0.6	0.6	0.6	0.6	0.5	0.5
19	0.9	0.9	0.9	0.9	0.9	0.9	0.8	0.8	0.8	0.8	0.7	0.7	0.7	0.7	0.6	0.6	0.6	0.6	0.5	0.5
18	0.9	0.9	0.9	0.9	0.9	0.9	0.8	0.8	0.8	0.8	0.7	0.7	0.7	0.6	0.6	0.6	0.6	0.6	0.5	0.5
17	0.95	0.9	0.9	0.9	0.9	0.9	0.8	0.8	0.8	0.8	0.7	0.7	0.7	0.6	0.6	0.6	0.6	0.5	0.5	0.5
16	0.95	0.9	0.9	0.9	0.9	0.9	0.9	0.8	0.8	0.8	0.7	0.7	0.7	0.6	0.6	0.6	0.6	0.5	0.5	0.5
15	0.95	0.9	0.9	0.9	0.9	0.9	0.9	0.8	0.8	0.8	0.7	0.7	0.7	0.6	0.6	0.6	0.5	0.5	0.5	0.5
14	0.95	0.95	0.9	0.9	0.9	0.9	0.9	0.8	0.8	0.8	0.7	0.7	0.7	0.6	0.6	0.6	0.5	0.5	0.5	0.4
13	0.95	0.95	0.95	0.9	0.9	0.9	0.9	0.8	0.8	0.8	0.7	0.7	0.7	0.6	0.6	0.6	0.5	0.5	0.5	0.4
12	0.95	0.95	0.95	0.9	0.9	0.9	0.9	0.9	0.8	0.8	0.7	0.7	0.6	0.6	0.6	0.5	0.5	0.5	0.4	0.4
11	0.95	0.95	0.95	0.95	0.9	0.9	0.9	0.9	0.8	0.8	0.7	0.7	0.6	0.6	0.6	0.5	0.5	0.4	0.4	0.4
10	1	0.95	0.95	0.95	0.9	0.9	0.9	0.9	0.8	0.8	0.7	0.7	0.6	0.6	0.5	0.5	0.5	0.4	0.4	0.4
9	1	1	0.95	0.95	0.95	0.9	0.9	0.9	0.8	0.8	0.7	0.7	0.6	0.6	0.5	0.5	0.4	0.4	0.4	0.3
8	1	1	1	0.95	0.95	0.9	0.9	0.9	0.8	0.8	0.7	0.6	0.6	0.6	0.5	0.4	0.4	0.4	0.3	0.3
7	1	1	1	1	0.95	0.95	0.9	0.9	0.9	0.8	0.7	0.6	0.6	0.5	0.5	0.4	0.4	0.3	0.3	0.3
6	1	1	1	1	1	0.95	0.95	0.9	0.9	0.8	0.7	0.6	0.5	0.5	0.4	0.4	0.3	0.3	0.3	0.3
5	1	1	1	1	1	1	0.95	0.9	0.9	0.8	0.7	0.6	0.5	0.4	0.4	0.3	0.3	0.3	0.3	0.3
4	1	1	1	1	1	1	1	0.95	0.9	0.8	0.7	0.5	0.4	0.4	0.3	0.3	0.3	0.3	0.2	0.2
3	1	1	1	1	1	1	1	1	0.95	0.8	0.7	0.5	0.3	0.3	0.3	0.3	0.3	0.2	0.2	0.2
2	1	1	1	1	1	1	1	1	1	0.9	0.5	0.4	0.3	0.3	0.3	0.2	0.2	0.2	0.2	0.2
1	1	1	1	1	1	1	1	1	1	1	0.4	0.3	0.3	0.2	0.2	0.2	0.2	0.2	0.2	0.2

X/L

Table B.1: Diffraction table for a semi-infinite breakwater, with s_{max} = 10 (Rijksinstituut voor Kust en Zee, 2004)

Y/L	10	9	8	7	6	5	4	3	2	1	-1	-2	-3	-4	-5	-6	-7	-8	-9	-10
20	1	1	1	1	1	1	0.9	0.9	0.9	0.8	0.7	0.7	0.6	0.5	0.5	0.4	0.4	0.3	0.3	0.3
19	1	1	1	1	1	1	0.9	0.9	0.9	0.8	0.7	0.7	0.6	0.5	0.5	0.4	0.4	0.3	0.3	0.3
18	1	1	1	1	1	1	0.9	0.9	0.9	0.8	0.7	0.7	0.6	0.5	0.4	0.4	0.4	0.3	0.3	0.3
17	1	1	1	1	1	1	1	0.9	0.9	0.8	0.7	0.6	0.6	0.5	0.4	0.4	0.3	0.3	0.3	0.2
16	1	1	1	1	1	1	1	0.9	0.9	0.8	0.7	0.6	0.6	0.5	0.4	0.4	0.3	0.3	0.3	0.2
15	1	1	1	1	1	1	1	0.9	0.9	0.8	0.7	0.6	0.6	0.5	0.4	0.3	0.3	0.3	0.2	0.2
14	1	1	1	1	1	1	1	0.9	0.9	0.8	0.7	0.6	0.5	0.5	0.4	0.3	0.3	0.3	0.2	0.2
13	1	1	1	1	1	1	1	1	0.9	0.9	0.7	0.6	0.5	0.4	0.4	0.3	0.3	0.2	0.2	0.2
12	1	1	1	1	1	1	1	1	0.9	0.9	0.7	0.6	0.5	0.4	0.3	0.3	0.3	0.2	0.2	0.2
11	1	1	1	1	1	1	1	1	0.9	0.9	0.7	0.6	0.5	0.4	0.3	0.3	0.2	0.2	0.2	0.2
10	1	1	1	1	1	1	1	1	0.9	0.9	0.7	0.5	0.5	0.4	0.3	0.3	0.2	0.2	0.2	0.2
9	1	1	1	1	1	1	1	1	0.9	0.9	0.7	0.5	0.4	0.3	0.3	0.2	0.2	0.2	0.2	0.2
8	1	1	1	1	1	1	1	1	0.9	0.9	0.7	0.5	0.4	0.3	0.3	0.2	0.2	0.2	0.2	0.2
7	1	1	1	1	1	1	1	1	1	0.9	0.7	0.5	0.4	0.3	0.2	0.2	0.2	0.2	0.2	0.1
6	1	1	1	1	1	1	1	1	1	0.9	0.7	0.5	0.3	0.3	0.2	0.2	0.2	0.2	0.1	0.1
5	1	1	1	1	1	1	1	1	1	0.9	0.7	0.4	0.3	0.2	0.2	0.2	0.2	0.1	0.1	0.1
4	1	1	1	1	1	1	1	1	1	0.9	0.7	0.4	0.3	0.2	0.2	0.2	0.2	0.1	0.1	0.1
3	1	1	1	1	1	1	1	1	1	1	0.7	0.3	0.2	0.2	0.2	0.2	0.1	0.1	0.1	0.1
2	1	1	1	1	1	1	1	1	1	1	0.7	0.3	0.2	0.2	0.2	0.1	0.1	0.1	0.1	0.1
1	1	1	1	1	1	1	1	1	1	1	0.7	0.2	0.2	0.2	0.2	0.1	0.1	0.1	0.1	0.1

X/L

Table B.2: Diffraction table for a semi-infinite breakwater, with s_{max} = 75 (Rijksinstituut voor Kust en Zee, 2004)

Y/L	0	0.2	0.4	0.6	0.8	1	1.2	1.4	1.6	1.8	2	2.2	2.4	2.6	2.8	3
	4	0.4	0.4	0.4	0.4	0.4	0.4	0.4	0.4	0.4	0.4	0.3	0.3	0.3	0.3	0.3
	3.8	0.4	0.4	0.4	0.4	0.4	0.4	0.4	0.4	0.4	0.4	0.3	0.3	0.3	0.3	0.3
	3.6	0.4	0.4	0.4	0.4	0.4	0.4	0.4	0.4	0.4	0.4	0.3	0.3	0.3	0.3	0.3
	3.4	0.4	0.4	0.4	0.4	0.4	0.4	0.4	0.4	0.4	0.4	0.4	0.3	0.3	0.3	0.3
	3.2	0.5	0.5	0.5	0.4	0.4	0.4	0.4	0.4	0.4	0.4	0.4	0.3	0.3	0.3	0.3
	3	0.5	0.5	0.5	0.5	0.4	0.4	0.4	0.4	0.4	0.4	0.4	0.3	0.3	0.3	0.3
	2.8	0.5	0.5	0.5	0.5	0.5	0.4	0.4	0.4	0.4	0.4	0.4	0.3	0.3	0.3	0.3
	2.6	0.5	0.5	0.5	0.5	0.5	0.4	0.4	0.4	0.4	0.4	0.3	0.3	0.3	0.3	0.3
	2.4	0.5	0.5	0.5	0.5	0.5	0.4	0.4	0.4	0.4	0.4	0.3	0.3	0.3	0.3	0.3
	2.2	0.5	0.5	0.5	0.5	0.5	0.5	0.4	0.4	0.4	0.4	0.3	0.3	0.3	0.3	0.3
	2	0.6	0.6	0.5	0.5	0.5	0.5	0.4	0.4	0.4	0.3	0.3	0.3	0.3	0.3	0.3
	1.8	0.6	0.6	0.6	0.5	0.5	0.5	0.4	0.4	0.4	0.3	0.3	0.3	0.3	0.3	0.3
	1.6	0.6	0.6	0.6	0.5	0.5	0.5	0.4	0.4	0.4	0.3	0.3	0.3	0.3	0.3	0.3
	1.4	0.7	0.6	0.6	0.6	0.5	0.5	0.4	0.4	0.3	0.3	0.3	0.3	0.3	0.2	0.2
	1.2	0.7	0.7	0.6	0.6	0.5	0.5	0.4	0.4	0.3	0.3	0.3	0.3	0.3	0.2	0.2
	1	0.8	0.7	0.7	0.6	0.5	0.4	0.4	0.4	0.3	0.3	0.3	0.3	0.2	0.2	0.2
	0.8	0.8	0.8	0.7	0.6	0.5	0.4	0.4	0.3	0.3	0.3	0.3	0.3	0.2	0.2	0.2
	0.6	0.9	0.8	0.7	0.6	0.5	0.4	0.4	0.3	0.3	0.3	0.3	0.2	0.2	0.2	0.2
	0.4	1.0	0.9	0.8	0.6	0.4	0.4	0.3	0.3	0.3	0.3	0.3	0.3	0.2	0.2	0.2
	0.2	1.0	1.0	1.0	0.5	0.4	0.4	0.3	0.3	0.3	0.3	0.3	0.3	0.2	0.2	0.2
	0	0.2	0.4	0.6	0.8	1	1.2	1.4	1.6	1.8	2	2.2	2.4	2.6	2.8	3
									X/L							

Table B.3: Diffraction table for a breakwater gap, with $B/L = 1.0$ and $s_{max} = 10$, relatively close to gap (Rijksinstituut voor Kust en Zee, 2004)

Y/L	0	1	2	3	4	5	6	7	8	9	10	11	12	13	14	15
	20	0.2	0.2	0.2	0.2	0.2	0.2	0.2	0.15	0.15	0.15	0.15	0.15	0.15	0.15	0.15
	19	0.2	0.2	0.2	0.2	0.2	0.2	0.2	0.2	0.15	0.15	0.15	0.15	0.15	0.15	0.15
	18	0.2	0.2	0.2	0.2	0.2	0.2	0.2	0.2	0.15	0.15	0.15	0.15	0.15	0.15	0.15
	17	0.2	0.2	0.2	0.2	0.2	0.2	0.2	0.2	0.15	0.15	0.15	0.15	0.15	0.15	0.15
	16	0.2	0.2	0.2	0.2	0.2	0.2	0.2	0.2	0.15	0.15	0.15	0.15	0.15	0.15	0.15
	15	0.2	0.2	0.2	0.2	0.2	0.2	0.2	0.2	0.2	0.15	0.15	0.15	0.15	0.15	0.15
	14	0.3	0.3	0.2	0.2	0.2	0.2	0.2	0.2	0.2	0.15	0.15	0.15	0.15	0.15	0.15
	13	0.3	0.3	0.3	0.2	0.2	0.2	0.2	0.2	0.15	0.15	0.15	0.15	0.15	0.15	0.15
	12	0.3	0.3	0.3	0.3	0.2	0.2	0.2	0.2	0.15	0.15	0.15	0.15	0.15	0.15	0.15
	11	0.3	0.3	0.3	0.3	0.3	0.2	0.2	0.2	0.15	0.15	0.15	0.15	0.15	0.15	0.15
	10	0.3	0.3	0.3	0.3	0.3	0.2	0.2	0.2	0.15	0.15	0.15	0.15	0.15	0.15	0.1
	9	0.3	0.3	0.3	0.3	0.3	0.2	0.2	0.2	0.15	0.15	0.15	0.15	0.15	0.1	0.1
	8	0.3	0.3	0.3	0.3	0.3	0.2	0.2	0.2	0.15	0.15	0.15	0.15	0.15	0.1	0.1
	7	0.3	0.3	0.3	0.3	0.3	0.2	0.2	0.15	0.15	0.15	0.15	0.15	0.1	0.1	0.1
	6	0.4	0.3	0.3	0.3	0.2	0.2	0.2	0.15	0.15	0.15	0.15	0.1	0.1	0.1	0.1
	5	0.4	0.4	0.3	0.3	0.2	0.2	0.15	0.15	0.15	0.15	0.15	0.1	0.1	0.1	0.1
	4	0.4	0.4	0.3	0.3	0.2	0.2	0.15	0.15	0.15	0.15	0.1	0.1	0.1	0.1	0.1
	3	0.5	0.4	0.3	0.2	0.2	0.15	0.15	0.15	0.15	0.1	0.1	0.1	0.1	0.1	0.1
	2	0.6	0.4	0.3	0.2	0.15	0.15	0.15	0.15	0.15	0.1	0.1	0.1	0.1	0.1	0.1
	1	0.6	0.3	0.3	0.2	0.2	0.2	0.15	0.15	0.15	0.15	0.15	0.1	0.1	0.1	0.1
	0	1	2	3	4	5	6	7	8	9	10	11	12	13	14	15
									X/L							

Table B.4: Diffraction table for a breakwater gap, with $B/L = 1.0$ and $s_{max} = 10$, relatively far from gap (Rijksinstituut voor Kust en Zee, 2004)

Y/L	0	2	4	6	8	10	12	14	16	18	20	22	24	26	28	30
8	0.4	0.4	0.4	0.4	0.4	0.4	0.4	0.4	0.4	0.4	0.4	0.3	0.3	0.3	0.3	0.3
7.6	0.4	0.4	0.4	0.4	0.4	0.4	0.4	0.4	0.4	0.4	0.4	0.4	0.3	0.3	0.3	0.3
7.2	0.5	0.5	0.5	0.4	0.4	0.4	0.4	0.4	0.4	0.4	0.4	0.4	0.3	0.3	0.3	0.3
6.8	0.5	0.5	0.5	0.5	0.4	0.4	0.4	0.4	0.4	0.4	0.4	0.4	0.3	0.3	0.3	0.3
6.4	0.5	0.5	0.5	0.5	0.5	0.4	0.4	0.4	0.4	0.4	0.4	0.4	0.3	0.3	0.3	0.3
6	0.5	0.5	0.5	0.5	0.5	0.4	0.4	0.4	0.4	0.4	0.4	0.3	0.3	0.3	0.3	0.3
5.6	0.5	0.5	0.5	0.5	0.5	0.5	0.4	0.4	0.4	0.4	0.4	0.3	0.3	0.3	0.3	0.3
5.2	0.5	0.5	0.5	0.5	0.5	0.5	0.4	0.4	0.4	0.4	0.4	0.3	0.3	0.3	0.3	0.3
4.8	0.6	0.5	0.5	0.5	0.5	0.5	0.4	0.4	0.4	0.4	0.4	0.3	0.3	0.3	0.3	0.3
4.4	0.6	0.6	0.5	0.5	0.5	0.5	0.4	0.4	0.4	0.4	0.3	0.3	0.3	0.3	0.3	0.2
4	0.6	0.6	0.6	0.5	0.5	0.5	0.4	0.4	0.4	0.4	0.3	0.3	0.3	0.3	0.3	0.2
3.6	0.6	0.6	0.6	0.5	0.5	0.5	0.4	0.4	0.4	0.4	0.3	0.3	0.3	0.3	0.2	0.2
3.2	0.7	0.6	0.6	0.6	0.5	0.5	0.4	0.4	0.4	0.3	0.3	0.3	0.3	0.3	0.2	0.2
2.8	0.7	0.7	0.6	0.6	0.5	0.5	0.4	0.4	0.4	0.3	0.3	0.3	0.3	0.2	0.2	0.2
2.4	0.7	0.7	0.6	0.6	0.5	0.4	0.4	0.4	0.3	0.3	0.3	0.3	0.2	0.2	0.2	0.2
2	0.8	0.7	0.7	0.6	0.5	0.4	0.4	0.4	0.3	0.3	0.3	0.2	0.2	0.2	0.2	0.15
1.6	0.8	0.8	0.7	0.6	0.5	0.4	0.3	0.3	0.3	0.3	0.2	0.2	0.2	0.2	0.15	0.15
1.2	0.9	0.8	0.7	0.6	0.4	0.4	0.3	0.3	0.3	0.3	0.2	0.2	0.2	0.15	0.15	0.15
0.8	1.0	0.9	0.7	0.5	0.4	0.3	0.3	0.3	0.3	0.2	0.2	0.2	0.15	0.15	0.15	0.15
0.4	1.0	1.0	0.8	0.5	0.3	0.3	0.3	0.3	0.3	0.2	0.2	0.2	0.2	0.15	0.15	0.15
0	0.4	0.8	1.2	1.6	2	2.4	2.8	3.2	3.6	4	4.4	4.8	5.2	5.6	6	

X/L

Table B.5: Diffraction table for a breakwater gap, with $B/L = 2.0$ and $s_{max} = 10$, relatively close to gap (Rijksinstituut voor Kust en Zee, 2004)

Y/L	0	2	4	6	8	10	12	14	16	18	20	22	24	26	28	30
40	0.2	0.2	0.2	0.2	0.2	0.2	0.2	0.2	0.2	0.15	0.15	0.15	0.15	0.15	0.15	0.15
38	0.2	0.2	0.2	0.2	0.2	0.2	0.2	0.2	0.2	0.2	0.15	0.15	0.15	0.15	0.15	0.15
36	0.2	0.2	0.2	0.2	0.2	0.2	0.2	0.2	0.2	0.2	0.15	0.15	0.15	0.15	0.15	0.15
34	0.2	0.2	0.2	0.2	0.2	0.2	0.2	0.2	0.2	0.2	0.15	0.15	0.15	0.15	0.15	0.15
32	0.2	0.2	0.2	0.2	0.2	0.2	0.2	0.2	0.2	0.2	0.15	0.15	0.15	0.15	0.15	0.15
30	0.3	0.3	0.2	0.2	0.2	0.2	0.2	0.2	0.2	0.2	0.15	0.15	0.15	0.15	0.15	0.15
28	0.3	0.3	0.3	0.2	0.2	0.2	0.2	0.2	0.2	0.2	0.15	0.15	0.15	0.15	0.15	0.15
26	0.3	0.3	0.3	0.3	0.2	0.2	0.2	0.2	0.2	0.2	0.15	0.15	0.15	0.15	0.15	0.1
24	0.3	0.3	0.3	0.3	0.2	0.2	0.2	0.2	0.2	0.15	0.15	0.15	0.15	0.15	0.15	0.1
22	0.3	0.3	0.3	0.3	0.3	0.2	0.2	0.2	0.2	0.15	0.15	0.15	0.15	0.15	0.1	0.1
20	0.3	0.3	0.3	0.3	0.3	0.2	0.2	0.2	0.2	0.15	0.15	0.15	0.15	0.1	0.1	0.1
18	0.3	0.3	0.3	0.3	0.3	0.2	0.2	0.2	0.15	0.15	0.15	0.15	0.15	0.1	0.1	0.1
16	0.3	0.3	0.3	0.3	0.3	0.2	0.2	0.2	0.15	0.15	0.15	0.15	0.1	0.1	0.1	0.1
14	0.4	0.3	0.3	0.3	0.3	0.2	0.2	0.15	0.15	0.15	0.15	0.1	0.1	0.1	0.1	0.1
12	0.4	0.3	0.3	0.3	0.2	0.2	0.2	0.15	0.15	0.15	0.1	0.1	0.1	0.1	0.1	0.1
10	0.4	0.4	0.3	0.3	0.2	0.2	0.2	0.15	0.15	0.1	0.1	0.1	0.1	0.1	0.1	0.1
8	0.5	0.4	0.3	0.3	0.2	0.15	0.15	0.15	0.1	0.1	0.1	0.1	0.1	0.1	0.1	0.1
6	0.5	0.4	0.3	0.2	0.15	0.15	0.1	0.1	0.1	0.1	0.1	0.1	0.1	0.1	0.1	0.1
4	0.6	0.4	0.2	0.15	0.15	0.15	0.1	0.1	0.1	0.1	0.1	0.1	0.1	0.1	0.1	0.1
2	0.6	0.3	0.2	0.15	0.15	0.1	0.1	0.1	0.1	0.1	0.1	0.1	0.1	0.1	0.1	0.1
0	2	4	6	8	10	12	14	16	18	20	22	24	26	28	30	

X/L

Table B.6: Diffraction table for a breakwater gap, with $B/L = 2.0$ and $s_{max} = 10$, relatively far from gap (Rijksinstituut voor Kust en Zee, 2004)

Y/L	0	0.8	1.6	2.4	3.2	4	4.8	5.6	6.4	7.2	8	8.8	9.6	10.4	11.2	12
16	0.4	0.4	0.4	0.4	0.4	0.4	0.4	0.4	0.4	0.4	0.4	0.3	0.3	0.3	0.3	0.3
15.2	0.5	0.5	0.4	0.4	0.4	0.4	0.4	0.4	0.4	0.4	0.4	0.4	0.3	0.3	0.3	0.3
14.4	0.5	0.5	0.5	0.5	0.4	0.4	0.4	0.4	0.4	0.4	0.4	0.4	0.3	0.3	0.3	0.3
13.6	0.5	0.5	0.5	0.5	0.5	0.4	0.4	0.4	0.4	0.4	0.4	0.4	0.3	0.3	0.3	0.3
12.8	0.5	0.5	0.5	0.5	0.5	0.4	0.4	0.4	0.4	0.4	0.4	0.4	0.3	0.3	0.3	0.3
12	0.5	0.5	0.5	0.5	0.5	0.5	0.4	0.4	0.4	0.4	0.4	0.4	0.3	0.3	0.3	0.3
11.2	0.5	0.5	0.5	0.5	0.5	0.5	0.4	0.4	0.4	0.4	0.4	0.4	0.3	0.3	0.3	0.3
10.4	0.5	0.5	0.5	0.5	0.5	0.5	0.4	0.4	0.4	0.4	0.4	0.3	0.3	0.3	0.3	0.3
9.6	0.6	0.6	0.5	0.5	0.5	0.5	0.4	0.4	0.4	0.4	0.4	0.3	0.3	0.3	0.3	0.2
8.8	0.6	0.6	0.5	0.5	0.5	0.5	0.4	0.4	0.4	0.4	0.4	0.3	0.3	0.3	0.2	0.2
8	0.6	0.6	0.6	0.5	0.5	0.5	0.4	0.4	0.4	0.4	0.3	0.3	0.3	0.3	0.2	0.2
7.2	0.6	0.6	0.6	0.6	0.5	0.5	0.4	0.4	0.4	0.4	0.3	0.3	0.3	0.2	0.2	0.2
6.4	0.7	0.6	0.6	0.6	0.5	0.5	0.4	0.4	0.4	0.3	0.3	0.3	0.3	0.2	0.2	0.2
5.6	0.7	0.7	0.6	0.6	0.5	0.5	0.4	0.4	0.4	0.3	0.3	0.3	0.2	0.2	0.2	0.15
4.8	0.7	0.7	0.7	0.6	0.5	0.4	0.4	0.3	0.3	0.3	0.3	0.2	0.2	0.2	0.15	0.15
4	0.8	0.7	0.7	0.6	0.5	0.4	0.3	0.3	0.3	0.3	0.2	0.2	0.2	0.15	0.15	0.15
3.2	0.9	0.8	0.7	0.6	0.4	0.4	0.3	0.3	0.2	0.2	0.2	0.2	0.15	0.15	0.15	0.15
2.4	0.9	0.9	0.7	0.6	0.4	0.3	0.3	0.2	0.2	0.15	0.15	0.15	0.15	0.15	0.15	0.15
1.6	1	0.9	0.8	0.4	0.3	0.3	0.2	0.2	0.15	0.15	0.15	0.15	0.15	0.15	0.15	0.15
0.8	1	1	0.9	0.3	0.3	0.2	0.2	0.15	0.15	0.15	0.15	0.15	0.15	0.15	0.15	0.15
0	0.8	1.6	2.4	3.2	4	4.8	5.6	6.4	7.2	8	8.8	9.6	10.4	11.2	12	

X/L

Table B.7: Diffraction table for a breakwater gap, with $B/L = 4.0$ and $s_{max} = 10$, relatively close to gap (Rijksinstituut voor Kust en Zee, 2004)

Y/L	0	4	8	12	16	20	24	28	32	36	40	44	48	52	56	60
80	0.2	0.2	0.2	0.2	0.2	0.2	0.2	0.2	0.2	0.15	0.15	0.15	0.15	0.15	0.15	0.15
76	0.2	0.2	0.2	0.2	0.2	0.2	0.2	0.2	0.2	0.15	0.15	0.15	0.15	0.15	0.15	0.15
72	0.2	0.2	0.2	0.2	0.2	0.2	0.2	0.2	0.2	0.2	0.15	0.15	0.15	0.15	0.15	0.15
68	0.2	0.2	0.2	0.2	0.2	0.2	0.2	0.2	0.2	0.2	0.15	0.15	0.15	0.15	0.15	0.15
64	0.3	0.3	0.2	0.2	0.2	0.2	0.2	0.2	0.2	0.15	0.15	0.15	0.15	0.15	0.15	0.15
60	0.3	0.3	0.3	0.2	0.2	0.2	0.2	0.2	0.2	0.15	0.15	0.15	0.15	0.15	0.15	0.15
56	0.3	0.3	0.3	0.3	0.2	0.2	0.2	0.2	0.2	0.15	0.15	0.15	0.15	0.15	0.15	0.15
52	0.3	0.3	0.3	0.3	0.2	0.2	0.2	0.2	0.2	0.15	0.15	0.15	0.15	0.15	0.15	0.1
48	0.3	0.3	0.3	0.3	0.3	0.2	0.2	0.2	0.2	0.15	0.15	0.15	0.15	0.15	0.1	0.1
44	0.3	0.3	0.3	0.3	0.3	0.2	0.2	0.2	0.2	0.15	0.15	0.15	0.15	0.15	0.1	0.1
40	0.3	0.3	0.3	0.3	0.3	0.2	0.2	0.2	0.2	0.15	0.15	0.15	0.15	0.1	0.1	0.1
36	0.3	0.3	0.3	0.3	0.3	0.2	0.2	0.2	0.2	0.15	0.15	0.15	0.1	0.1	0.1	0.1
32	0.3	0.3	0.3	0.3	0.3	0.2	0.2	0.2	0.15	0.15	0.15	0.15	0.1	0.1	0.1	0.1
28	0.4	0.3	0.3	0.3	0.3	0.2	0.2	0.2	0.15	0.15	0.15	0.1	0.1	0.1	0.1	0.1
24	0.4	0.4	0.3	0.3	0.2	0.2	0.2	0.15	0.15	0.15	0.1	0.1	0.1	0.1	0.1	0.1
20	0.4	0.4	0.3	0.3	0.2	0.15	0.15	0.15	0.15	0.1	0.1	0.1	0.1	0.1	0.1	0.1
16	0.5	0.4	0.3	0.3	0.2	0.15	0.15	0.1	0.1	0.1	0.1	0.1	0.1	0.1	0.1	0.1
12	0.5	0.4	0.3	0.2	0.15	0.15	0.1	0.1	0.1	0.1	0.1	0.1	0.1	0.1	0.1	0.05
8	0.6	0.4	0.2	0.15	0.15	0.1	0.1	0.1	0.1	0.1	0.1	0.1	0.1	0.1	0.05	0.05
4	0.6	0.2	0.15	0.15	0.1	0.1	0.1	0.1	0.1	0.1	0.1	0.1	0.1	0.1	0.1	0.1
0	4	8	12	16	20	24	28	32	36	40	44	48	52	56	60	

X/L

Table B.8: Diffraction table for a breakwater gap, with $B/L = 4.0$ and $s_{max} = 10$, relatively far from gap (Rijksinstituut voor Kust en Zee, 2004)

Y/L	0	1.6	3.2	4.8	6.4	8	9.6	11.2	12.8	14.4	16	17.6	19.2	20.8	22.4	24
32	0.5	0.5	0.5	0.5	0.4	0.4	0.4	0.4	0.4	0.4	0.4	0.4	0.4	0.3	0.3	0.3
30.4	0.5	0.5	0.5	0.5	0.4	0.4	0.4	0.4	0.4	0.4	0.4	0.4	0.4	0.3	0.3	0.3
28.8	0.5	0.5	0.5	0.5	0.5	0.4	0.4	0.4	0.4	0.4	0.4	0.4	0.3	0.3	0.3	0.3
27.2	0.5	0.5	0.5	0.5	0.5	0.4	0.4	0.4	0.4	0.4	0.4	0.4	0.3	0.3	0.3	0.3
25.6	0.5	0.5	0.5	0.5	0.5	0.4	0.4	0.4	0.4	0.4	0.4	0.3	0.3	0.3	0.3	0.3
24	0.5	0.5	0.5	0.5	0.5	0.5	0.4	0.4	0.4	0.4	0.4	0.3	0.3	0.3	0.3	0.3
22.4	0.5	0.5	0.5	0.5	0.5	0.5	0.4	0.4	0.4	0.4	0.3	0.3	0.3	0.3	0.3	0.3
20.8	0.5	0.5	0.5	0.5	0.5	0.5	0.4	0.4	0.4	0.4	0.4	0.3	0.3	0.3	0.3	0.3
19.2	0.6	0.6	0.5	0.5	0.5	0.5	0.4	0.4	0.4	0.4	0.4	0.3	0.3	0.3	0.3	0.2
17.6	0.6	0.6	0.6	0.5	0.5	0.5	0.4	0.4	0.4	0.4	0.3	0.3	0.3	0.3	0.2	0.2
16	0.6	0.6	0.6	0.5	0.5	0.5	0.4	0.4	0.4	0.4	0.3	0.3	0.3	0.3	0.2	0.2
14.4	0.6	0.6	0.6	0.6	0.5	0.5	0.4	0.4	0.4	0.3	0.3	0.3	0.3	0.2	0.2	0.2
12.8	0.7	0.6	0.6	0.6	0.5	0.5	0.4	0.4	0.4	0.3	0.3	0.3	0.2	0.2	0.2	0.2
11.2	0.7	0.7	0.6	0.6	0.5	0.5	0.4	0.4	0.4	0.3	0.3	0.2	0.2	0.2	0.2	0.2
9.6	0.7	0.7	0.7	0.6	0.5	0.4	0.4	0.4	0.3	0.3	0.3	0.2	0.2	0.2	0.2	0.2
8	0.8	0.7	0.7	0.6	0.5	0.4	0.3	0.3	0.3	0.3	0.2	0.2	0.2	0.2	0.2	0.2
6.4	0.9	0.8	0.7	0.6	0.4	0.4	0.3	0.3	0.2	0.2	0.2	0.2	0.2	0.2	0.2	0.1
4.8	0.9	0.8	0.7	0.6	0.4	0.3	0.3	0.2	0.2	0.2	0.2	0.2	0.2	0.1	0.1	0.1
3.2	1	0.9	0.7	0.4	0.3	0.2	0.2	0.2	0.2	0.2	0.2	0.2	0.1	0.1	0.1	0.1
1.6	1	1	0.8	0.3	0.2	0.2	0.2	0.2	0.2	0.2	0.2	0.1	0.1	0.1	0.1	0.1

X/L

Table B.9: Diffraction table for a breakwater gap, with $B/L = 8.0$ and $s_{max} = 10$, relatively close to gap (Rijksinstituut voor Kust en Zee, 2004)

Y/L	0	8	16	24	32	40	48	56	64	72	80	88	96	104	112	120
160	0.2	0.2	0.2	0.2	0.2	0.2	0.2	0.2	0.2	0.15	0.15	0.15	0.15	0.15	0.15	0.15
152	0.2	0.2	0.2	0.2	0.2	0.2	0.2	0.2	0.2	0.2	0.15	0.15	0.15	0.15	0.15	0.15
144	0.2	0.2	0.2	0.2	0.2	0.2	0.2	0.2	0.2	0.2	0.15	0.15	0.15	0.15	0.15	0.15
136	0.3	0.2	0.2	0.2	0.2	0.2	0.2	0.2	0.2	0.2	0.15	0.15	0.15	0.15	0.15	0.15
128	0.3	0.3	0.2	0.2	0.2	0.2	0.2	0.2	0.2	0.2	0.15	0.15	0.15	0.15	0.15	0.15
120	0.3	0.3	0.3	0.2	0.2	0.2	0.2	0.2	0.2	0.2	0.15	0.15	0.15	0.15	0.15	0.15
112	0.3	0.3	0.3	0.2	0.2	0.2	0.2	0.2	0.2	0.2	0.15	0.15	0.15	0.15	0.15	0.1
104	0.3	0.3	0.3	0.3	0.2	0.2	0.2	0.2	0.2	0.2	0.15	0.15	0.15	0.15	0.15	0.1
96	0.3	0.3	0.3	0.3	0.2	0.2	0.2	0.2	0.2	0.15	0.15	0.15	0.15	0.15	0.1	0.1
88	0.3	0.3	0.3	0.3	0.3	0.2	0.2	0.2	0.2	0.15	0.15	0.15	0.15	0.1	0.1	0.1
80	0.3	0.3	0.3	0.3	0.3	0.2	0.2	0.2	0.2	0.15	0.15	0.15	0.15	0.1	0.1	0.1
72	0.3	0.3	0.3	0.3	0.3	0.2	0.2	0.2	0.2	0.15	0.15	0.15	0.1	0.1	0.1	0.1
64	0.3	0.3	0.3	0.3	0.3	0.2	0.2	0.15	0.15	0.15	0.15	0.1	0.1	0.1	0.1	0.1
56	0.4	0.3	0.3	0.3	0.3	0.2	0.2	0.15	0.15	0.15	0.15	0.1	0.1	0.1	0.1	0.1
48	0.4	0.4	0.3	0.3	0.2	0.2	0.15	0.15	0.15	0.1	0.1	0.1	0.1	0.1	0.1	0.05
40	0.4	0.4	0.3	0.3	0.2	0.2	0.15	0.15	0.1	0.1	0.1	0.1	0.1	0.1	0.05	0.05
32	0.5	0.4	0.3	0.2	0.2	0.15	0.15	0.1	0.1	0.1	0.1	0.1	0.05	0.05	0.05	0.05
24	0.5	0.4	0.3	0.2	0.15	0.15	0.1	0.1	0.1	0.1	0.1	0.05	0.05	0.05	0.05	0.05
16	0.5	0.4	0.2	0.15	0.1	0.1	0.1	0.1	0.05	0.05	0.05	0.05	0.05	0.05	0.05	0.05
8	0.5	0.3	0.15	0.1	0.1	0.1	0.1	0.1	0.1	0.1	0.1	0.05	0.05	0.05	0.05	0.05

X/L

Table B.10: Diffraction table for a breakwater gap, with $B/L = 8.0$ and $s_{max} = 10$, relatively far from gap (Rijksinstituut voor Kust en Zee, 2004)

Y/L	0	0.2	0.4	0.6	0.8	1	1.2	1.4	1.6	1.8	2	2.2	2.4	2.6	2.8	3
4	0.5	0.5	0.5	0.5	0.5	0.5	0.4	0.4	0.4	0.4	0.4	0.3	0.3	0.3	0.3	0.3
3.8	0.5	0.5	0.5	0.5	0.5	0.5	0.4	0.4	0.4	0.4	0.4	0.3	0.3	0.3	0.3	0.3
3.6	0.6	0.5	0.5	0.5	0.5	0.5	0.5	0.4	0.4	0.4	0.4	0.3	0.3	0.3	0.3	0.3
3.4	0.6	0.6	0.5	0.5	0.5	0.5	0.5	0.4	0.4	0.4	0.3	0.3	0.3	0.3	0.3	0.3
3.2	0.6	0.6	0.6	0.5	0.5	0.5	0.5	0.4	0.4	0.4	0.3	0.3	0.3	0.3	0.3	0.3
3	0.6	0.6	0.6	0.6	0.5	0.5	0.5	0.4	0.4	0.4	0.3	0.3	0.3	0.3	0.3	0.2
2.8	0.6	0.6	0.6	0.6	0.5	0.5	0.5	0.4	0.4	0.4	0.3	0.3	0.3	0.3	0.3	0.2
2.6	0.6	0.6	0.6	0.6	0.5	0.5	0.5	0.4	0.4	0.3	0.3	0.3	0.3	0.3	0.3	0.2
2.4	0.7	0.6	0.6	0.6	0.5	0.5	0.4	0.4	0.4	0.3	0.3	0.3	0.3	0.3	0.2	0.2
2.2	0.7	0.7	0.6	0.6	0.5	0.5	0.4	0.4	0.4	0.3	0.3	0.3	0.3	0.3	0.2	0.2
2	0.7	0.7	0.6	0.6	0.5	0.5	0.4	0.4	0.3	0.3	0.3	0.3	0.3	0.2	0.2	0.2
1.8	0.7	0.7	0.7	0.6	0.5	0.5	0.4	0.4	0.3	0.3	0.3	0.3	0.3	0.2	0.2	0.2
1.6	0.8	0.7	0.7	0.6	0.5	0.4	0.4	0.3	0.3	0.3	0.3	0.3	0.2	0.2	0.2	0.2
1.4	0.8	0.8	0.7	0.6	0.5	0.4	0.4	0.3	0.3	0.3	0.2	0.2	0.2	0.2	0.2	0.15
1.2	0.9	0.8	0.7	0.6	0.5	0.4	0.3	0.3	0.3	0.3	0.2	0.2	0.2	0.2	0.2	0.15
1	0.9	0.8	0.7	0.5	0.4	0.4	0.3	0.3	0.3	0.2	0.2	0.2	0.2	0.2	0.15	0.15
0.8	1.0	0.8	0.7	0.5	0.4	0.4	0.3	0.3	0.3	0.2	0.2	0.2	0.2	0.2	0.15	0.15
0.6	1.0	0.9	0.7	0.5	0.4	0.3	0.3	0.3	0.2	0.2	0.2	0.2	0.2	0.2	0.15	0.15
0.4	1.1	1.0	0.7	0.5	0.4	0.3	0.3	0.3	0.2	0.2	0.2	0.2	0.2	0.2	0.15	0.15
0.2	1.1	1.1	0.9	0.5	0.4	0.3	0.3	0.3	0.2	0.2	0.2	0.2	0.2	0.2	0.15	0.15
0	0.2	0.4	0.6	0.8	1	1.2	1.4	1.6	1.8	2	2.2	2.4	2.6	2.8	3	
								X/L								

Table B.11: Diffraction table for a breakwater gap, with $B/L = 1.0$ and $s_{max} = 75$, relatively close to gap (Rijksinstituut voor Kust en Zee, 2004)

Y/L	0	1	2	3	4	5	6	7	8	9	10	11	12	13	14	15
20	0.3	0.3	0.3	0.3	0.2	0.2	0.2	0.2	0.2	0.2	0.15	0.15	0.15	0.15	0.15	
19	0.3	0.3	0.3	0.3	0.3	0.2	0.2	0.2	0.2	0.2	0.15	0.15	0.15	0.15	0.15	
18	0.3	0.3	0.3	0.3	0.3	0.2	0.2	0.2	0.2	0.15	0.15	0.15	0.15	0.15	0.15	
17	0.3	0.3	0.3	0.3	0.3	0.2	0.2	0.2	0.2	0.15	0.15	0.15	0.15	0.15	0.1	
16	0.3	0.3	0.3	0.3	0.3	0.2	0.2	0.2	0.2	0.15	0.15	0.15	0.15	0.15	0.1	
15	0.3	0.3	0.3	0.3	0.3	0.2	0.2	0.2	0.2	0.15	0.15	0.15	0.15	0.1	0.1	
14	0.3	0.3	0.3	0.3	0.3	0.2	0.2	0.2	0.2	0.15	0.15	0.15	0.15	0.1	0.1	
13	0.3	0.3	0.3	0.3	0.3	0.2	0.2	0.2	0.15	0.15	0.15	0.15	0.1	0.1	0.1	
12	0.3	0.3	0.3	0.3	0.3	0.2	0.2	0.2	0.15	0.15	0.15	0.15	0.1	0.1	0.1	
11	0.3	0.3	0.3	0.3	0.3	0.2	0.2	0.2	0.15	0.15	0.15	0.1	0.1	0.1	0.1	
10	0.4	0.3	0.3	0.3	0.3	0.2	0.2	0.15	0.15	0.15	0.15	0.1	0.1	0.1	0.1	
9	0.4	0.4	0.3	0.3	0.3	0.2	0.2	0.15	0.15	0.15	0.1	0.1	0.1	0.1	0.1	
8	0.4	0.4	0.3	0.3	0.3	0.2	0.15	0.15	0.1	0.1	0.1	0.1	0.1	0.1	0.1	
7	0.4	0.4	0.3	0.3	0.2	0.2	0.15	0.15	0.1	0.1	0.1	0.1	0.1	0.1	0.1	
6	0.4	0.4	0.3	0.3	0.2	0.15	0.15	0.15	0.1	0.1	0.1	0.1	0.1	0.1	0.1	
5	0.5	0.4	0.3	0.3	0.2	0.15	0.15	0.1	0.1	0.1	0.1	0.1	0.1	0.1	0.1	
4	0.5	0.4	0.3	0.2	0.15	0.15	0.1	0.1	0.1	0.1	0.1	0.1	0.1	0.1	0.1	
3	0.6	0.4	0.3	0.15	0.15	0.15	0.1	0.1	0.1	0.1	0.1	0.1	0.1	0.1	0.1	
2	0.7	0.3	0.2	0.15	0.15	0.15	0.1	0.1	0.1	0.1	0.1	0.1	0.1	0.1	0.1	
1	0.7	0.3	0.2	0.15	0.15	0.1	0.1	0.1	0.1	0.1	0.1	0.1	0.1	0.1	0.1	
0	1	2	3	4	5	6	7	8	9	10	11	12	13	14	15	
								X/L								

Table B.12: Diffraction table for a breakwater gap, with $B/L = 1.0$ and $s_{max} = 75$, relatively far from gap (Rijksinstituut voor Kust en Zee, 2004)

Y/L																
8	0.6	0.6	0.6	0.5	0.5	0.5	0.4	0.4	0.4	0.3	0.3	0.3	0.3	0.2	0.2	
7.6	0.6	0.6	0.6	0.6	0.5	0.5	0.5	0.4	0.4	0.3	0.3	0.3	0.3	0.2	0.2	
7.2	0.6	0.6	0.6	0.6	0.5	0.5	0.4	0.4	0.4	0.3	0.3	0.3	0.3	0.2	0.2	
6.8	0.7	0.7	0.6	0.6	0.5	0.5	0.4	0.4	0.4	0.3	0.3	0.3	0.2	0.2	0.2	
6.4	0.7	0.7	0.6	0.6	0.5	0.5	0.4	0.4	0.3	0.3	0.3	0.3	0.2	0.2	0.2	
6	0.7	0.7	0.6	0.6	0.5	0.5	0.4	0.4	0.3	0.3	0.3	0.3	0.2	0.2	0.15	
5.6	0.7	0.7	0.7	0.6	0.5	0.5	0.4	0.4	0.3	0.3	0.3	0.2	0.2	0.2	0.15	
5.2	0.7	0.7	0.7	0.6	0.5	0.5	0.4	0.4	0.3	0.3	0.3	0.2	0.2	0.15	0.15	
4.8	0.8	0.7	0.7	0.6	0.5	0.5	0.4	0.3	0.3	0.3	0.2	0.2	0.2	0.15	0.15	
4.4	0.8	0.8	0.7	0.6	0.5	0.4	0.4	0.3	0.3	0.3	0.2	0.2	0.15	0.15	0.15	
4	0.8	0.8	0.7	0.6	0.5	0.4	0.4	0.3	0.3	0.3	0.2	0.2	0.15	0.15	0.15	
3.6	0.8	0.8	0.7	0.6	0.5	0.4	0.3	0.3	0.3	0.2	0.2	0.15	0.15	0.15	0.15	
3.2	0.9	0.8	0.7	0.6	0.5	0.4	0.3	0.3	0.3	0.2	0.2	0.15	0.15	0.15	0.15	
2.8	0.9	0.8	0.7	0.5	0.4	0.4	0.3	0.3	0.2	0.2	0.15	0.15	0.15	0.15	0.15	
2.4	0.9	0.9	0.7	0.5	0.4	0.3	0.3	0.2	0.2	0.2	0.15	0.15	0.15	0.15	0.15	
2	1	0.9	0.6	0.5	0.4	0.3	0.3	0.2	0.2	0.15	0.15	0.15	0.15	0.15	0.1	
1.6	1.0	0.9	0.6	0.5	0.3	0.3	0.2	0.2	0.2	0.15	0.15	0.15	0.15	0.15	0.1	
1.2	1.1	1	0.6	0.4	0.3	0.3	0.2	0.2	0.15	0.15	0.15	0.15	0.15	0.1	0.1	
0.8	1.1	1.0	0.6	0.4	0.3	0.3	0.2	0.2	0.15	0.15	0.15	0.15	0.15	0.1	0.1	
0.4	1.1	1.1	0.6	0.4	0.3	0.2	0.2	0.2	0.15	0.15	0.15	0.15	0.15	0.1	0.1	
0	0.4	0.8	1.2	1.6	2	2.4	2.8	3.2	3.6	4	4.4	4.8	5.2	5.6	6	
								X/L								

Table B.13: Diffraction table for a breakwater gap, with $B/L = 2.0$ and $s_{max} = 75$, relatively close to gap (Rijksinstituut voor Kust en Zee, 2004)

Y/L																
40	0.3	0.3	0.3	0.3	0.3	0.2	0.2	0.2	0.15	0.15	0.15	0.15	0.1	0.1	0.1	
38	0.3	0.3	0.3	0.3	0.3	0.2	0.2	0.2	0.15	0.15	0.15	0.15	0.1	0.1	0.1	
36	0.3	0.3	0.3	0.3	0.3	0.2	0.2	0.2	0.15	0.15	0.15	0.1	0.1	0.1	0.1	
34	0.3	0.3	0.3	0.3	0.3	0.2	0.2	0.2	0.15	0.15	0.15	0.1	0.1	0.1	0.1	
32	0.3	0.3	0.3	0.3	0.3	0.2	0.2	0.15	0.15	0.15	0.15	0.1	0.1	0.1	0.1	
30	0.3	0.3	0.3	0.3	0.3	0.2	0.2	0.15	0.15	0.15	0.1	0.1	0.1	0.1	0.1	
28	0.4	0.3	0.3	0.3	0.3	0.2	0.2	0.15	0.15	0.15	0.1	0.1	0.1	0.1	0.1	
26	0.4	0.4	0.3	0.3	0.3	0.2	0.2	0.15	0.15	0.1	0.1	0.1	0.1	0.1	0.1	
24	0.4	0.4	0.3	0.3	0.3	0.2	0.15	0.15	0.15	0.1	0.1	0.1	0.1	0.1	0.1	
22	0.4	0.4	0.3	0.3	0.3	0.2	0.15	0.15	0.1	0.1	0.1	0.1	0.1	0.1	0.1	
20	0.4	0.4	0.3	0.3	0.2	0.2	0.15	0.15	0.1	0.1	0.1	0.1	0.1	0.1	0.1	
18	0.4	0.4	0.3	0.3	0.2	0.15	0.15	0.1	0.1	0.1	0.1	0.1	0.1	0.1	0.1	
16	0.5	0.4	0.3	0.3	0.2	0.15	0.15	0.1	0.1	0.1	0.1	0.1	0.1	0.1	0.05	
14	0.5	0.4	0.3	0.3	0.2	0.15	0.1	0.1	0.1	0.1	0.1	0.1	0.1	0.1	0.05	
12	0.5	0.4	0.3	0.2	0.15	0.15	0.1	0.1	0.1	0.1	0.1	0.1	0.1	0.05	0.05	
10	0.5	0.4	0.3	0.2	0.15	0.1	0.1	0.1	0.1	0.1	0.1	0.1	0.1	0.05	0.05	
8	0.6	0.4	0.2	0.15	0.15	0.1	0.1	0.1	0.1	0.1	0.1	0.1	0.05	0.05	0.05	
6	0.6	0.3	0.2	0.15	0.1	0.1	0.1	0.1	0.1	0.1	0.1	0.1	0.05	0.05	0.05	
4	0.7	0.2	0.15	0.1	0.1	0.1	0.1	0.1	0.1	0.1	0.1	0.05	0.05	0.05	0.05	
2	0.7	0.2	0.15	0.1	0.1	0.1	0.1	0.1	0.1	0.1	0.1	0.05	0.05	0.05	0.05	
0	2	4	6	8	10	12	14	16	18	20	22	24	26	28	30	
								X/L								

Table B.14: Diffraction table for a breakwater gap, with $B/L = 2.0$ and $s_{max} = 75$, relatively far from gap (Rijksinstituut voor Kust en Zee, 2004)

Y/L	0	0.8	1.6	2.4	3.2	4	4.8	5.6	6.4	7.2	8	8.8	9.6	10.4	11.2	12
	16	0.7	0.6	0.6	0.6	0.5	0.5	0.4	0.4	0.4	0.3	0.3	0.3	0.3	0.2	0.2
	15.2	0.7	0.7	0.6	0.6	0.5	0.5	0.4	0.4	0.4	0.3	0.3	0.3	0.2	0.2	0.2
	14.4	0.7	0.7	0.6	0.6	0.5	0.5	0.4	0.4	0.4	0.3	0.3	0.3	0.2	0.2	0.2
	13.6	0.7	0.7	0.7	0.6	0.5	0.5	0.4	0.4	0.3	0.3	0.3	0.3	0.2	0.2	0.2
	12.8	0.7	0.7	0.7	0.6	0.5	0.5	0.4	0.4	0.3	0.3	0.3	0.2	0.2	0.2	0.2
	12	0.7	0.7	0.7	0.6	0.5	0.5	0.4	0.4	0.3	0.3	0.3	0.2	0.2	0.2	0.2
	11.2	0.8	0.7	0.7	0.6	0.5	0.5	0.4	0.3	0.3	0.3	0.2	0.2	0.2	0.2	0.2
	10.4	0.8	0.8	0.7	0.6	0.5	0.4	0.4	0.3	0.3	0.3	0.2	0.2	0.2	0.2	0.2
	9.6	0.8	0.8	0.7	0.6	0.5	0.4	0.4	0.3	0.3	0.2	0.2	0.2	0.2	0.2	0.2
	8.8	0.8	0.8	0.7	0.6	0.5	0.4	0.3	0.3	0.3	0.2	0.2	0.2	0.2	0.2	0.2
	8	0.9	0.8	0.7	0.6	0.5	0.4	0.3	0.3	0.2	0.2	0.2	0.2	0.2	0.2	0.1
	7.2	0.9	0.8	0.7	0.6	0.5	0.4	0.3	0.3	0.2	0.2	0.2	0.2	0.2	0.2	0.1
	6.4	0.9	0.9	0.7	0.6	0.5	0.4	0.3	0.2	0.2	0.2	0.2	0.2	0.2	0.1	0.1
	5.6	1	0.9	0.7	0.6	0.4	0.3	0.3	0.2	0.2	0.2	0.2	0.2	0.1	0.1	0.1
	4.8	1	0.9	0.7	0.6	0.4	0.3	0.2	0.2	0.2	0.2	0.2	0.1	0.1	0.1	0.1
	4	1	1	0.7	0.6	0.4	0.3	0.2	0.2	0.2	0.2	0.2	0.1	0.1	0.1	0.1
	3.2	1	1	0.8	0.6	0.3	0.2	0.2	0.2	0.2	0.2	0.1	0.1	0.1	0.1	0.1
	2.4	1.1	1	0.8	0.4	0.3	0.2	0.2	0.2	0.2	0.1	0.1	0.1	0.1	0.1	0.1
	1.6	1.1	1.1	0.9	0.4	0.3	0.2	0.2	0.2	0.2	0.1	0.1	0.1	0.1	0.1	0.1
	0.8	1.1	1.1	0.9	0.3	0.2	0.2	0.2	0.2	0.2	0.1	0.1	0.1	0.1	0.1	0.1
	0	0.8	1.6	2.4	3.2	4	4.8	5.6	6.4	7.2	8	8.8	9.6	10.4	11.2	12
									X/L							

Table B.15: Diffraction table for a breakwater gap, with $B/L = 4.0$ and $s_{max} = 75$, relatively close to gap (Rijksinstituut voor Kust en Zee, 2004)

Y/L	0	4	8	12	16	20	24	28	32	36	40	44	48	52	56	60
	80	0.3	0.3	0.3	0.3	0.3	0.2	0.2	0.2	0.2	0.2	0.2	0.1	0.1	0.1	0.1
	76	0.3	0.3	0.3	0.3	0.3	0.2	0.2	0.2	0.2	0.2	0.2	0.1	0.1	0.1	0.1
	72	0.4	0.3	0.3	0.3	0.3	0.3	0.2	0.2	0.2	0.2	0.2	0.1	0.1	0.1	0.1
	68	0.4	0.3	0.3	0.3	0.3	0.3	0.2	0.2	0.2	0.2	0.1	0.1	0.1	0.1	0.1
	64	0.4	0.4	0.3	0.3	0.3	0.2	0.2	0.2	0.2	0.2	0.1	0.1	0.1	0.1	0.1
	60	0.4	0.4	0.3	0.3	0.3	0.2	0.2	0.2	0.2	0.2	0.1	0.1	0.1	0.1	0.1
	56	0.4	0.4	0.3	0.3	0.3	0.2	0.2	0.2	0.2	0.1	0.1	0.1	0.1	0.1	0.1
	52	0.4	0.4	0.3	0.3	0.3	0.2	0.2	0.2	0.1	0.1	0.1	0.1	0.1	0.1	0.1
	48	0.4	0.4	0.3	0.3	0.3	0.2	0.2	0.2	0.1	0.1	0.1	0.1	0.1	0.1	0.1
	44	0.4	0.4	0.3	0.3	0.3	0.2	0.2	0.1	0.1	0.1	0.1	0.1	0.1	0.1	0.05
	40	0.4	0.4	0.4	0.3	0.2	0.2	0.2	0.1	0.1	0.1	0.1	0.1	0.05	0.05	0.05
	36	0.5	0.4	0.4	0.3	0.2	0.2	0.1	0.1	0.1	0.1	0.1	0.05	0.05	0.05	0.05
	32	0.5	0.4	0.4	0.3	0.2	0.2	0.1	0.1	0.1	0.1	0.05	0.05	0.05	0.05	0.05
	28	0.5	0.4	0.3	0.2	0.2	0.1	0.1	0.1	0.1	0.05	0.05	0.05	0.05	0.05	0.05
	24	0.5	0.4	0.3	0.2	0.2	0.1	0.1	0.1	0.05	0.05	0.05	0.05	0.05	0.05	0.05
	20	0.6	0.4	0.3	0.2	0.1	0.1	0.1	0.05	0.05	0.05	0.05	0.05	0.05	0.05	0.05
	16	0.6	0.4	0.2	0.2	0.1	0.1	0.1	0.05	0.05	0.05	0.05	0.05	0.05	0.05	0.05
	12	0.7	0.3	0.2	0.1	0.1	0.1	0.05	0.05	0.05	0.05	0.05	0.05	0.05	0.05	0.05
	8	0.7	0.2	0.1	0.1	0.1	0.1	0.05	0.05	0.05	0.05	0.05	0.05	0.05	0.05	0.05
	4	0.7	0.2	0.1	0.1	0.1	0.1	0.05	0.05	0.05	0.05	0.05	0.05	0.05	0.05	0.05
	0	4	8	12	16	20	24	28	32	36	40	44	48	52	56	60
									X/L							

Table B.16: Diffraction table for a breakwater gap, with $B/L = 4.0$ and $s_{max} = 75$, relatively far from gap (Rijksinstituut voor Kust en Zee, 2004)

Y/L	0	1.6	3.2	4.8	6.4	8	9.6	11.2	12.8	14.4	16	17.6	19.2	20.8	22.4	24
32	0.7	0.7	0.6	0.6	0.5	0.5	0.4	0.4	0.3	0.3	0.3	0.3	0.2	0.2	0.15	
30.4	0.7	0.7	0.6	0.6	0.6	0.5	0.4	0.4	0.3	0.3	0.3	0.2	0.2	0.15	0.15	
28.8	0.7	0.7	0.7	0.6	0.6	0.5	0.4	0.4	0.3	0.3	0.3	0.2	0.2	0.15	0.15	
27.2	0.7	0.7	0.7	0.6	0.6	0.5	0.4	0.4	0.3	0.3	0.2	0.2	0.2	0.15	0.15	
25.6	0.7	0.7	0.7	0.6	0.6	0.5	0.4	0.3	0.3	0.3	0.2	0.2	0.15	0.15	0.15	
24	0.8	0.7	0.7	0.6	0.6	0.5	0.4	0.3	0.3	0.3	0.2	0.2	0.15	0.15	0.15	
22.4	0.8	0.8	0.7	0.6	0.5	0.5	0.4	0.3	0.3	0.2	0.2	0.15	0.15	0.15	0.1	
20.8	0.8	0.8	0.7	0.6	0.5	0.4	0.4	0.3	0.3	0.2	0.2	0.15	0.15	0.15	0.1	
19.2	0.8	0.8	0.7	0.6	0.5	0.4	0.3	0.3	0.3	0.2	0.15	0.15	0.15	0.1	0.1	
17.6	0.9	0.8	0.7	0.6	0.5	0.4	0.3	0.3	0.2	0.2	0.15	0.15	0.15	0.1	0.1	
16	0.9	0.8	0.7	0.6	0.5	0.4	0.3	0.3	0.2	0.15	0.15	0.15	0.1	0.1	0.1	
14.4	0.9	0.9	0.7	0.6	0.5	0.4	0.3	0.2	0.2	0.15	0.15	0.1	0.1	0.1	0.1	
12.8	0.9	0.9	0.7	0.6	0.4	0.3	0.3	0.2	0.15	0.15	0.1	0.1	0.1	0.1	0.1	
11.2	1	0.9	0.7	0.5	0.4	0.3	0.2	0.15	0.15	0.15	0.1	0.1	0.1	0.1	0.05	
9.6	1	0.9	0.7	0.5	0.4	0.3	0.2	0.15	0.15	0.1	0.1	0.1	0.1	0.05	0.05	
8	1	0.9	0.7	0.4	0.3	0.2	0.15	0.1	0.1	0.1	0.1	0.1	0.1	0.05	0.05	
6.4	1	1	0.7	0.4	0.3	0.2	0.15	0.1	0.1	0.1	0.1	0.1	0.05	0.05	0.05	
4.8	1.1	1	0.7	0.3	0.2	0.15	0.1	0.1	0.1	0.1	0.1	0.1	0.05	0.05	0.05	
3.2	1.1	1	0.7	0.3	0.15	0.15	0.1	0.1	0.1	0.1	0.1	0.1	0.1	0.05	0.05	
1.6	1.1	1.1	0.7	0.2	0.15	0.15	0.1	0.1	0.1	0.1	0.1	0.1	0.1	0.05	0.5	

X/L

Table B.17: Diffraction table for a breakwater gap, with $B/L = 8.0$ and $s_{max} = 75$, relatively close to gap (Rijksinstituut voor Kust en Zee, 2004)

Y/L	0	8	16	24	32	40	48	56	64	72	80	88	96	104	112	120
160	0.3	0.3	0.3	0.3	0.3	0.2	0.2	0.2	0.2	0.2	0.2	0.2	0.1	0.1	0.1	
152	0.4	0.3	0.3	0.3	0.3	0.2	0.2	0.2	0.2	0.2	0.2	0.1	0.1	0.1	0.1	
144	0.4	0.3	0.3	0.3	0.3	0.2	0.2	0.2	0.2	0.2	0.1	0.1	0.1	0.1	0.1	
136	0.4	0.3	0.3	0.3	0.3	0.2	0.2	0.2	0.2	0.2	0.1	0.1	0.1	0.1	0.1	
128	0.4	0.3	0.3	0.3	0.2	0.2	0.2	0.2	0.2	0.1	0.1	0.1	0.1	0.1	0.1	
120	0.4	0.4	0.3	0.3	0.2	0.2	0.2	0.2	0.2	0.1	0.1	0.1	0.1	0.1	0.1	
112	0.4	0.4	0.3	0.3	0.2	0.2	0.2	0.2	0.1	0.1	0.1	0.1	0.1	0.1	0.05	
104	0.4	0.4	0.3	0.3	0.2	0.2	0.2	0.2	0.1	0.1	0.1	0.1	0.1	0.05	0.05	
96	0.5	0.4	0.3	0.3	0.2	0.2	0.2	0.1	0.1	0.1	0.1	0.1	0.05	0.05	0.05	
88	0.5	0.4	0.3	0.3	0.2	0.2	0.2	0.1	0.1	0.1	0.1	0.05	0.05	0.05	0.05	
80	0.5	0.4	0.3	0.3	0.2	0.2	0.1	0.1	0.1	0.1	0.1	0.05	0.05	0.05	0.05	
72	0.5	0.4	0.3	0.2	0.2	0.2	0.1	0.1	0.1	0.1	0.05	0.05	0.05	0.05	0.05	
64	0.5	0.4	0.3	0.2	0.2	0.1	0.1	0.1	0.1	0.05	0.05	0.05	0.05	0.05	0.05	
56	0.5	0.4	0.3	0.2	0.2	0.1	0.1	0.1	0.05	0.05	0.05	0.05	0.05	0.05	0.05	
48	0.6	0.4	0.3	0.2	0.2	0.1	0.1	0.05	0.05	0.05	0.05	0.05	0.05	0.05	0.05	
40	0.6	0.4	0.2	0.2	0.1	0.1	0.05	0.05	0.05	0.05	0.05	0.05	0.05	0.05	0.05	
32	0.7	0.3	0.2	0.2	0.1	0.05	0.05	0.05	0.05	0.05	0.05	0.05	0.05	0.05	0.05	
24	0.7	0.3	0.2	0.1	0.05	0.05	0.05	0.05	0.05	0.05	0.05	0.05	0.05	0.05	0.05	
16	0.7	0.2	0.1	0.05	0.05	0.05	0.05	0.05	0.05	0.05	0.05	0.05	0.05	0.05	0.05	
8	0.7	0.1	0.1	0.05	0.05	0.05	0.05	0.05	0.05	0.05	0.05	0.05	0.05	0.05	0.05	

X/L

Table B.18: Diffraction table for a breakwater gap, with $B/L = 8.0$ and $s_{max} = 75$, relatively far from gap (Rijksinstituut voor Kust en Zee, 2004)

C. List of genetic algorithm terminology

As genetic algorithms still do not play a large role within the field of hydraulic engineering, more clarification regarding the terminology of genetic algorithms is desired. Therefore, a complete list with the definition of *GA* terms is provided below, including its relation to the research topic. Optimisation parameter definitions are given in Section 5.5.2.

Evolution	The iterative process that is represented by a genetic algorithm.
Chromosome/individual	A breakwater layout alternative satisfying the model constraints.
Gene	A certain decision variable that characterises an individual (e.g. coordinates of the breakwater nodes).
Allele	Value corresponding to a certain gene.
Locus	The position of a gene within the chromosome it belongs to.
Genotype	The coded representation of a chromosome (as a string of genes).
Phenotype	The decoded representation of a chromosome (as a breakwater layout alternative).
Population	A collection of a certain amount of chromosomes that is generated by the algorithm.
Parents	A pair of chromosomes that is selected to transfer their genetic material to create a new chromosome.
Mating pool	The collection of parent chromosomes belonging to a population.
Offspring	The new population that is created by applying evolutionary processes to the current population.
Child	A single chromosome that belongs to the offspring population.
Generation	A loop within the evolution process, represented by a single population of alternatives.
Objective function	A function defining one of the optimisation objectives that need to be minimised by the model.
Fitness function	A function that serves as an indicator of the performance of a certain individual, leading to a balance between both objectives.
Neighbourhood	A certain area within the solution space that a certain group of layout configurations – having approximately equal characteristics – belongs to. This group can consequently be called a species, therefore to be considered as the same breakwater layout alternative.
Alternative	A solution of the parametric model (a breakwater layout configuration in this case) that is located in the same neighbourhood as another solution, therewith having comparable characteristics.
Genetic operator	Component within the genetic algorithm that guides individuals towards a solution. It corresponds to an evolutionary process, such as selection, crossover or mutation.

Selection	A genetic operator that is used to select parents to form the mating pool and to select chromosomes that move on to the next generation.
Crossover	A genetic operator that recombines the genes of parent chromosomes to form a child.
Mutation	A genetic operator that randomly introduces changes to certain genes to maintain diversity in the population.
Elitism	A specific form of selection that guarantees to pass on the best alternatives to the next generation.
Fitness evaluation	Ranking of chromosomes within a population based on their objective scores.
Dominance	Better performance of an alternative with respect to another alternative on all considered objectives.
Non-dominated sorting	Sorting strategy that makes use of the level of domination of the chromosomes in a population.
Crowding distance	Sum of the differences of two neighbouring solutions within the considered domination front with respect to all objectives.
Binary tournament selection	Selection type that randomly picks to alternatives within a population and chooses one of them based on their fitness evaluation.
Optimisation parameter	Parameter influencing the performance of the genetic algorithm.

D. Input parameter tables

D.1. Overview

Symbol	Description	Default	Unit
(x_{max}, y_{max})	Outermost point defined for primary breakwater	(4000, 3000)	m
L_{max}	Outermost distance for secondary breakwater in x-direction	4000	m

Table D.1: Input parameters for 'constraints'

Symbol	Description	Default	Unit
H_n	Limiting wave height for navigational downtime	1.5	m
H_{od}	Limiting wave height for operational downtime	0.5	m
$u_{w,od}$	Limiting wind speed for operational downtime	20	m/s
$u_{cw,n}$	Limiting cross-wind speed for navigational downtime	18	m/s
$u_{lw,n}$	Limiting longitudinal wind speed for navigational downtime	18	m/s
$u_{cc,n}$	Limiting cross-current speed for navigational downtime	0.5	m/s
$u_{lc,n}$	Limiting longitudinal current speed for navigational downtime	2.0	m/s
$v_{s,min}$	Minimum vessel speed	2.0	m/s
t_{tug}	Tugging time	10	min

Table D.2: Input parameters for 'navigation'

Symbol	Description	Default	Unit
L_s	Length over all of design vessel	300	m
B_s	Beam of design vessel	32	m
D	Draught of design vessel	12	m
v_s	Vessel entrance speed	3.0	m/s

Table D.3: Input parameters for 'vessel'

Symbol	Description	Default	Unit
C_{core}	Unit price for breakwater core layer	30	€/m^3
C_{under}	Unit price for breakwater underlayer	25	€/m^3
C_{armour}	Unit price for breakwater armour layer	400	€/unit
C_{dd}	Dredging-dumping costs of sediment	5	€/m^3
C_{df}	Dredging-filling costs of sediment	4	€/m^3
C_{TEU}	Unit rate per TEU	60	€/TEU
C_{land}	Land costs per running metre of coastline stretch	2000	€/m'
$\Phi_{bw,m}$	Ratio of annual breakwater maintenance costs w.r.t. construction	0.02	-
r	Discount rate for present-day value	0.05	-
T_L	Design lifetime of the breakwater	50	yr

Table D.4: Input parameters for 'costs' (unit prices include manufacturing, transport & construction)

Symbol	Description	Default	Unit
n_b	Number of berths	-	-
n_{bf}	Number of berths in future	-	-
y_f	Fill-up distance of terminal in y-direction	-	m
m_b	Berth occupancy factor	0.6	-
P_b	Hourly berth productivity	35	moves/hr
f_{TEU}	TEU-factor	1.5	-

Table D.5: Input parameters for 'terminal'

Symbol	Description	Default	Unit
z_0	Ground level at $y = 0$	-	m (+ MSL)
$1 : \alpha_b$	Slope of the sea bed	-	-
θ_s	Orientation of normal to coastline with respect to North	-	°

Table D.6: Input parameters for 'bathymetry' and 'coast'

Symbol	Description	Default	Unit
HAT	High Astronomical Tide	-	m (+ MSL)
LAT	Low Astronomical Tide	-	m (- MSL)

Table D.7: Input parameters 'water levels'

Symbol	Description	Default	Unit
h_l	Level of leeward armour layer level	3	m (- MSL)
h_c	Top level of core layer	0.5	m (+ HAT)
B_{crest}	Average breakwater crest width	10	m
n_v	Armour layer porosity	0.5	-
D_n	Nominal diameter of armour units	1.5	m
t_a	Armour layer thickness	3.0	m
t_u	Underlayer thickness	1.0	m
$1 : x_f$	Front slope of breakwater	1 : 1.5	-
$1 : x_r$	Rear slope of breakwater	1 : 1.5	-

Table D.8: Input parameters for 'breakwater'

Symbol	Description	Default	Unit
$H_{0,s}$	Significant wave height in deep water	-	m
$T_{0,p}$	Peak period in deep water	-	s
θ_0	Wave direction in deep water with respect to North	-	°
u_w	Wind speed at sea	-	m/s
θ_w	Wind direction at sea with respect to North	-	°
u_c	Current speed at sea	-	m/s
θ_c	Current direction at sea with respect to North	-	°
Pr	Probability of occurrence of a certain environmental condition	-	-
s_{max}	Maximum directional concentration parameter	10	-

Table D.9: Input parameters for 'environment'

Symbol	Description	Default	Unit
$t_{s,0}$	Annual siltation thickness (no secondary breakwater)	0.4	m/yr
$t_{s,min}$	Annual siltation thickness (breakwater gap ≥ 1000 m)	0.3	m/yr
$t_{s,max}$	Annual siltation thickness (breakwater gap width equal to channel width)	0.25	m/yr
s_{type}	Soil type (1 = mud, 2 = sand/clay, 3 = rock/coral)	2	-

Table D.10: Input parameters for 'sedimentation'

Symbol	Description	Default	Unit
h_f	Average fill level of terminal	-	m (+ MSL)
$1:x_b$	Bank slope of the approach channel	1 : 4	-

Table D.11: Input parameters for 'dredging'

D.2. Sensitivity analysis

Symbol	Description	Value	Unit
n_b	Number of berths	3	-
n_{bf}	Number of berths in future	5	-
y_f	Fill-up distance of terminal in y-direction	200	m
z_0	Ground level at $y = 0$	2.5	m (+ MSL)
$1:\alpha_b$	Slope of the sea bed	100	-
θ_s	Orientation of normal to coastline with respect to North	0	°
HAT	High Astronomical Tide	1.5	m (+ MSL)
LAT	Low Astronomical Tide	1.5	m (- MSL)
h_f	Average fill level of terminal	2.5	m (+ MSL)

Table D.12: Non-default parameters for sensitivity analysis

D.3. Case study

Symbol	Description	Value	Unit
(x_{max}, y_{max})	Outermost point defined for primary breakwater	(3000, 3000)	m
L_{max}	Outermost distance for secondary breakwater in x-direction	3000	m
$u_{cw,n}$	Limiting cross-wind speed for navigational downtime	10	m
$u_{lw,n}$	Limiting longitudinal wind speed for navigational downtime	12	m
L_s	Length over all of design vessel	400	m
B_s	Beam of design vessel	59	m
D	Draught of design vessel	16	m
n_b	Number of berths	6	-
n_{bf}	Number of berths in future	6	-
y_f	Fill-up distance of terminal in y-direction	400	m
m_b	Berth occupancy factor	0.65	-
P_b	Hourly berth productivity	55	moves/hr
z_0	Ground level at $y = 0$	1.5	m (+ MSL)
$1:\alpha_b$	Slope of the sea bed	45	-
θ_s	Orientation of normal to coastline with respect to North	-50	°
HAT	High Astronomical Tide	0.5	m (+ MSL)
LAT	Low Astronomical Tide	0.5	m (- MSL)
h_f	Average fill level of terminal	1.5	m (+ MSL)

Table D.13: Parameters with non-default values for the case study of Tanger Med 2

E. Environmental conditions

Several sets of environmental conditions are used in Chapter 6 to 8. These sets are given below. The direction convention is 'from' for waves and 'to' for winds and currents, always with respect to the coastline normal. Also some supporting figures are provided for the case study.

E.1. Sensitivity analysis

$H_{0,s}$ (m)	$T_{0,p}$ (s)	θ_0 (°)	u_w (m/s)	θ_w (°)	u_c (m/s)	θ_c (°)	Pr (-)
5.5	8	40	15	-100	0.2	-100	0.005
4.5	8	40	15	-100	0.2	-100	0.015
4.0	8	40	15	-100	0.2	-100	0.04
3.0	8	40	15	-100	0.2	-100	0.15
2.0	8	40	15	-100	0.2	-100	0.22
5.0	8	-20	15	-100	0.2	-100	0.005
4.0	8	-20	15	-100	0.2	-100	0.015
3.5	8	-20	15	-100	0.2	-100	0.06
2.5	8	-20	15	-100	0.2	-100	0.22
1.5	8	-20	15	-100	0.2	-100	0.27

Table E.1: Environmental conditions for model tuning, double wave direction

$H_{0,s}$ (m)	$T_{0,p}$ (s)	θ_0 (°)	u_w (m/s)	θ_w (°)	u_c (m/s)	θ_c (°)	Pr (-)
5.5	8	30	15	-100	0.2	-100	0.01
4.5	8	30	15	-100	0.2	-100	0.02
4.0	8	30	15	-100	0.2	-100	0.04
3.0	8	30	15	-100	0.2	-100	0.13
2.0	8	30	15	-100	0.2	-100	0.30
1.0	8	30	15	-100	0.2	-100	0.50

Table E.2: Environmental conditions for a single wave direction

$H_{0,s}$ (m)	$T_{0,p}$ (s)	θ_0 (°)	u_w (m/s)	θ_w (°)	u_c (m/s)	θ_c (°)	Pr (-)
3.5	9	30	17	-150	0.2	-100	0.005
3.0	9	20	12	160	0.2	60	0.015
2.5	9	-70	15	170	0.2	-90	0.04
2.0	8	-50	11	-10	0.1	70	0.15
1.5	8	0	16	-50	0.1	100	0.22
1.2	8	-30	15	-140	0.4	90	0.005
1.1	7	30	12	-75	0.1	-90	0.015
1.0	7	-60	10	150	0.3	90	0.06
0.8	7	30	8	90	0.2	-120	0.22
0.5	6	-80	12	-175	0.2	90	0.27

Table E.3: Environmental conditions for a mild wave climate

$H_{0,s}$ (m)	$T_{0,p}$ (s)	θ_0 (°)	u_w (m/s)	θ_w (°)	u_c (m/s)	θ_c (°)	Pr (-)
6.5	9	30	17	-150	0.2	-100	0.005
5.5	9	20	12	160	0.2	60	0.015
5.0	9	-70	15	170	0.2	-90	0.04
4.5	8	-50	11	-10	0.1	70	0.15
4.2	8	0	16	-50	0.1	100	0.22
4.0	8	-30	15	-140	0.4	90	0.005
3.8	7	30	12	-75	0.1	-90	0.015
3.5	7	-60	10	150	0.3	90	0.06
2.3	7	30	8	90	0.2	-120	0.22
1.8	6	-80	12	-175	0.2	90	0.27

Table E.4: Environmental conditions for a rough wave climate

E.2. Case study

$H_{0,s}$ (m)	$T_{0,p}$ (s)	θ_0 (°)	u_w (m/s)	θ_w (°)	u_c (m/s)	θ_c (°)	Pr (-)
0.5	7	88	7	-45	0.8	110	0.45
1.0	8	-35	6	145	1.0	-92	0.43
0.8	8	85	8	-40	1.1	-92	0.012
0.6	8	-10	9	-40	1.2	-92	0.04
1.8	8	-20	9	160	1.2	110	0.02
2.0	9	-35	10	140	1.3	110	0.025
2.1	9	-35	10	140	1.3	110	0.01
2.2	10	-35	10	140	1.5	110	0.005
1.2	8	88	9	-40	1.2	-92	0.005
1.5	8	-30	13	-40	1.0	110	0.003

Table E.5: Environmental conditions for the case study of Tanger Med 2

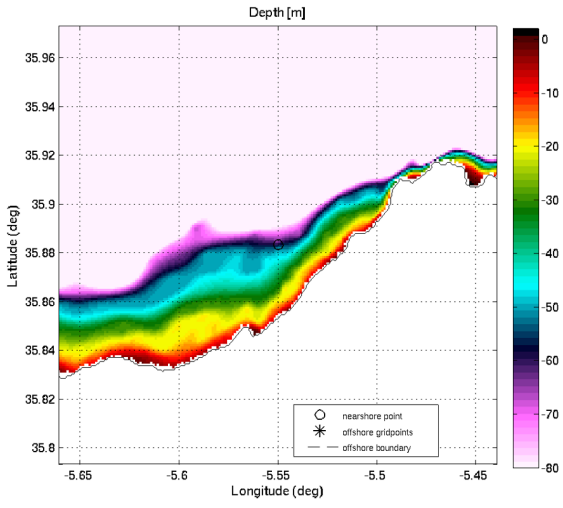

Figure E.1: Bathymetry at port location

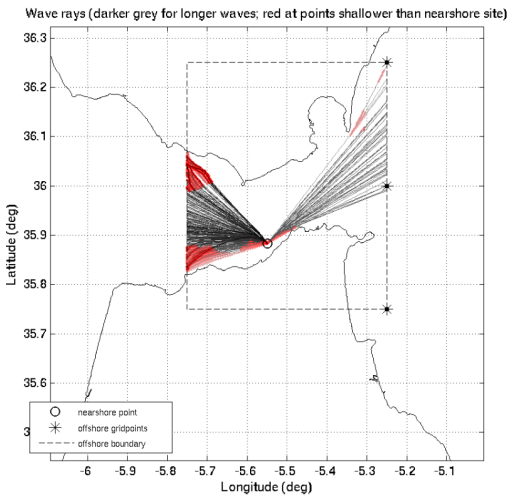

Figure E.2: Wave rays until port location